The Institute of Paper Chemistry

Appleton, Wisconsin

Doctor's Dissertation

The Wettability of Cellulose Film as Affected by Vapor-Phase Adsorption of Amphipathic Molecules

James L. Ferris

June, 1974

THE WETTABILITY OF CELLULOSE FILM AS AFFECTED BY VAPOR-PHASE ADSORPTION OF AMPHIPATHIC MOLECULES

A thesis submitted by

James L. Ferris

B.S. 1966, University of Washington

M.S. 1969, Lawrence University

In partial fulfillment of the requirements
of The Institute of Paper Chemistry
for the degree of Doctor of Philosophy
from Lawrence University
Appleton, Wisconsin

June, 1974

TABLE OF CONTENTS

SUMMARY

Alteration of the absorbent nature of cellulose is commercially accomplished by adsorption of low energy hydrophobic molecules from solution onto the cellulose surface. This operation, called sizing, promotes water repellency in many cellulosic products. This study was initiated to determine the relationship between the amount and orientation of sizing molecules adsorbed from the vapor phase and the subsequent water repellency developed on the sized surface.

Cellulose film was hand cast from cellulose xanthate on smooth glass plates and dried against a polymethylmethacrylate surface to provide a smooth and clean adsorption surface. This surface was exposed to radioactively labelled stearic acid in the vapor phase. The stearic acid adsorbed both physically and chemically onto the cellulose surface in a reproducible manner.

The amount of adsorption on the film was determined by radioactive counting. The amount of chemically bonded acid was determined by extraction of the film in benzene and water to remove physically adsorbed and trapped molecules. The remaining molecules were assumed to be chemically bonded.

The water contact angle on treated cellulose film was measured by photographic means which enabled the determination of a contact angle within one second after placement of the liquid drop on the surface. Methylene iodide contact angles were also determined and a surface energy parameter was calculated from the Owens-Wendt equations.

Adsorption temperatures of 65, 85, and 105°C were used in a closed adsorption system with infinite stearic acid source. Total adsorption increased with temperature due to the increased vapor pressure. Adsorption isotherms as a function of time rapidly increased to a constant equilibrium value then

increased again as massive amounts of acid began to penetrate into the film. The chemical bonding reaction followed zero-order kinetics but was highly temperature dependent. The reaction essentially stopped above 23% geometric monolayer coverage.

Water contact angles increased linearly with time at each temperature from the initial value of 28° to approximately 60° where the rate slowed considerably, reaching 90° only after 290 hours at 105°C. Physically, adsorbed molecules appear to have no effect on the water contact angle, all increases in repellency being directly attributable to chemically bonded molecules.

INTRODUCTION

Since cellulose is a very hydrophilic material, any purely cellulosic material will tend to absorb water. Paper, as a cellulosic product, therefore has a natural tendency to absorb aqueous liquids. Unfortunately, in only a few special cases is absorbency desired in paper. Therefore, it falls to the papermaker to artifically produce water resistance in his products. This is typically accomplished by adsorbing hydrophobic molecules onto the hydrophilic fiber surface to mask the absorbent character of the cellulose. This operation is referred to as sizing.

There are two primary methods used to size paper commercially. Internal sizing involves addition of sizing agents into the pulp slurry at some point before the wet end of the machine. In this way, individual fibers are sized and the water repellency of the paper exists throughout the sheet. In the second method, surface sizing, film-forming agents are applied to the surface of the already formed sheet by a roll application technique. In this way, only the water repellency of the surface of the sheet is altered.

A third conceivable method is surface sizing in the vapor phase. This technique would be far superior economically to internal sizing as much less sizing agent would be required. Vapor-phase application would not require a solvent for the sizing agent and would be exceedingly adaptable in controlling the amount of size added to the surface. It could possibly be added to the drying machine.

The eventual development of commercial vapor-phase sizing processes is the ultimate desired application of this work. This, the first step, will address the question of how sizing develops from the vapor phase.

LITERATURE REVIEW

INTRODUCTION TO THE SURFACE ENERGY OF SOLIDS

Molecules deep in a nonstressed solid are entirely surrounded by other molecules. Each molecule in the solid exerts forces on every other molecule to some extent. These may be ubiquitous London dispersion forces, electrostatic attractive or repulsive forces, chemical bonding or quasi-chemical bonding interactions such as hydrogen bonding. Whatever the sources of the intermolecular forces acting on a molecule in the bulk, they are balanced in the nonstressed solid; that is, the summation of forces acting on a molecule is zero. On the surface of a solid, however, these forces cannot be balanced. This results in a tension, or energy, in the surface which is unique to this layer of molecules. On an ideal surface under vacuum, the magnitude of this surface energy is dependent only on the molecular species of the solid. For a real surface, however, there are several factors which affect the surface energy, causing it to vary from point to point on a microscopic scale. Causes of this heterogeneity include surface roughness, chemical impurity of the solid, adsorption of foreign molecules onto the surface, and stresses frozen into the solid when formed. Surface energy varies with roughness, for example, as the forces acting on surface molecules of flat planes, ridges, and points become increasingly unbalanced in one, two, and three dimensions, respectively. Chemical impurity and adsorption of foreign molecules can affect the surface properties in obvious ways. This heterogeneity of a real surface can cause point to point differences in adsorption, wetting, and chemical reactivity of the surface.

THEORETICAL ASPECTS OF SURFACE ENERGY

Surface energy is conventionally denoted by a gamma, γ, and is defined as the energy in ergs required to create one square centimeter of nonstressed surface. That is, it is the energy per square centimeter of new surface required to separate the bulk matter into two pieces, infinitely distant. It is always positive in natural systems (i.e., energy must be consumed to create the surface), and it is mathematically equal to the surface tension for all pure liquid surfaces (1). The surface tension is a force in the plane of the surface. Subscripts are used to designate phases as follows: s°, sv, sl indicate the surface energy of the solid in equilibrium with a vacuum, vapor, and liquid, respectively; while the subscript lv is usually used to indicate the surface energy (or tension) of the liquid in equilibrium with its own vapor.

Although there are many difficulties in experimental determination of the surface energy of solids, the concept is the basis for many theoretical as well as experimental investigations of surface wetting.

Wetting or spreading involves the interaction of a liquid with a solid surface. The degree of wetting of a solid by a liquid is determined by the surface energy of the two phases and the interfacial attractive energy.

Keeping in mind that the definitions of surface energy and surface tensions apply to liquids as well as solids, the work of adhesion between a liquid and a solid is defined by Dupre (2) in Equation (1):

$$W_A = \gamma_{sv} + \gamma_{lv} - \gamma_{sl}, \qquad (1)$$

where W_A is the reversible work of adhesion and γ_{sv}, γ_{lv}, and γ_{sl} are the surface energies as defined by the subscripts above. The term W_A quantifies the energy required to separate one square centimeter of wetted solid interface into one square centimeter each of liquid surface and solid surface.

A thermodynamic requirement for a liquid to spread on a solid has been taken as a positive spreading coefficient, S, defined as $S = W_A - W_C$. The work of cohesion, W_C, is equal to twice the surface energy of the pure liquid. That is, spreading can initiate where the liquid has more attraction for the solid than for itself.

A more readily visualized but dangerously simple concept of the interrelation of the surface energies involves interpretation in terms of the surface tensions of the system as shown in Fig. 1. As noted by Johnson (1), the surface tension and surface energy of solid surfaces are not equal where a third component is adsorbed on the surface.

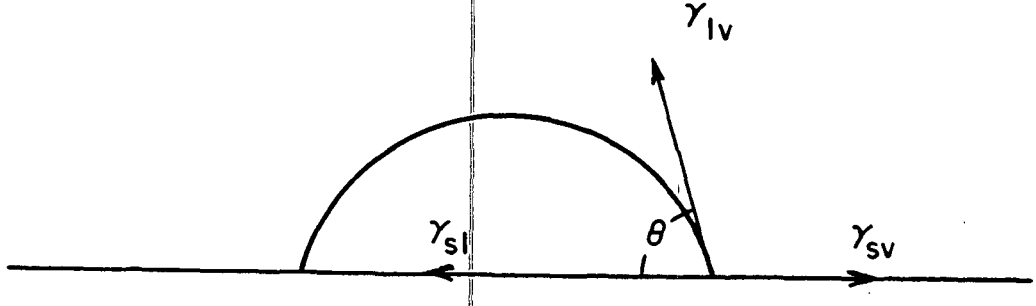

Figure 1. Surface Tension Forces at Equilibrium for Liquid Drop on Flat Plate

From considerations of a drop in equilibrium on a smooth flat plate, such as shown in Fig. 1, Young (3) in 1805 postulated the mathematical relationship of the surface tensions in the famous Young's equation:

$$\gamma_{lv}\cos\theta = \gamma_{sv} - \gamma_{sl}. \qquad (2)$$

Here, the surface tension subscripts are as previously defined and θ is the contact angle of the liquid on the solid measured in the liquid phase. This equation, easily derived from a balance of forces, can also be derived thermodynamically (1), but Adamson and Ling (4) have pointed out the difficulties involved in experimentally testing the results. Lester (5) calculated that Equation (2) is valid only if the solid is not too deformable. Softer solids will develop a deformation around the periphery of the liquid drop according to this hypothesis. Michaels and Dean (6) have experimentally found this deformation of soft silica gels under a water drop.

Bangham and Razouk (7) emphasized that the value of γ_{sv} should not be equated to γ_{s^o} without due consideration. That is, the surface of a solid in equilibrium with a saturated vapor is not necessarily equal to the pure solid surface tension itself. The value of $\gamma_s - \gamma_{sv}$, which he calls π_e, must not be assumed negligible, especially where the liquid is volatile or the solid has an affinity for the vapor. Bangham has proposed that the value of π_e can be calculated from the Gibbs adsorption isotherm when ideal gas behavior of the vapor is assumed. Young's equation in terms of the pure solid surface tension, γ_s, is therefore $\gamma_{lv}\cos = \gamma_s - \pi_e - \gamma_{sl}$. If π_e is not negligible, great care must be taken that it is included in the interpretation of the surface properties.

CONTACT ANGLE

The measurement of Young's contact angle is so seemingly straightforward that its experimental use has been widespread since first proposed over 160 years ago. However, the results obtained have been extremely difficult to

reproduce, and not until recently have characteristic contact angles for liquid-solid systems been established with any validity. Only the most rigorously reproduced surface preparations and measurement procedures result in comparable angles. Indeed, the best reproducibility reported is normally ±2°.

Modification of Young's equation has been attempted to improve the significance of the angle on real surfaces — specifically rough and porous surfaces. Wenzel (8) proposed that roughness could be taken into account by introduction of a roughness factor, r, equal to the ratio of the actual surface area to the geometric surface area of the solid. This factor is introduced into the Young's equation as shown.

$$\gamma_{lv}\cos\theta_A = r\,\gamma_{sv} - r\,\gamma_{sl} = r(\gamma_{sv} - \gamma_{sl})$$

or

$$\cos\theta_A = r(\cos\theta_o). \qquad (3)$$

Here, θ_A is the experimentally measured angle referred to as the apparent contact angle, θ_o is the real contact angle which would be found for a perfectly smooth surface, and all other terms are as previously defined. This correction factor has been subject to criticism (9-11) but is generally supported. Its use follows from a surface energy interpretation by adjusting planar surfaces to rough surfaces.

On a microscopic level, several investigators have found that the contact angle varies with the angle the roughness makes with the plane of the surface, but is independent of the height of the deformities on the surface (9,12).

A further correction equation for contact angles which includes the modification by Wenzel, is the 1944 proposal by Cassie and Baxter (13) for

contact angle measurement on rough porous surfaces such as textiles. Equation (4) is the Cassie-Baxter equation,

$$\cos \theta_A = f_1 \cos \theta_o - f_2, \qquad (4)$$

where θ_A and θ_o are the contact angles as defined above: f_1 is Wenzel's roughness factor, r; and f_2 is a porosity factor — the ratio of pore area to geometric surface area. There is not a clearly defined border between the two factors for roughness and porosity since some deep surface asperities may appear as pores to the wetting liquid. This is especially true for obtuse contact angles.

The roughness factor r, or f_1, causes more of an effect on the measured contact angle near 0 or 180° than at less extreme cases. For example, a 5° difference between the apparent and real angles will occur with r = 2.0 and θ_A = 80°. However, for this same 5° difference to be maintained when θ_A is 10°, r must only be 1.02. (If r = 2.0 when θ_A is 10°, θ_o is 60°.) It should also be noted that increased roughness increases θ_A for $\theta_o > 90°$, and decreases θ_A for $\theta_o < 90°$. An increasing porosity factor, however, always increases θ_A.

One of the most difficult experimental aspects of the contact angle is the existence in many systems of a hysteresis of contact angles between the liquid drop advancing over the dry surface and the liquid receding from the surface as the size of the drop is reduced (14). These two angles are denoted as θ_{AA} for the apparent advancing angle and θ_R for the receding angle. θ_{AA} is almost always larger than θ_R. Dettre and Johnson (15,16) have thoroughly studied contact angle hysteresis both theoretically and experimentally. Various theories have been proposed for hysteresis attributing the phenomena

to roughness (16), surface energy differences (17), and molecular volume of the contact angle liquid (18). The latter hypothesis suggests hysteresis will occur when the molecular volume of the drop liquid is smaller than the pore size of the substrate. Timmons and Zisman (18) have shown that if a large enough molecule is used for the contact angle measurements, hysteresis can be eliminated. Water, as a small molecule, will produce this hysteresis in most systems.

The temperature dependence of contact angles has been difficult to assess since so many other variables have not been controlled. This relation has recently been investigated, however, by Neumann, et al. (19) and Petke and Ray (20) who found, in general, the advancing contact angle has a negative coefficient of about 0.2° per °C, while the receding angle has a positive coefficient of the same general magnitude.

The effect of drop size on contact angles measured by the sessile drop method has been specifically studied by Herzberg and Marian (21) who found only a slight increase in angle in the water-polymethylmethacrylate-air system as the drop size was increased from 1 to 20 µl. In general, their results are confusing, however.

Despite the variances in contact angles, they can be used with considerable success in studying changes in a substrate. Most of the variable and experimental problems involved in determining absolute contact angles cancel out when only a relative angle is desired. Ellison and Zisman (22) and Fox and Zisman (23), for example, have found that the contact angle varies smoothly and predictably as the chemical composition of an organic substrate is altered by substitution of fluorine into the polymer. Furthermore, contact

angles have been shown to be sensitive to molecular packing of methyl groups on solid surfaces (24). Ray, et al. (25) have noticed differences between the air side and solid side of polymers cast on solids, and have attributed this difference to induced orientation of the polymer molecules brought about by the polarizing effect of the substrate. Other workers have studied the relation of surface morphology and chemical constitution to the contact angle (24,26,27). These examples indicate the sensitivity and usefulness of the relative contact angle measurement.

The contact angle has also been used for characterizing the solid surface energy or approximations to it. Zisman (23) has defined what he terms "a convenient concept" of the critical surface tension of wetting. This value, denoted as γ_c, is determined by plotting cos θ vs. γ_{lv} for a series of liquids of different surface tension and extrapolating this line to cos θ = 1 to obtain the maximum surface tension of a liquid which will spread on this solid. Interpretation of this value of γ_c as some estimate of γ_s was discouraged by Zisman who found that solids could have different γ_c values depending on the type of liquids used in the experiments. For example, a series of homologous polar liquids would result in a different γ_c than a series of nonpolar liquids. The cause of these variations is the interaction between the liquid and the solid. However, γ_c can be used for comparative correlations of surface energies. The temperature dependence of γ_c has recently been reported (20,28).

In recent years, contact angles have been related to solid surface energies by Fowkes (29), Girifalco and Good (30), Owens and Wendt (31), and Wu (32). These treatments have become increasingly sophisticated until they now specify polar, and dispersion force components of the surface energy of the solids from contact angle measurements. These calculations will be reviewed in a later section.

MONOLAYER MASKING OF SURFACE PROPERTIES

To this point, only pure noncontaminated surfaces have been considered. Attention is now turned to surfaces covered with an adsorbed layer of foreign molecules. Langmuir (33) was the first to report the masking effect of a single layer of molecules on the properties of a solid. In an address to the Faraday Society in 1919, he reported striking changes in the wetting and frictional properties of solids covered with an adsorbed layer of polar organic molecules. From his experiments, he proposed that only those atoms at the interface between the solid and the liquid controlled the wettability of the system. That is, other atoms (even of the same molecule) not in direct contact at the interface have no effect on the adsorption or wetting properties of the solid. This hypothesis became known as Langmuir's Principle of Independent Surface Action. A good example of the masking effect on high energy solids was observed by Bernett and Zisman (34), who found that fourteen metals of widely varying surface energy all exhibited the same critical surface tension of wetting (γ_c) at constant relative humidity. These observations were interpreted to mean that the adsorbed layer of water completely masked the individual surface energies of the metals. These experiments held true for samples conditioned as low as 0.6% RH. The masking of mineral properties is very readily shown in data by Bartell and Bristol (35).

If a solid is covered with a monolayer of amphipathic fatty acid molecules — as in Langmuir's experiments — the acid molecules will orient so as to produce an outer surface with the lowest free energy. That is, the low energy methyl groups will extend outward from the surface and the high energy polar end will adsorb at the solid surface. Therefore, the terminal end methyl group will dictate the apparent surface energy for the monolayer covered solid (36).

There are two characteristics of adsorbed amphipathic molecules that affect interpretation of wetting behavior. First, Langmuir (37) reported that the polar end of an adsorbed amphipathic molecule will normally stay at the solid surface unless a polar liquid is placed on the film, in which case the molecule may actually overturn and expose its polar end to the wetting liquid. This phenomenon of overturning will cause a lowering of the contact angle dependent on the number of overturned molecules (38). The amount of overturning depends on the relative attraction of the substrate and the liquid for the polar group of the adsorbed molecule. Yiannos (39) has determined that 50% of the top layer of a stearic acid multilayer will overturn when exposed to a water drop. This phenomenon explains the time dependence of contact angles of adsorbed films of fatty acids on some solids.

Rideal and Tadayon (40) have investigated the related topic of surface diffusion of molecules adsorbed onto a surface and have determined that, as expected, diffusivity is a function of temperature and substrate composition. At 25°C little surface diffusion of stearic acid on mica was noted. At the other extreme, however, the monolayer melted at 52°C.

The second characteristic of amphipathic or fatty acid films is the ability of the molecule to form chemical bonds with the substrate. This formation is a time-dependent reaction whose rate is a function of the adsorbate-adsorbent properties. Stearic acid on mica (41), copper (42), and iron (43), amine films on platinum and chromium (44), and ethyl hydrogen octadecanoate on germanium (45) have all shown evidence of chemical bonding to some degree. A majority of this evidence is based on the observation that part of an adsorbed monolayer can be desorbed easily whereas the remainder of the film can only be removed by the most vigorous action (41,44). The

difference in rate is attributed to the different energy of activation required to remove physically and chemically adsorbed molecules.

Contact angle measurements on a monolayer of amphipathic molecules must be interpreted in light of the above two characteristics. Some of the film molecules may be anchored (chemically bonded) and unable to overturn, while some fraction of the remaining molecules may overturn and alter the surface energy of the layer.

ADSORPTION OF FATTY ACIDS

The theory of adsorption at solid-vapor and solid-liquid interfaces is presented in good reviews by Adamson (46) and Gregg (47). Zettlemoyer (48) has reviewed adsorption on hydrophobic surfaces. Most adsorption studies involving fatty acid adsorbate molecules have been concerned with adsorption from solution. Unless otherwise mentioned, the following refers to adsorption from solution.

Bigelow, et al. (49) established that the most likely configuration of adsorbed fatty acid films is a closely packed array of molecules with polar groups adsorbed at the solid surface and the hydrocarbon chains projecting nearly normal to it. Bigelow and Brockway (50) observed by reflection electron diffraction techniques that the fatty acid molecules tilted slightly away from the perpendicular, 2 to 8°, depending on the acid chain length. Langmuir (51) had previously suggested the cause of the tilt is that the carboxyl groups of the molecule have a larger cross-sectional area than the hydrocarbon tail so that, as clusters form, the tails tend to tilt inward (grossly analogous to corn shocks). Obviously at a critical diameter, it would be energetically more favorable to start a new micelle rather than add to the present one.

Epstein (52), from electron microscopy work, postulated the existence of two-dimensional micelles of associated stearic acid molecules. He estimated the critical size of a stearic acid micelle to be about 100 A. Some evidence has been found for the existence of these micelles or islands in monolayers spread on water as well as solids (53).

Brockway and Jones (53) studied by electron microscopy and contact angle measurements the progress of adsorption of various fatty acids on glass. They found that adsorption did take place by growth of patches of stearic acid on the glass. The ultimate size of the patches was 5-10 times the size of Epstein's suggested micelles for stearic acid, however. The growth process varied with size of the acid and with the type of solvent. In some cases, the adsorbed molecules formed lace networks which encompassed large holes in the film, while others grew in patches.

Gaines (54) and Young (41) reported the initial adsorption of stearic acid on various solids at certain active sites on the surface. Subsequent adsorption spread out from these sites. Furthermore, upon desorption, the acid desorbed last from these areas. This is in agreement with Cook and Ries (43) who found increasing difficulty in removing all radiostearic acid from metal surfaces with boiling benzene and concluded that some acid is held more firmly than others.

Brockway and Jones (53) observed a linear relation between the degree of coverage and the contact angle. Correlations between the contact angle and the extent of monolayer coverage from depletion of the monolayer was studied by Bartell and Ruch (44) who depleted n-octadecylamine monolayers from platinum by a boiling benzene treatment and found the measured contact angle remained constant until half of the monolayer had been removed, then dropped off

gradually to zero as the remainder of the monolayer was depleted. Later work by the same authors (55) indicated that the initial work was misleading because the n-hexane used for the contact angle measurements had been filling into the depleted areas of the film and exposing the same type of surface (methyl groups) to the drop. That is, although amine molecules were being removed, the hexane molecules of the drop were taking their place and the solid properties were still masked. When 50% of the amine had been removed, the skeleton of amine film was no longer able to support the pseudo-methyl surface.

A similar nonhomogeneous variation from a complete monolayer is found as adsorption continues into multilayers. Here, the solid surface remains completely covered, but discrete patches of double layer adsorption are found (17). Ruch and Bartell (17) have shown that the contact angle of amines adsorbed on platinum increases to 90° then decreases to zero as adsorption continues. They suggest that the maximum contact angle corresponds to the complete monolayer coverage and the decrease in contact angle occurs as the double layer adsorption builds up. This second layer can overturn under the water drop and produce a more wettable surface. The first layer does not overturn due to interaction with the platinum.

Ruch and Bartell demonstrated fairly successfully that contributions from each of the types of surface on the solid can be mathematically incorporated into a revised Young's equation to calculate an expected contact angle. The mathematical model of their system involved a surface with P% adsorbed water, R% monolayer, and S% double layer. Each of these areas has a different interfacial tension expression and are summed in Equation (5) to give the conventional Young's equation form.

$$\gamma_{la}\cos\theta = P(\gamma_{wa} - \gamma_{wl}) + R(\gamma_{ma} - \gamma_{ml}) + S(\gamma_{da} - \gamma_{dl}). \qquad (5)$$

Subscripts on the surface tensions are w, water; a, air; l, contact angle liquid; m, monolayer; and d, double layer.

Vapor-phase adsorption of n-alkane vapors (C_5-C_{12}) on graphon has been studied by Clint (56). Area per molecule results indicate the alkanes lie flat on the surface in the first layer.

CELLULOSE FILMS

Cellulose films can be prepared in many ways, but whatever the process, the films have a characteristic smoothness and purity which make them far superior to paper for cellulose surface studies. Surfaces of the finest paper are still fibrous and contact angle measurements are difficult to interpret (57). Films, on the other hand, are essentially nonfibrous and present surfaces of extraordinary smoothness.

Jayme and Balser (58) reviewed previous surface studies of regenerated cellulose films and by use of electron microscopy have studied the physical appearance of viscose films produced under a variety of conditions. They have drawn the following conclusions from their studies.

- Surface character is determined by production technique.
- Hand-cast films are isotropic in surface structure.
- Machine-cast films exhibit a machine-direction striation 100-200 A in width. This ordered layer covers an amorphous layer which occasionally includes bubbles, vacuoles, and blisters.
- Slow drying under natural tension produces the smoothest film.

Stone, et al. (59) have determined by solute exclusion that the median pore diameter of a water swollen, hand-cast cellulose film is 40 A, with a maximum diameter of 165 A for never-dried films and 110 A for dried and re-swollen films. Chemically, the following must be kept in mind with regard to the surface of the cellulose film.

> "The free hydroxyl groups of the cellulose molecule are very much responsible for the chemical behavior of the cellulose, and they react, at least partly, as a polyvalent alcohol to form hydrates, addition compounds, esters, and ethers. They can be converted into aldehydic and carboxylic groups, and they react to form some compounds analogous to simple alcoholates.
>
> "Furthermore, in a solid system consisting of cellulose there are areas where the molecules are arranged in such a way that certain interatomic spacings repeat themselves in three dimensions as in a crystal lattice. In these areas the molecules are highly oriented, the density is high, and the arrangement gives rise to x-ray diffraction. In the rest of the solid the molecules are much less oriented, the density lower with an arrangement of the molecules that corresponds to an amorphous body." (61)

Crystalline regions in cellulose films are not as predominant as in cellulose fibers, but are present.

CONTACT ANGLES ON CELLULOSE FILMS

Contact angles on regenerated cellulose films have been intensively studied by Borgin (60-63). The most significant part of his work characterized the effect of changes in time, relative humidity, water content of the film, and temperature on the water-cellulose film-air contact angle.

The measured contact angle decreased continuously in all unsaturated atmospheres for 10-15 minutes until an apparent equilibrium was reached. A true equilibrium, corresponding to stable contact angles over long periods of time (1 to 24 hours) was obtained only in atmospheres near 100% RH. These data are shown in Fig. 2 and 3. From Fig. 3 it can be seen that below 40% RH the

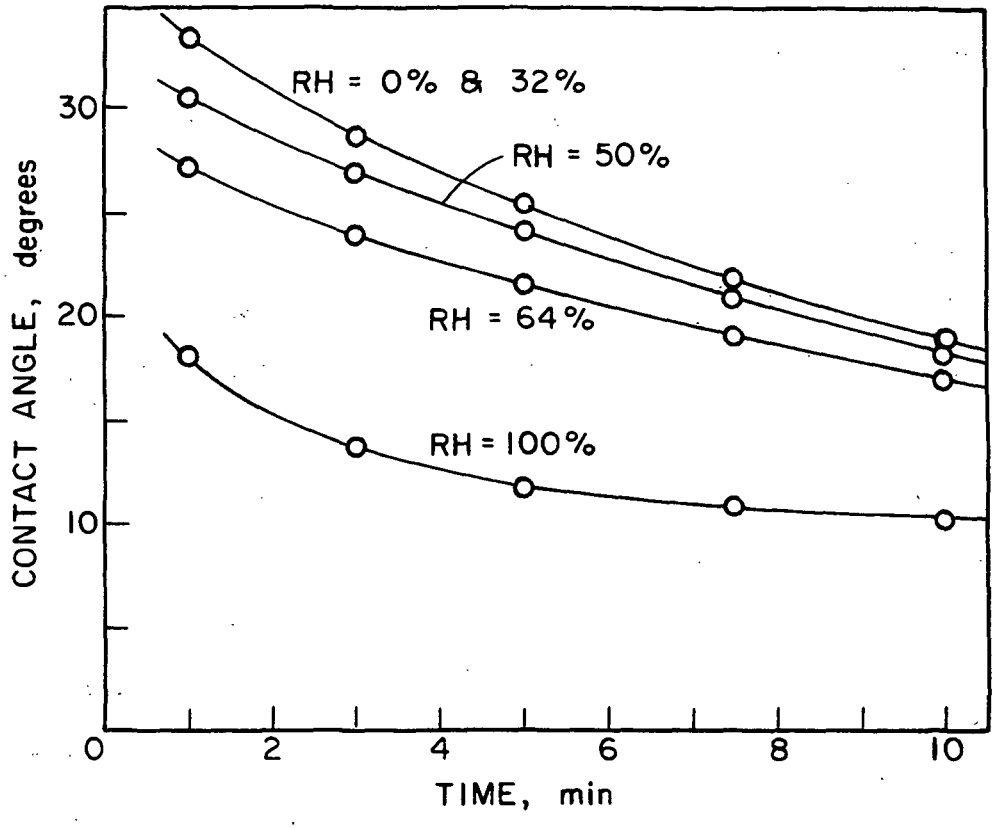

Figure 2. Time Dependence of Water Contact Angle on Cellulose Film (61)

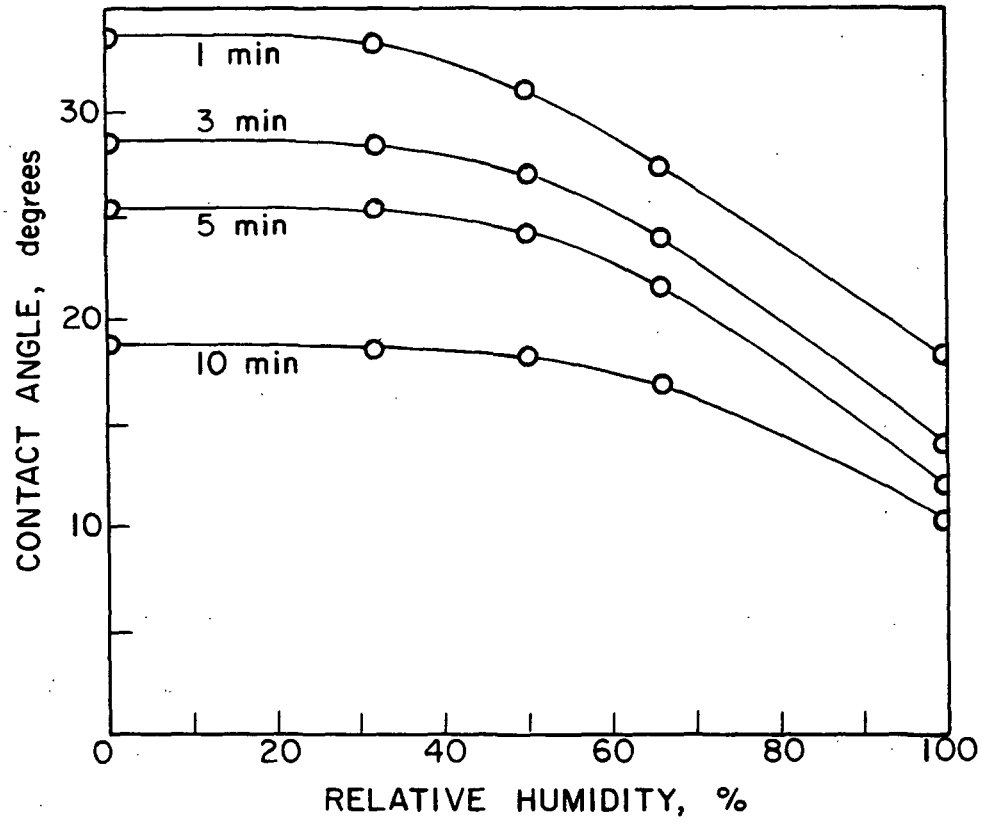

Figure 3. Relative Humidity Dependence of Water Contact Angle (61)

contact angle varies little with the relative humidity. Above this value, the angle decreases as the humidity increases. Since the films were preconditioned in equilibrium with the atmosphere, the water content of the film increased with the RH. Borgin has determined that the cellulose film will absorb up to 12% moisture (corresponding to 50% RH) before the contact angle will change significantly. He, therefore, concluded that the first 12% of water takeup is bound in a true hydrate form with the cellulose. Additional water is absorbed as a free water layer which does alter the contact angle. That the angle at 100% RH does not go to zero leads Borgin to conclude that the surface of the film is never completely covered with an adsorbed water film. Furthermore, Hermans (64) in a separate approach by x-ray diffraction studies, determined that regenerated cellulose films contain 12.1% chemically bound water. That this agrees so well with Borgin's findings adds validity to his conclusions.

Temperature dependence of the water-cellulose-air system was also studied as a function of relative humidity. The results in all cases are a decreasing angle with increasing temperature. This relationship is composed of two opposing forces, however. The increase in temperature lowers the liquid surface tension but also lowers the moisture content of the film.

Borgin has also studied organic liquids on cellulose and the effect of chemical modification of the surface. Wetting characteristics of cellulose derivatives have been studied by Bartell and Ray (65,66). Luner and Sandell (67) have studied the wetting character of cellulose and hemicellulose films hand-cast in various ways. The wetting properties of their films are compared in terms of Zisman's critical surface tension γ_c. Hand-cast regenerated cellulose films are compared with hemicellulose films, and differences found

in glass and air sides of cast film, casting methods, and cellulose sources are reported.

RELATION OF CONTACT ANGLE TO INTERFACIAL TENSION

Fowkes (29) was the first to mathematically combine Young's equation and an interfacial tension term to obtain a method for determination of the dispersion force contribution of the surface energy of a solid from contact angle data. Fowkes' derivation is as follows: Consider an interface between two dissimilar nonpolar substances whose intermolecular forces are dispersion forces only. As noted previously, a surface tension γ is present in all surfaces due to the unbalanced forces on the surface molecules. When two surfaces which independently exhibit surface tensions, γ_1 and γ_2, are placed in intimate contact, an interfacial tension, γ_{12}, arises. This force occurs in exactly the same manner as the free surface γ, that is, from unbalanced forces on the surface or interfacial molecules. Here, the unbalance results since the forces exerted on the surface 1 molecules by substance 2 are not equal to those exerted on surface 1 by substance 1. Fowkes, following Girifalco and Good (30), used a geometric mean term $\sqrt{\gamma_1^d \gamma_2^d}$ to approximate the magnitude of the effect on the individual surface tensions by the presence of the other substance. The surface tension of surface 1 is, therefore, $\gamma_1 - \sqrt{\gamma_1^d \gamma_2^d}$ and likewise for surface 2, $\gamma_2 - \sqrt{\gamma_1^d \gamma_2^d}$. The total interfacial tension is the sum of the two contributions so that $\gamma_{12} = \gamma_1 + \gamma_2 - 2\sqrt{\gamma_1^d \gamma_2^d}$. Fowkes justifies the use of the geometric mean historically, empirically, and theoretically, and recognizes that strictly its use is limited to cases where the molecules of the two substances or their volume elements (e.g., CH_2 groups in hydrocarbons) are of the same size. Differences in ionization potential or polarizability of the two species also affect the results. Despite these drawbacks, Fowkes used the

geometric mean relation because of its empirically good agreement with a variety of interfacial tensions in liquid-liquid systems he studied.

Young's equation for the same system in terms of a solid (Phase 2) and liquid (Phase 1) is shown in Equation (6).

$$\gamma_1 \cos \theta = \gamma_2 - \gamma_{12}. \tag{6}$$

Substituting the above equation for γ_{12} into Young's equation results in Equation (7).

$$\gamma_1 \cos \theta = -\gamma_1 + 2\sqrt{\gamma_1^d \gamma_2^d}\ . \tag{7}$$

Rearranging and substituting conventional subscripts for the solid, and liquid phases gives Equation (8),

$$\cos \theta = -1 + 2\sqrt{\gamma_s^d}\left(\frac{\sqrt{\gamma_1^d}}{\gamma_1}\right) \tag{8}$$

where the superscript $\underline{d}$ recognizes that these surface tensions represent the dispersion force contributions to the surface tension of the solid. Therefore, a plot of cos θ vs. $\sqrt{\gamma_{\underline{1}}^{\underline{d}}}/\gamma_{\underline{1}}$ gives a straight line with the origin at cos θ = -1 and slope of $2\sqrt{\gamma_{\underline{s}}^{\underline{d}}}$. Only one measurement is theoretically needed to obtain $\gamma_{\underline{s}}^{\underline{d}}$ in this way. This value is the dispersion force contribution to the total $\gamma_{\underline{s}}$, but will equal $\gamma_{\underline{s}}$ in nonpolar systems.

Owens and Wendt (31) extend Fowkes relations by adding a term for nondispersion forces across an interface. This term includes hydrogen bonding, dipole-dipole and induced dipole attractive terms. Mathematically, they assume $\gamma_{\underline{s}} = \gamma_{\underline{s}}^{\underline{d}} + \gamma_{\underline{s}}^{\underline{h}}$ where $\underline{d}$ and $\underline{h}$ are the dispersion and nondispersion (hydrogen bonding) components, respectively. Equation (9) applies in this system.

$$\gamma_{sl} = \gamma_{sv} + \gamma_{lv} - 2\sqrt{\gamma_s^d \gamma_l^d} - 2\sqrt{\gamma_s^h \gamma_l^h} \quad . \tag{9}$$

Once again the geometric mean relation for the hydrogen bonding interaction is assumed. In operating form, Owens and Wendt use Equation (10).

$$\cos\theta = -1 + 2\sqrt{\gamma_s^d}\left(\frac{\sqrt{\gamma_l^d}}{\gamma_l}\right) + 2\sqrt{\gamma_s^h}\left(\frac{\sqrt{\gamma_l^h}}{\gamma_l}\right). \tag{10}$$

Two measurements with two different liquids and knowledge of $\gamma_{\underline{l}}^{\underline{d}}$ and $\gamma_{\underline{l}}^{\underline{h}}$ from literature or related experiments are needed to calculate the dispersion and nondispersion components to $\gamma_{\underline{s}}$. They point out also that when nonpolar liquids are used $\gamma_{\underline{s}}^{\underline{d}} = \gamma_{\underline{c}}$, Zisman's critical surface tension of wetting. When either liquid is polar, $\gamma_{\underline{c}}$ is less than $\gamma_{\underline{s}}$.

Wu (32) has suggested an improvement on the geometric mean relationship, indicating the "reciprocal mean" empirically gives better results on polar polymers. His basic relationship is presented in Equation (11),

$$\gamma_{12} = \gamma_1 + \gamma_2 - \frac{4\gamma_1^d \gamma_2^d}{\gamma_1^d + \gamma_2^d} - \frac{4\gamma_1^p \gamma_2^p}{\gamma_1^p + \gamma_2^p} \quad , \tag{11}$$

where superscript $\underline{p}$ is the polar (nondispersion) components. Wu uses a set of two simultaneous equations for determination of the components of $\gamma_{\underline{s}}$. The equations require two contact angle measurements be made with different liquids. Use of the reciprocal mean is shown to give improvements on the Owens and Wendt values for molten polar polymer systems. Justification for use of the reciprocal mean is strictly empirical.

Dann (68,69) has compared Zisman's $\gamma_{\underline{c}}$ to Fowkes $\gamma_{\underline{s}}^{\underline{d}}$ and considered deviations of the two as the polar component of the liquid and/or solid increases.

PRESENTATION OF THE PROBLEM

In papermaking, water repellency is imparted to the paper sheet by adsorbing low energy molecules onto the cellulose fibers. The degree of sizing depends on the amount of adsorption. The amount of sizing required to make a cellulose surface water repellent has not been determined. However, a monolayer coverage on all surfaces would theoretically make cellulose nonwettable. Swanson (70) has reported some intriguing data on the problem. Working with radioactive stearic acid as a model sizing agent, Swanson and Cordingly (71) found a respectable sizing time developed as stearic acid was adsorbed from the vapor phase onto paper sheets. However, when the paper was extracted in boiling benzene to remove the stearic acid and dried, the water repellency was not reduced but increased to infinity (70). The sheets were totally water repellent. Furthermore, radiochemical analysis of these sheets indicated that the equivalent of 6% of a monolayer remained on the nonbonded surface area of the fibers. That this small amount of surface coverage could completely mask the natural hydrophilic nature of paper was astonishing. Yet when these sheets were dipped in dilute sodium hydroxide, neutralized, and again washed in boiling benzene and dried, they were now totally absorbent.

These facts fit the hypothesis that physically adsorbed stearic acid is removed by the benzene treatment, leaving 6% of a monolayer which is chemically bonded to the cellulose. This sufficient and possibly excessive amount of stearic acid completely changes the surface energy of the paper. Upon treatment with sodium hydroxide, these stearate bonds are saponified and the stearic acid is subsequently removed by benzene extraction.

STATEMENT OF THE PROBLEM

Determine how water repellency develops when a cellulose surface is exposed to a vapor-phase sizing agent. Determine how the extent of monolayer coverage and the degree of chemical bonding affect the ability of the film to repel aqueous liquids.

APPROACH TO THE PROBLEM

There are two experimental measurements necessary to study the problem as stated: a method to measure repellency and a method to measure degree of coverage. For both measurements, current technology limits the available choices.

Repellency is best measured by contact angles. For optimum results, a smooth surface, such as a cellulose film is required. Determination of the degree of monolayer coverage could only be accomplished by radioactive methods which can be sensitive to relatively small numbers of molecules.

The basic experimental approach is thereby to adsorb a radioactive sizing agent onto the surface of a smooth cellulose film and to determine the response of the water contact angle. This response is dependent to some degree on the type of sizing molecule. For this basic study, however, the very simple model, stearic acid, is used. This linear molecule has the desirable amphipathic properties of a sizing agent: the low-energy hydrophobic tail to repel water, and the high-energy, reactive carboxyl group to interact with the cellulose and thereby anchor the molecule to the surface.

The choice of adsorption conditions must be selected for the type of data desired. The scope of this study does not include the kinetics of

adsorption. Therefore, a very simple "infinite reservoir" system was chosen. The variables in the adsorption process are limited to time and temperature at saturated conditions.

By measuring contact angles with two liquids, the Owens-Wendt Surface Energy Parameter can be followed throughout the experiments and considered in interpretation of the data.

FUNDAMENTAL CONSIDERATIONS

The approach to the problem poses four areas of concern on a fundamental level: the interpretation of the initial contact angle, the character of the adsorbed stearic acid, the validity of the Owens-Wendt calculations, and an evaluation of the roughness factor.

INTERPRETATION OF THE INITIAL CONTACT ANGLE

The contact angle formed by a small drop of liquid on a solid surface is undoubtedly a direct resultant of forces exerted on the liquid drop at any given time. A changing contact angle is therefore indicative of changes in one or more of the forces which produce this angle. A true equilibrium contact angle occurs only when all forces are in balance and remain constant. In systems where the liquid and solid do not interact, the equilibrium contact angle may occur quite rapidly; but in interacting systems such as the cellulose-water system, equilibrium will not occur until the cellulose-water reaction is complete. It is this problem which creates the special difficulties of water-cellulose contact angle measurement.

Cellulose has a great affinity for water. Dry cellulose will adsorb moisture very rapidly and the absorption will continue until the cellulose has absorbed more than its own weight of water. At this point the cellulose-water equilibrium has been reached.

As absorption and adsorption progress on cellulose toward equilibrium, the character of the cellulose surface is changed by the adsorption of water molecules. As the water concentration increases at the surface, more and more of the surface becomes waterlike in its behavior toward water drops.

If the surface were to become totally masked by water molecules, the contact angle would approach zero degrees (i.e., the angle of water on water). However, at equilibrium near 100% RH, the water-cellulose contact angle is 10.8°, whereas dry cellulose has an initial angle of 34° (61).

For this reason, it is important to specify the moisture content or relative humidity at which cellulose film is conditioned before measuring the contact angle. However, perhaps more important, is the time elapsed before the angle is measured (after the drop is placed). Immediately upon contact of water with the cellulose film (if not before), the water-cellulose reactions begin and the surface character begins to change. In addition, water vapor near the perimeter of the drop probably migrates to the adjacent film and adsorbs. These mechanisms alter the character of the surface significantly and rapidly.

For these reasons, if it is desired to measure the contact angle of water on cellulose conditioned at less than 100% RH, the measurement must immediately follow the placement of the drop. This may appear to be in opposition to the equilibrium of forces concept upon which the very definition of the contact angle rests, but it is proposed that the angle is indeed in a quasi-equilibrium with the forces that exist at any instantaneous time. However, due to the changes in these forces as the water-cellulose interaction proceeds, the angle must respond accordingly.

If this view is accepted, a limited case can be made for back-extrapolation to zero time of contact angle *vs.* time measurements. While this technique is not used in this work, it has been used by others (72).

In the more complex case of a heterogeneous surface where a third component is adsorbed onto the cellulose, the same principles apply. The presence of water on the surface will alter the contact angle with time. Overturning of adsorbed molecules, swelling of cellulose by either water or water vapor penetrating the adsorbed film, and adsorption of water onto exposed cellulose surfaces will all lower the contact angle with time. Therefore, an immediate contact angle will most closely approach the conditions of interest.

CHARACTER OF THE ADSORBED ACID

In a classical Langmuir-Blodgett deposition of stearic acid onto a solid surface by withdrawal from liquid, the molecules emerge closely packed, oriented perpendicularly to the surface, covering 20.1 A^2 of surface per molecule (54). It is an organized reproducible system upon which much work has been done. Vapor-phase adsorption is another matter.

In classical vapor-phase adsorption onto solids, the molecules collide with the surface where they remain for some average period of time and then desorb back into the vapor phase. In a more complex case, the molecules may chemically bond in a relatively irreversible reaction with the solid, and thereby remain on the surface. As the molecular population on the surface increases, interactions between adsorbed molecules become increasingly important, adding to the complexity. This is especially true for long-chain molecules.

The adsorption of stearic acid onto cellulose includes these possibilities and more. In the vapor phase at low pressures, the acid will exist primarily in monomer form (Appendix I). However, once adsorbed to the film

surface, the much higher concentrations will allow almost complete association of the acid into dimers. The dimer will react differently than the monomer as a sizing agent. It cannot chemically bond to the cellulose without first dissociating. It will also have a lower vapor pressure and mobility than the monomer form.

Another consideration of the adsorbed layer is the penetration of acid molecules into the porous film or adsorption into surface irregularities. In either case, the acid will fail to participate at the water-cellulose interface but will be detected as present on the cellulose surface by radioactive counting procedures. Both occurrences will be minimized by use of cellulose film.

The final, and perhaps overwhelming, consideration is the orientation of the molecules. Monomers may adsorb from the vapor with polar end up or down, and both monomers and dimers may recline on the surface or be perpendicular to it (or any position in between in an adsorbed layer). Molecules may adsorb on top of one another or intermingle, oriented neither like a forest nor like spaghetti. Furthermore, they may adsorb in patches or be well dispersed on the cellulose surface.

The primary point is that a monolayer of stearic acid adsorbed from the vapor phase is totally unlike the classical Langmuir-Blodgett monolayer. Concepts developed from such monolayers need not necessarily apply in the vapor deposited case.

SURFACE ENERGY ESTIMATION

Estimates of the surface energy by the methods of both Owens and Wendt, and Wu have recently been criticized by Panzer (73). It has been shown that the use of various liquid pairs gives totally different results on the same surface. In addition, the calculations are based on contact angle measurements of two liquids, and surface roughness will affect the angle made by each liquid to a different extent (if the real angles are different). Therefore, without knowledge of the true contact angles, an erroneous surface energy would result.

However, for a substrate of constant roughness, and for the same set of liquids, the Owens-Wendt equations should give a useful surface energy parameter.

Of more fundamental concern is the effect of the presence of a third species, stearic acid, at the liquid-solid interface. The Owens-Wendt derivation applies strictly to a two-substance system, and the effect of the third component is not clear.

For these reasons, the surface energy value calculated is considered to be an empirical parameter only. To emphasize this, no units are associated with the values obtained from the Owens-Wendt calculations.

EVALUATION OF ROUGHNESS FACTOR

Knowledge of the roughness factor (real to geometric surface area) would be useful for discussion of two areas: 1) the evaluation of a real contact angle (θ_o) as opposed to an apparent (measured) contact angle (θ_A)

on cellulose, and 2) the conversion of geometric percent monolayer coverage to a real percent monolayer coverage.

The use of Wenzel's relationship to determine a real contact angle θ_o for a surface is normally avoided in the literature. A pertinent example of why this is so may possibly be seen from a few calculations of water-cellulose contact angles. For example, if θ_A is 34° as reported by Borgin (61) and the roughness factor varied from 2 to 4 to 6, the corresponding θ_o values are 65, 78, and 82°, respectively. If θ_A then increased to 60°, the corresponding θ_o values are 75, 83, and 85°. These are extremely small differences in θ_o values compared to the 26° change in θ_A.

From another viewpoint, if θ_o was 82° and the roughness factor varied as before, the apparent contact angle would vary from 75° for r = 2 to 34° for r = 6. It is not likely that the real contact angle of cellulose film of perfect smoothness is as high as 82°; therefore, the relatively good agreement of reported measured contact angles near 34° would require that all investigators have essentially the identical roughness factor on their films. This is definitely not the case. In view of these calculations it is understandable why Wenzel's correction factor is not used.

The second area where a roughness factor might be employed is in determining true monolayer coverage from a known molecular concentration on a geometric area. The value of an accurate knowledge of the roughness factor is greatly reduced by the existence of two physical characteristics of the system which add great uncertainty to the true monolayer calculations. The first complication is the orientation of the molecules. If a stearic acid molecule tilts away from the perpendicular and reclines on the surface, the projected area increases by a factor of 5. This projected area directly

affects the monolayer coverage. The second characteristic of the system which will greatly hinder the determination of a true monolayer coverage is the fact that the adsorbed molecules will not be uniformly distributed on the surface. The stearic acid molecules will tend to have some degree of preference for the rough areas of the film. This means that the molecular concentration measured per unit area is only an average value which includes higher concentrations in the surface deformities. The existence of these two variables makes the determination of an exact roughness factor unnecessary.

However, an estimate of the roughness factor is worthwhile and can be used in the interpretation of the results. The factors for several surfaces are listed in Table I (74).

TABLE I

ROUGHNESS FACTORS OF SEVERAL SURFACES

Surface	r
Electropolished steel	1.12
Glass beads (once cleaned)	1.6
Nickel foil	2.15
Silver foil	5.0

The cellulose films have been formed by casting against glass and drying against Lucite. The Campbell forces evolved during drying will cause the roughness of the relatively conformable cellulose film to approach that of the Lucite surface. Electron microscopic results indicate similar roughness of Lucite and glass surfaces, and only a slightly rougher cellulose surface. The glass surface value would be the lower limit on the roughness

factor. An upper limit of 8.0, or five times the glass roughness is arbitrarily assumed. The roughness factor for cellulose film is therefore taken to lie between 1.6 and 8.0.

EXPERIMENTAL MATERIALS AND EQUIPMENT

CHEMICALS

Commercially available reagent-grade chemicals were used throughout this work. Chemicals of special interest or treatment are noted below.

WATER

All water used in the experimental process was deionized and triply distilled. The first stage, separate from the last two, was a Corning Model AG-3 still. This was followed by a permanganate distillation and a pure distillation into clean containers. Eight gallons of this water could be produced per day.

STEARIC ACID

Two millicuries of stearic — [1 - ^{14}C] — acid were purchased from Dhom Products, Ltd. As received, each millicurie was dissolved in one milliliter of benzene at an activity of 58 millicuries per millimole. The composition of this radioactive stearic acid was 99.9% stearic and 0.1% palmitic by gas chromatography (Appendix II).

Nonradioactive crystalline stearic acid purchased by Neuman (75) from the Fluka Company was used for dilution. GLC testing indicated 99.64% stearic and 0.28% palmitic (Appendix II).

METHYLENE IODIDE

Eastman diiodomethane was tested for purity by measuring the surface tension by the ring method. The surface tension was found to be 50.70 vs. 50.76 literature value.

SATURATED METHYLENE IODIDE

This liquid is methylene iodide mixed thoroughly with excess crystalline stearic acid and filtered. (See Procedure section.)

ADSORPTION APPARATUS

Vapor-phase adsorption of stearic acid onto cellulose film was performed in adsorption trays of simple design. The tray was constructed of two 4-inch × 8-inch stainless steel plates. The bottom 1/4-inch thick plate was machined to 1/8-inch thickness in the center 3-inch × 7-inch area. Stearic acid was placed in this bottom tray. The top of the tray was 1/8-inch thick with ten threaded holes to hold a 1.5-inch × 5-inch aluminum bracket and teflon gasket centered on the stainless. This aluminum-teflon assembly clamped cellulose film flat against the top stainless plate and exposed 1 inch × 4 inches of the film to the acid vapor. This apparatus is shown in Fig. 4. Eighteen wing nuts clamped the two pieces together with a teflon seal. In this way, the film was supported 1/8-inch above the stearic acid bed.

Identical thickness of the top and bottom stainless was necessary to obtain an even distribution of acid on the cellulose film after cooling. Uneven cooling in the tray caused acid to either desorb from or condense onto the film.

RADIOACTIVITY COUNTER

A Nuclear Chicago Model 182 scaler connected to a Model D-47 gas flow detector was operated in the β-proportional mode with "Micromil" window in place. Flow gas of 90% helium and 10% argon passed through the chamber at

50 ml/min. Background counts of 50-60 cpm were standard and uniform. An operating potential of 2050 volts was determined (Appendix III).

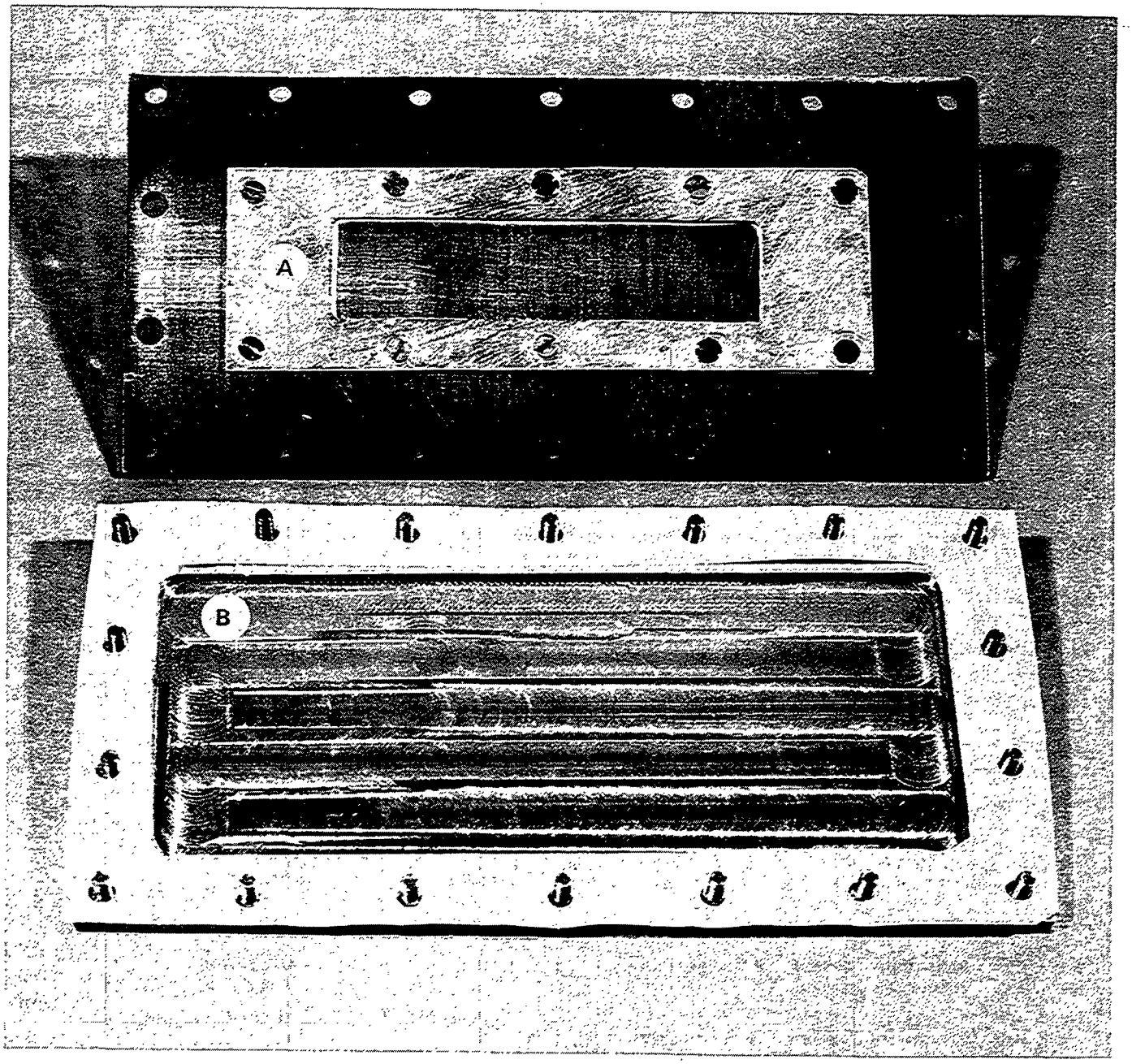

Figure 4. Stainless Steel Adsorption Apparatus. A. Tray Top with Centered Clamp Holding Film; B. Bottom of Tray with Stearic Acid Bed

Efficiency of counting for stearic acid on cellulose film was 17% based on quantitative transfer techniques (Appendix VIII).

CONTACT ANGLE EQUIPMENT

The basic contact angle goniometer used by Brown (76) was modified by the addition of a variable relative humidity gas purge system and a rapid automatic advancing 35-mm camera system. The complete apparatus is shown in Fig. 5.

A stream of prepurified nitrogen is passed through three gas washing bottles filled with distilled water to provide a "wet" stream of nitrogen (B). A dry stream from the second prepurified nitrogen tank (C) is mixed with the wet stream as the nitrogen enters the contact angle chamber (G). A calibrated electric hygrometer probe in the chamber indicates the relative humidity on the readout scale (A). A light and copper sulfate filter system (D) provide illumination for the 35-mm rapid advancing Minolta SR-M camera (H). This camera is capable of taking from three frames per second to one per minute automatically and is attached to the petrographic microscope with a 5X magnifying eyepiece. The lab jack (E) lowers an ultramicropipet (F) smoothly and uniformly to place the water drops. Three Gilmont ultramicropipets are available, each filled with a different contact angle liquid, and each easily interchangeable in the lab jack holder.

In Fig. 6, a more detailed view of the chamber, the gas streams enter at A and exit through an opening in the stopper at D. The hygrometer probe, a sample positioning rod, and thermometer all extend into the chamber through this stopper. The ultramicropipet (B) passes through an opening in the top of the chamber. Gas is prevented from exiting through this aperture by a

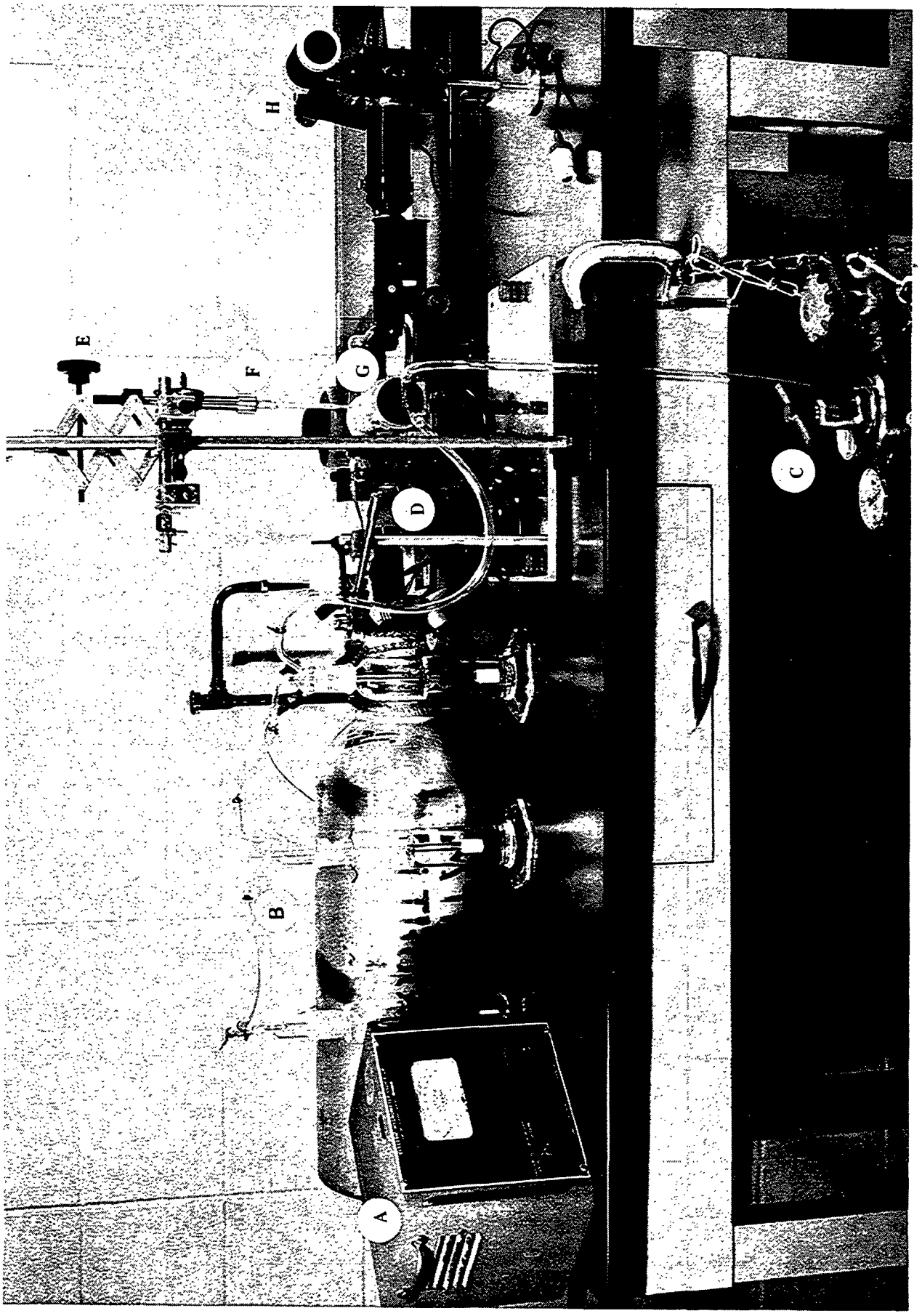

Figure 5. Apparatus for Measuring Contact Angles

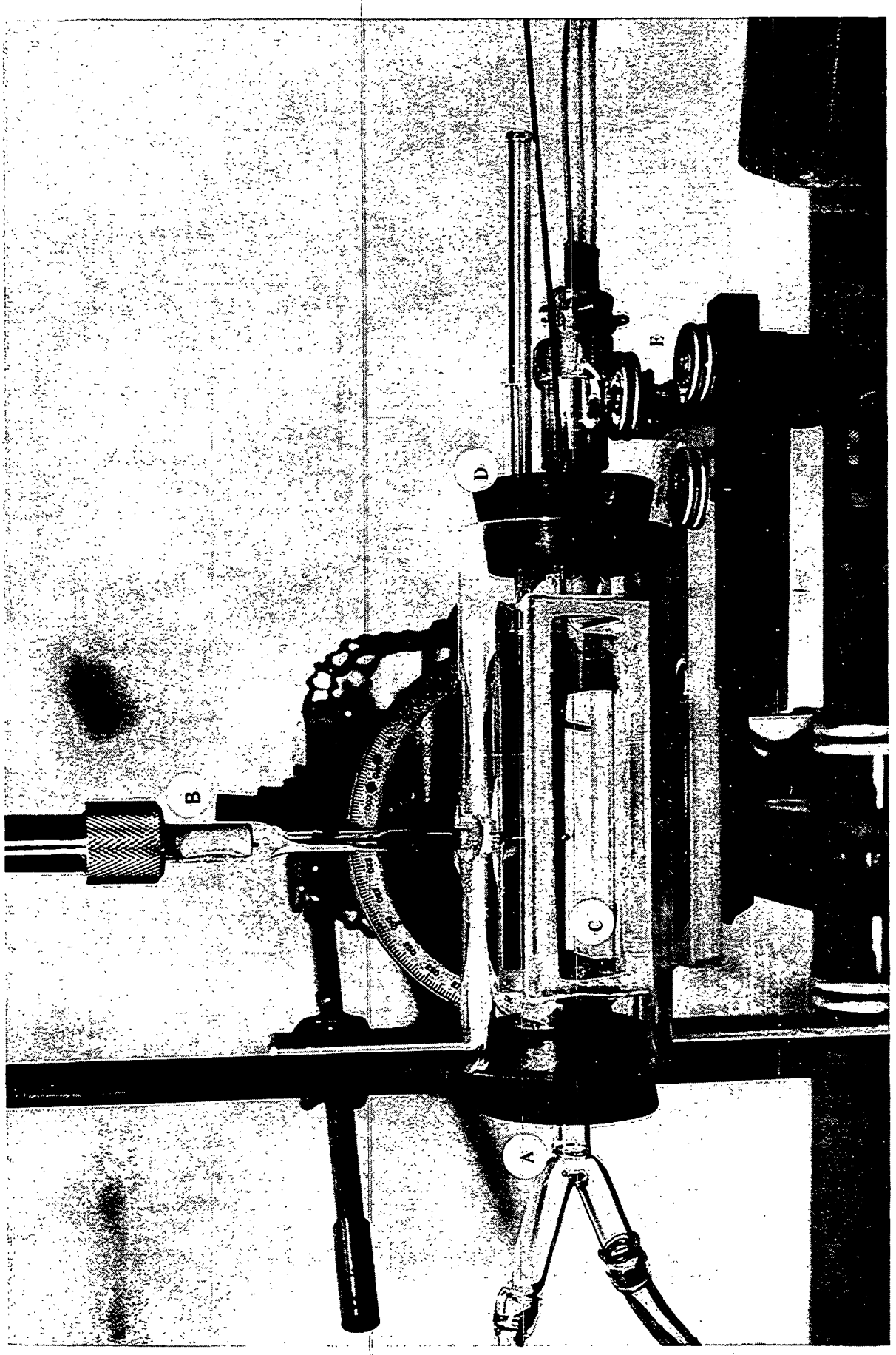

Figure 6. Close-up of Contact Angle Chamber

thin rubber seal not shown. Samples mounted on flat microscope slides are placed on the surface at C. This entire chamber can be moved in three dimensions by the controls at E.

The relative humidity sensing equipment is an Aminco Electric Hygrometer with remote probe calibrated over known solutions of sulfuric acid. A scale value of 86 corresponded to 40% relative humidity.

The entire contact angle apparatus was operated in a controlled temperature, relative humidity room (72°F, 50% RH).

DEVELOPMENT OF EXPERIMENTAL PROCEDURES

PREPARATION OF CELLULOSE XANTHATE

Cellulose films were hand-cast in the laboratory from cellulose xanthate. The viscose was prepared following the methods of Browning (77) and the films cast and regenerated following the two bath procedure of Luner and Sandell (67).

The film preparation process involved a 48-hour alcohol-benzene (1:2 by volume) extraction of Hercules cotton linters in a Soxhlet apparatus followed by complete washing in distilled water. The fibers were pressed dry and sufficient caustic solution added at room temperature to mercerize the cotton in 18% NaOH at 5% consistency for 90 minutes. The mercerized fibers were filtered and pressed to a pressed weight ratio (total weight after pressing/fiber o.d. weight) of 3.0-3.5. The pad was picked apart and stored 72 hours in a loosely stoppered container for aging.

Xanthation of the aged fibers was accomplished by adding an amount of carbon disulfide equal to one half of the ovendry fiber weight to the cotton in a sealed jar and mixing continuously for five hours. At this point, the fibers are a dark crumbly orange and have a visibly compacted volume. Sufficient caustic was added to make a final mixture of 7.0% cellulose, 6.0% caustic, 3.0-3.5% carbon disulfide, and about 84% water. This solution is rotated for a few hours to bring the xanthated fibers into solution, then ripened for 72 hours at room temperature. Midway in the ripening process, the solution was centrifuged at approximately 25,000 g for 30 minutes on an ultracentrifuge (Sorvaal Model RC-1) to remove fine undissolved fiber and dirt. The viscose is returned to a clean container for the remainder of the ripening period.

Laboratory casting of the films followed 72 hours of ripening at 72°F. No viscosity measurements were made. A proper amount of the viscose solution is poured across the top of a clean, dry 3-inch × 8-inch glass plate. A 0.012-inch clearance Bird Bar is drawn down the plate spreading the film smoothly and evenly across the glass. The upper left corner of the spread film is wiped off to identify the glass side of the film as the smooth side. The glass plate is transferred to a 15% ammonium sulfate solution for about 5 minutes or until the film coagulates and decolorizes, losing the orange color of the viscose. The film is then transferred by plastic tipped forceps to a 12% sulfuric acid bath for regeneration of the pure cellulose. Once the film, which has turned white upon contact with the acid, has again cleared, it is washed in a hot, 1% Na_2S-0.25% NaOH bath at 65°C for 10-15 minutes. A final soak in 0.25% NaOH for three hours ends the chemical treatment of the films. A thorough washing in distilled water over a period of days completes the preparation of the cellulose films which are stored under refrigeration in triply distilled water until used. Elemental analysis results for the cellulose films are presented in Appendix IV.

DRYING OF THE CELLULOSE FILM

Drying of cellulose film for reliable contact angle work requires special techniques to obtain a surface of optimum smoothness and cleanliness.

The smoothest surface was obtained by drying the side of the cellulose film formed against glass against a clean Lucite (polymethylmethacrylate) sheet. The effect of drying technique on roughness is shown by the series of three electron micrographs (11,000X) in Fig. 7. It is readily apparent from films dried (A) air-formed side against air, (B) glass-formed side against air,

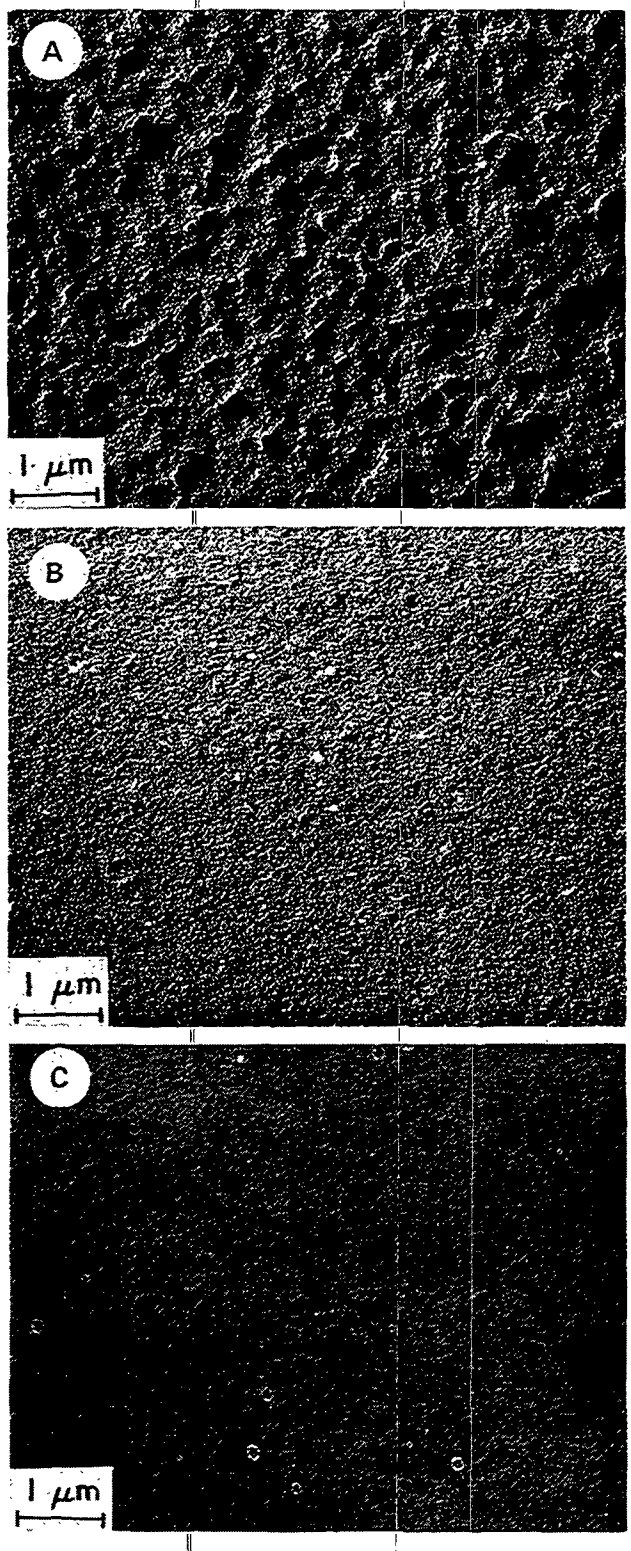

Figure 7. Electron Micrographs of Cellulose Film Surfaces.
A. Film Formed Against Air, Dried Against Air;
B. Film Formed Against Glass, Dried Against Air;
C. Film Formed Against Glass, Dried Against Lucite;
11,000X

and (C) glass-formed side against Lucite, that final roughness of the dry film is highly dependent on film drying procedure. The smoother the surface, the more accurate the measured contact angle and the smaller the amount of adsorbed stearic acid not participating at the water-cellulose interface.

Contamination of the films during drying was found to be a serious problem even with the most exacting handling procedures. Contamination by low molecular weight spreadable (LMWS) material was detected by passing a piece of the dry contaminated film perpendicularly through a clean air-water interface sprinkled with ignited talc. As the film touched the water surface, the LMWS material spread on the water and pushed away the talc in an easily observed manner. It was not possible to eliminate this contamination under any circumstances involving drying in air. When the films were dried under prepurified nitrogen, however, the LMWS material on the film was greatly reduced. Apparently, dust particles in the air contacted the wet film surface during drying and transferred some oily material to the film. This material would dry on the film surface and when a water drop was placed on the film for contact angle measurements, the LMWS material would spread on the water-air interface, lowering the surface tension and decreasing the contact angle.

The following drying procedure was developed to obtain a clean, smooth surface after drying. A 3-inch × 8-inch Lucite sheet was cleaned with Alconox and then with ethanol, rinsed in triply distilled water, dried briefly at 105°C to evaporate any residual ethanol, and rinsed again in water. Then, under water, a piece of cellulose film was positioned smooth side down on the Lucite plate, and both removed from the water. A 3-inch × 8-inch Lucite frame with the center 1.5 inch × 4.5 inch cut out was placed over the film to hold it in place. Four large Bulldog clips were used to hold the Lucite plates together.

This sandwich was then slowly lowered into a Lucite cylinder (7-inch diameter × 14-inch high) filled with triply distilled water. Any LMWS material which may have been on the surface of the film or the Lucite assembly would transfer to the water surface and be swept away by overflowing water from the cylinder. The top was then bolted onto the cylinder and sealed tight against an "O" ring. Prepurified nitrogen was blown into the cylinder through a port in the top and ejected through the bottom. The film was allowed to dry in the chamber for 12 hours with an automatic purging device flowing dry nitrogen through the chamber five out of every thirty minutes. After twelve hours, the film was transferred to a 30% relative humidity desiccator for 24 hours to come to a standard equilibrium prior to use. Aluminum pellets previously heated in the muffle furnace to destroy organics were placed in the desiccator to adsorb organic contaminants (78). Immediately before use, the cellulose film was removed from the Lucite by simply cutting around the edges of the film with a razor blade. The cellulose would snap off the Lucite and could be inverted to expose the clean, smooth surface.

ADSORPTION TECHNIQUE

The bottom portion of the stainless steel tray was filled with 10 ml of benzene containing approximately 200 monolayers of stearic acid in an 11.3 to 1.0 ratio of nonlabelled to labelled molecules. (At this ratio, 10,000 cpm is equivalent to 100% POML.) The benzene was evaporated slowly until almost dry, when a piece of lens paper was used to evenly distribute the acid/benzene. The tray bottom was then placed in the oven for 5 minutes at 105°C to remove the last traces of benzene. This bed of stearic acid acts as an infinite reservoir in attaining equilibrium within the closed chamber.

A piece of cellulose film is clamped to the top of the tray with the aluminum-teflon bracket. The top is bolted on and the sealed tray placed in the oven.

Adsorption time refers to the elapsed time the sample is in the oven. Neither the time to come to temperature nor the cooling time once removed from the oven are accounted for in this value. At 105°C, cooling time is approximately 45 minutes.

During the period in the oven, the system comes to equilibrium — the air becoming saturated with stearic acid vapor. At any temperature, the system is saturated due to the infinite reservoir.

When the tray is removed from the oven, the walls begin to cool and the stearic acid in the vapor begins to condense on the coolest surface. The amount of acid in the vapor at 105°C is approximately 0.5% of a POML. If the tray dimensions are such that the tray top cools faster than the rest of the stainless, stearic acid apparently condenses on the film; if the top is warmer than the remainder of the tray, it appears that the physically adsorbed stearic acid desorbs from the film. Uniform cooling of the entire tray and equal wall thicknesses are therefore necessary to prevent nonuniform or misleading adsorption on the film. Adsorption of acid onto the back of the film did not occur with the teflon gasket in place.

CONTACT ANGLE MEASUREMENT

The nitrogen streams of the contact angle equipment are adjusted to give a 40% RH atomosphere in the chamber and an ultramicropipet is placed in the holder. A film sample, mounted on a microscope slide, is removed from the

40% RH desiccator and placed in the chamber by briefly removing the end stopper. Since the room is at 50% RH, there is little effect on the chamber conditions. The pipet tip is brought into close proximity of the film and aligned so as to place the drop very near the front edge of the slide. This is necessary to keep the drop and film in the same focal plane to obtain a sharp image on the photograph. Liquid is then forced from the pipet to form a hemisphere of liquid clinging to the pipet tip. (This entire operation is observed through the camera lens.) Very slowly, the lab jack is lowered until the drop contacts the film and begins to spread. The pipet is then quickly raised until the liquid breaks away from the glass tip to form the drop. Care must be taken to insure that the perimeter of the formed drop is along film not wetted by the placement operation — that is, an advancing contact angle must be measured.

Since the drop is immediately in focus, a picture may be taken within one second. Three methods of measuring the initial contact angles were tested. Contact angles were calculated from 1) the average of the first three frames taken over one second, 2) the first frame only, and 3) data of the first three frames back-extrapolated to zero time. As would be expected, the water-cellulose contact angle thus determined did increase in the order shown, but the back-extrapolated values were less than 0.5 degree higher than the averaging method and less than 0.2 degree higher than the first frame method. The first frame method was, therefore, chosen for its simplicity.

Three drops per slide are taken over approximately thirty seconds. Thirty-six exposure rolls of Kodak High Contrast Film are used in the camera. This film is developed by standard photographic procedures (Appendix VI).

Conversion of the photographic image to contact angles was accomplished using the geometric method of Guide (79) adapted for computer solution. Guide shows that for small drops of spherical surface, the contact angle, θ, is related to two dimensions of the drop by Equation (12).

$$\text{Tan } \theta/2 = 2H/B, \qquad (12)$$

where H is the height of the drop and B is the base measurement. For computer solution, five-digit coordinates of the three points shown in Fig. 8 are automatically determined and punched on computer cards by coordinate comparator equipment. These cards are used with specially written computer programs to calculate contact angles, statistical data, and surface energy values by the Owens-Wendt equations (Appendix VII).

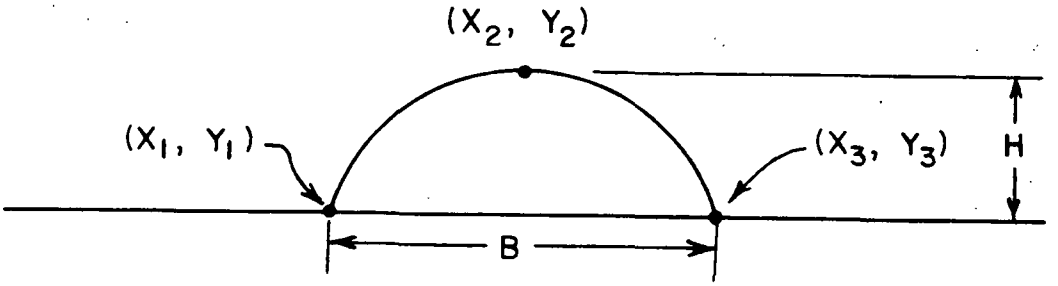

Figure 8. Coordinates for Conversion of Drop Image to Numerical Data

CONTACT ANGLE LIQUIDS

Contact angles of at least two different liquids of varying surface tension and polarity are required to calculate the polar and dispersion components of the solid surface by the methods of Owens-Wendt. Water was chosen as one liquid due to its importance in this work. The second liquid must also have a significant contact angle on cellulose, and have a polar component of surface tension different than water. Methylene iodide was chosen as the second liquid as it readily satisfied both of these requirements.

During initial experiments it was observed that autoradiograms of stearic acid-covered cellulose film which had been used for contact angle measurements showed major disruptions of the stearic acid uniformity wherever a liquid drop had been placed. During further investigation it was found that water drops did not disrupt the stearic acid until drying took place. The methylene iodide, however, appeared to disrupt the uniformity within a few seconds. It was not possible to determine the amount of disruption for shorter periods of time. Therefore, a third test liquid was prepared. Methylene iodide (MI) was mixed thoroughly with crystalline stearic acid and referred to as saturated methylene iodide (SMI). Both methylene iodide and saturated methylene iodide were tested on an adsorbed film and it was apparent that the saturated methylene iodide did reduce the amount of disruption of the radioactivity on autoradiograms. Since it had not been established that any stearic acid-methylene iodide reaction would occur in the fraction of a second required to measure the contact angle, both liquids were retained in the experimental program.

Surface tensions of all three test liquids were measured with the Cenco-DuNuoy Interfacial Tensiometer Model 10403. The ring factors of Brown (76) were used for methylene iodide measurements. Measured values of the surface tension, corresponding literature values, and the polar and dispersion components (76) are listed in Table II. The $\gamma_{\underline{1}}^{p}$, $\gamma_{\underline{1}}^{d}$ values calculated for saturated methylene iodide were modified by computer analysis to give the same values for the cellulose surface as obtained from pure methylene iodide.

TABLE II

PROPERTIES OF CONTACT ANGLE LIQUIDS

Liquid	γ_l, measured	γ_l, literature	Polar Component	Dispersion Component
Water	72.83	72.80	51.00	21.80
SMI[a], measured	47.6	--	1.1	46.5
SMI, modified	48.1	--	0.1	48.0
MI	50.70	50.76	0.38	50.38

[a]Calculations shown in Appendix V.

AUTORADIOGRAPHY

The simple technique of autoradiography performed quite well in monitoring uniformity of adsorption of the radioactive stearic acid on cellulose films. Kodak No-Screen x-ray film is pressed against the radioactive film in a light-tight box at room temperature. The reaction time for a good image depends on the acid concentration on the film and ranges from approximately 12 hours to 72 hours over the concentration range studied. Development procedures are presented in Appendix VI.

Reaction at refrigerated temperatures to reduce latent image fading appeared to cause spotting on the films due apparently to some mechanism of migration of stearic acid to surface deformities.

DESORPTION, EXTRACTION, PENETRATION, AND CHEMICAL BONDING OF STEARIC ACID

Desorption of stearic acid into the air after removal from the oven was monitored for 24 hours with the following results (Table III).

TABLE III

DESORPTION OF STEARIC ACID INTO AIR

Time, hr	Cpm on Film, % original
0.25	100
1.0	98
2.0	96
3.0	96
11.0	96
24.0	93

The stearic acid apparently does not leave the cellulose surface at room temperature to any great extent after two hours.

Separation of physically and chemically adsorbed species on various surfaces has been reported with hot benzene treatment (43,80). As indicated in Fig. 9, the hot benzene extraction of cellulose film containing adsorbed stearic acid exhibits the characteristic two-slope curve. The fast rate, complete in less than two minutes, most likely corresponds to the removal of physically adsorbed stearic acid from the surface of the film. The remaining radioactivity probably represents chemically bonded molecules and physically adsorbed molecules trapped in the film interior.

That physically adsorbed molecules are trapped in the film following benzene treatment is evident from Fig. 10. Here, additional stearic acid is extracted with water and ethanol at room temperature. As water will not cause any rupture of chemical bonds at this temperature, the swelling effect of the water on the cellulose must cause a release of previously trapped molecules. In these experiments, the films were extracted in the initial liquid, dipped into ethanol for 30 seconds to exchange water for ethanol,

then boiled in benzene for two minutes. In this way, the films emerged clear and smooth, suitable for contact angle measurements.

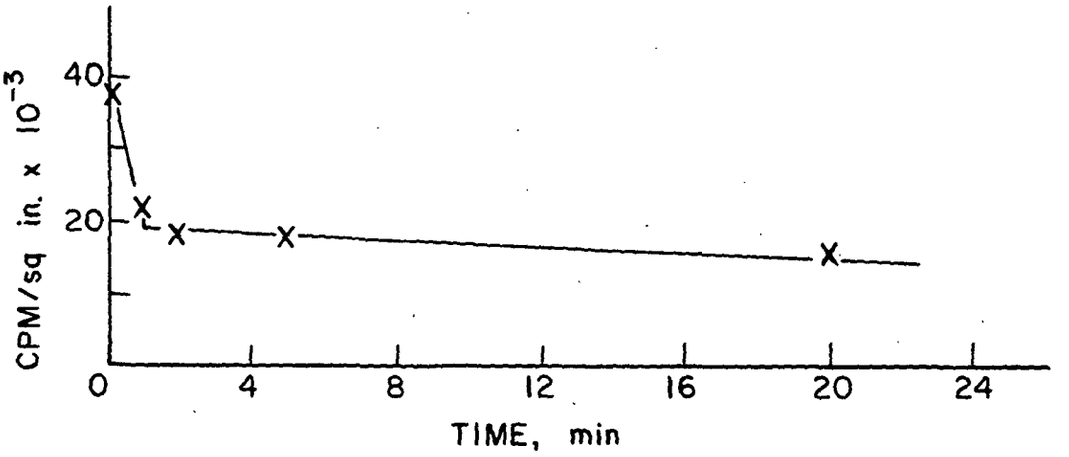

Figure 9. Benzene Extraction of Stearic Acid from Cellulose Film, 80°C

Essentially identical water contact angles were measured on cellulose film extracted only in benzene and on film extracted in a benzene-water-ethanol-benzene sequence. The radioactivity level, however, was decreased by 40%. This indicates that the surface character of the film has not changed and that the radioactivity removed was most likely associated with a form of trapped molecule. The possibility of water removing a hydrogen bonded species from the surface is considered to be a less likely phenomenon based on the constant contact angle results.

Contact angles of the caustic-extracted films, however, fall with the radioactivity content, suggesting that the caustic removes the surface molecules. Parenthetical numbers on curves in Fig. 10 are the corresponding water contact angles.

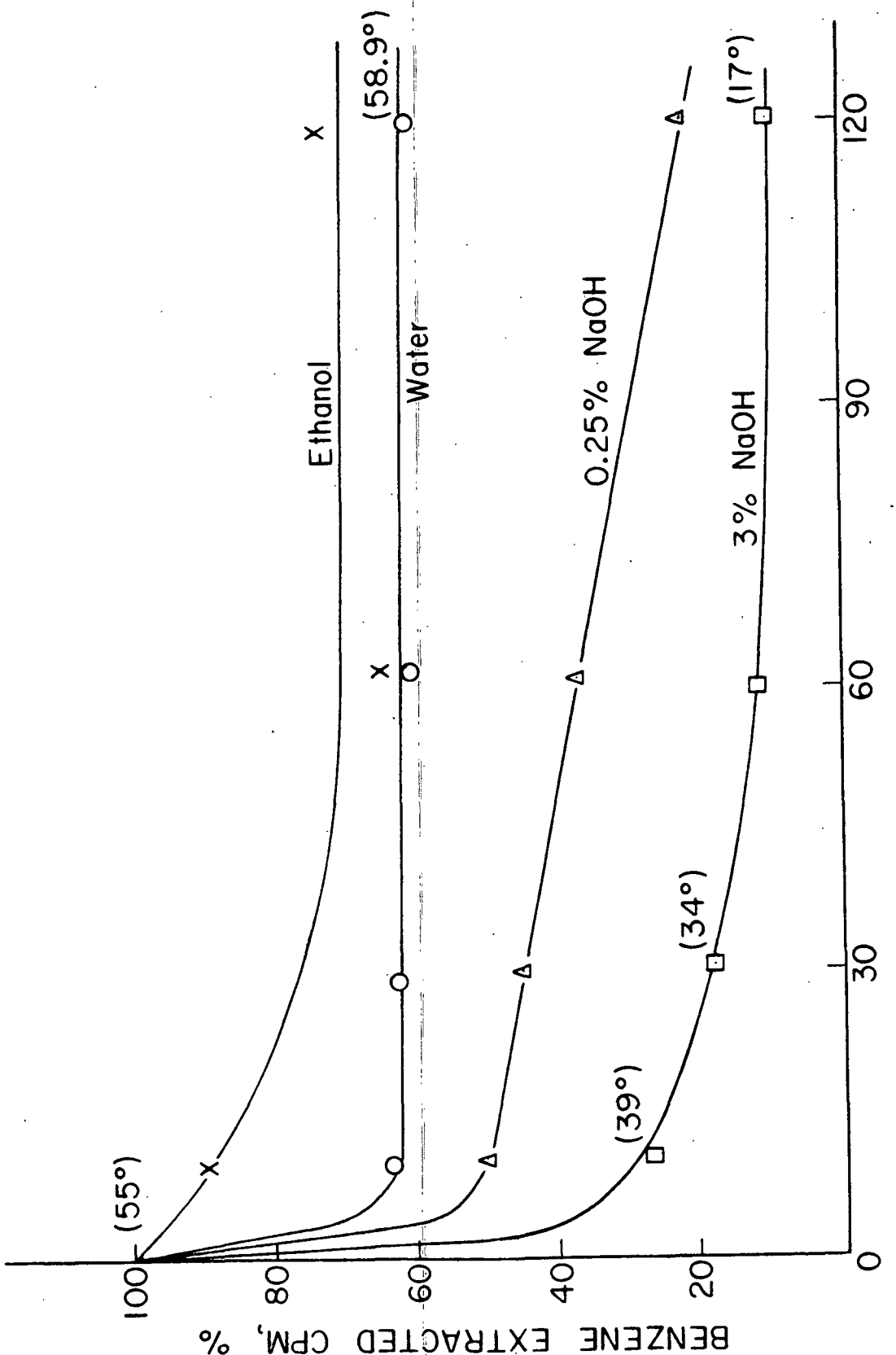

Figure 10. Extraction of Stearic Acid from Cellulose Film in Various Solvents, 20°C

The radioactivity remaining after caustic extraction must represent stearic acid molecules trapped in the film, i.e., molecules which have penetrated into the film interior. Although it is true that some radiation will be captured by cellulose depending on the depth of penetration (50% of the β-radiation entering one side of a film emerges from the opposite side), the level of radiation emerging from the film is the important value. That this level remains essentially constant from 30 to 120 seconds of extraction suggests relatively little migration of trapped molecules out of the film is taking place in this time interval. Therefore, the penetrated stearic acid contributes to a residual radioactivity which must be subtracted as an additional background value in counting. This residual will be less than the amount of radiation actually emitted by the trapped molecules by the amount of radiation absorbance.

From these experiments, the following procedure was developed to determine the amount of chemically bonded acid in the film.

1. Six pieces (0.4 inch × 1 inch) of a treated film are boiled in benzene at 80°C for two minutes, dried in air, and the cpm radiation determined.
2. These benzene-extracted films are then further extracted in water, with agitation, for two minutes, transferred to ethanol for 30 seconds to exchange water with ethanol, then extracted again in hot benzene for two minutes. After drying, the water-extracted cpm value is determined.
3. Two of the films are dipped into 3% caustic at 80°C for 30-60 seconds depending on the level of chemical bonding. They are

then washed in water to remove salts, rinsed in ethanol and extracted in benzene as before. The remaining (residual) cpm is determined.

4. The water contact angle on the two caustic-extracted films is determined and, if necessary, used to make adjustments to the residual cpm. These adjustments decrease the residual cpm by the amount of chemically bonded acid necessary to give the measured water contact angle. These adjustments are made from low contact angle data which did not require adjustment.
5. The chemically bonded cpm is equated to the cpm removed by caustic plus the cpm necessary to give the water contact angle on the caustic-extracted film.

RADIOACTIVITY MEASUREMENT AND CALIBRATION

Measurement of radioactivity in counts per minute (cpm) can be converted to any convenient value for reporting purposes. In this work, the amount of radioactivity determined is converted to %POML units. This value corresponds to percentage Planar Oriented MonoLayer (POML), where 100% POML is the number of molecules contained in a completely packed monolayer of stearic acid molecules oriented perpendicular to and cast upon a planar surface. Such a monolayer contains 31.8×10^{14} molecules per square inch and each molecule occupies 20.1 A^2 of surface area (54). True monolayer coverage is a function of the roughness factor, r, and the molecular orientation, i.e.,

$$\text{true monolayer coverage} = \frac{\%\text{POML}}{r} \times \frac{\text{effective } A^2/\text{molecule}}{20.1} .$$

To determine the correlation between %POML and cpm, 1.0 ml of radioactive stearic acid-benzene solution (0.172 μm) was diluted to 100 ml with benzene. A volume of 0.01 ml of this solution was transferred quantitatively to a cellulose film and the cpm determined. The amount of stearic acid on the film can be converted to %POML by mathematical techniques. Once this cpm-%POML relation is determined, nonlabelled stearic acid can be added to give any desired numerical ratio of cpm to %POML. In these experiments 11.3 to 1.0 nonlabelled to labelled acid is used to give 100% POML equivalent to 10,000 cpm. In this way, conversion of cpm to %POML is a simple matter of shifting the decimal point. Preparation of this solution is outlined in Appendix VIII.

Electronic counting equipment changes its efficiency day-to-day by a few percent. To correct for this, a radioactive source averaging 700 cpm was counted over 30 minutes preceding each experimental run. The average cpm for this period divided into 700 was then used as a correction factor to adjust the experimental results to the same counter efficiency.

Background counts were determined over a thirty-minute interval prior to counting the standard.

All counting of experimental data was sufficient to make the standard deviation of the count less than 2% of the total cpm.

EXPERIMENTAL RUN PROCEDURE

The following procedure, incorporating the results of the above preliminary experiments, was used to obtain the primary data of this work.

1. Film is dried in the Lucite chamber for 12 hours.
2. The film is conditioned in a 30% RH desiccator for 24 hours.
3. Stearic acid is adsorbed onto the film for a preselected time/temperature in the adsorption tray.
4. The tray is removed from the oven and cooled in laboratory ambient air for one hour.
5. The tray is opened and the top, with film attached, is placed in a 50% RH desiccator for two hours. This interval conditions the film so it will not curl up when released from the bracket. Also, the radioactivity level comes to equilibrium.
6. The film is removed from the bracket and the edges trimmed off so that only the film exposed to the vapor remains. The film is cut into ten pieces approximately 0.4 × 1.0 inch. Each piece is placed on a clean microscope slide.
7. The area of each piece of film is determined by measuring the dimensions in 1/32's of an inch and converting these measurements to the equivalent decimal fraction area.
8. The initial cpm on each piece is determined and converted to cpm/sq inch, adjusting for background.
9. Four of the film pieces are mounted immediately for initial contact angle measurements. To mount the films, two microscope slides are placed side-by-side and a 0.5 × 1.0-inch piece of two-sided tape centered over the joined edges. This tape is pressed tight against the glass. The film is then lowered onto the center of the tape and the edges pressed flat with a clean razor blade. The slides are flexed to pull the center of the film against the tape. The two slides are then cut apart with a clean razor blade by slitting

the film-tape laminate along the juncture of the two glass slides, making two contact angle samples from the single piece of film.

10. The remaining six films are benzene extracted, counted, water extracted, counted, and four of the pieces mounted for extracted film contact angle measurements.
11. The remaining two pieces are caustic extracted, counted, and mounted.
12. All films are placed in a 40% RH desiccator for four hours for conditioning prior to contact angle measurements.
13. Contact angle measurements are made with two rolls of 36-exposure film. The number of drops for each liquid are 24 water, 12 saturated methylene iodide, and 12 methylene iodide. Each liquid is equally divided between extracted and unextracted films. In addition, 10-12 water angles on caustic-treated films are taken.
14. Autoradiograms are started on the slides used for contact angle measurements. This step is not done where cpm data are uniform and experience indicates spotting is unlikely. The autoradiograms are developed 12-24 hours later.
15. The photographic film is developed, cards punched, and data calculated by computer.

EXPERIMENTAL RESULTS

CONTACT ANGLES AND SURFACE ENERGY PARAMETERS ON PURE CELLULOSE

Cellulose films conditioned 24 hours in a 30% RH atmosphere were removed from the Lucite plates and mounted directly on microscope slides. Following conditioning for 4 hours in a 40% RH desiccator, the contact angles of water, saturated methylene iodide (SMI), and methylene iodide (MI) were measured. The results are presented in Table IV along with the calculated surface energy parameters from the Owens-Wendt equations.

TABLE IV

PURE CELLULOSE CONTACT ANGLES AND SURFACE ENERGY PARAMETERS

Contact Angles

Liquid	Mean ±95% Conf. Lim.
Water	28.1 ± 0.71
Saturated methylene iodide	29.3 ± 0.50
Methylene iodide	26.4 ± 0.76

Surface Energy Parameter

Owens-Wendt Component	Liquid Pair	
	Water-SMI	Water-MI
Total	69.4	69.7
Dispersion	39.0	39.7
Polar	30.4	30.0
Fractional polarity	0.44	0.43

These water contact angles are lower by 5-6° than those previously reported in the literature (61,65,67). The methylene iodide contact angles are 12° lower than those reported by Bartell and Ray (65). However, the

Owens-Wendt polarity parameter of 0.44 for this work is in reasonable agreement with the similarly calculated value of 0.47 for Ray's data. An explanation of these differences based on roughness seems unlikely since the surfaces in this work have been prepared under conditions far more conducive to smoothness than any of the films reported in the literature. Contamination of the films by a spreadable material is eliminated as a possible cause since a) all data extrapolate back to 28°, and b) negative results are obtained from the surface-active talc test (see p. 45). The cause of these unusually low contact angles can, therefore, only be hypothesized. Perhaps the drying technique causes a reduction in the number of deep asperities in the surface which would reduce the effective porosity of the film and lower the contact angle. Whatever the cause of the low values, the angles measured were very reproducible and uniform.

The water-SMI and water-MI liquid pairs exhibit the agreement in surface energy parameter developed by computer refinement of the saturated methylene iodide properties. The calculation of a parameter based on the MI-SMI pair is not possible since the two liquids are too similar in polarity.

ADSORPTION OF STEARIC ACID

The adsorption isotherms of stearic acid on cellulose film is presented in Fig. 11 for the three temperatures. The adsorption curves can be separated into three regions. In the initial region, the adsorption of stearic acid onto cellulose increases to an apparent equilibrium level dependent on temperature. This level of adsorption remains constant throughout the equilibrium region, the length of which is also temperature dependent. After this period, a dramatic increase in stearic acid pickup develops as the acid begins massive

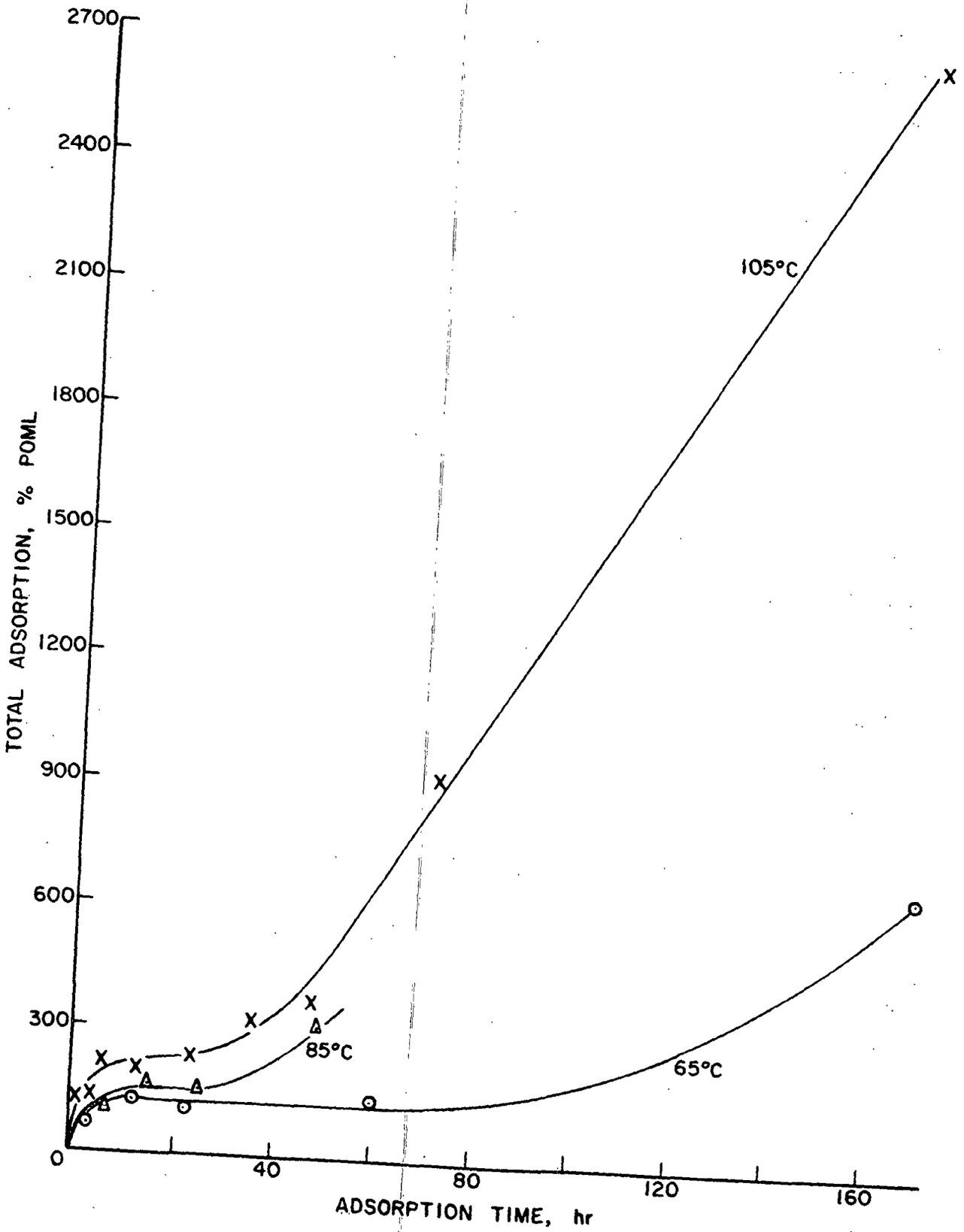

Figure 11. Adsorption of Stearic Acid

penetration into the film. This penetration interpretation is developed in the Discussion section.

The temperature dependence of the first two regions is presented in Fig. 12. From this figure, it is apparent that the equilibrium adsorption level is approximately 120, 160, and 240% POML at 65, 85, and 105°C, respectively.

The observation that higher temperatures lead to increased adsorption appears erroneous at first and would not be found in systems where temperature and partial pressure were independent. However, estimates of the vapor pressure of stearic acid at the three operating temperatures indicate that the ratio of the vapor pressures is 1:14.5:134 as the temperature is increased (Appendix I). This leads to an increased number of collisions with the surface at the higher temperatures, and although a smaller proportion of the collisions are sticking collisions, more total acid is adsorbed onto the surface. This phenomenon is a result of the use of the infinite bed system where an increase in temperature must cause an increase in the concentration of acid molecules in the vapor.

CHEMICAL ADSORPTION OF STEARIC ACID

The amount of stearic acid determined to be chemically bonded to the cellulose film increases linearly with time over the first two adsorption regions as shown in Fig. 13. Within these regions, the rates of chemical bonding are 0.11, 0.33, and 0.96% POML/hour at 65, 85, and 105°C, respectively.

Once penetration of the stearic acid into the film begins, the physically adsorbed acid which has penetrated is no longer totally extractable with benzene and/or water and the amount of chemically bonded acid can no longer be determined correctly. In addition, significant amounts of acid become

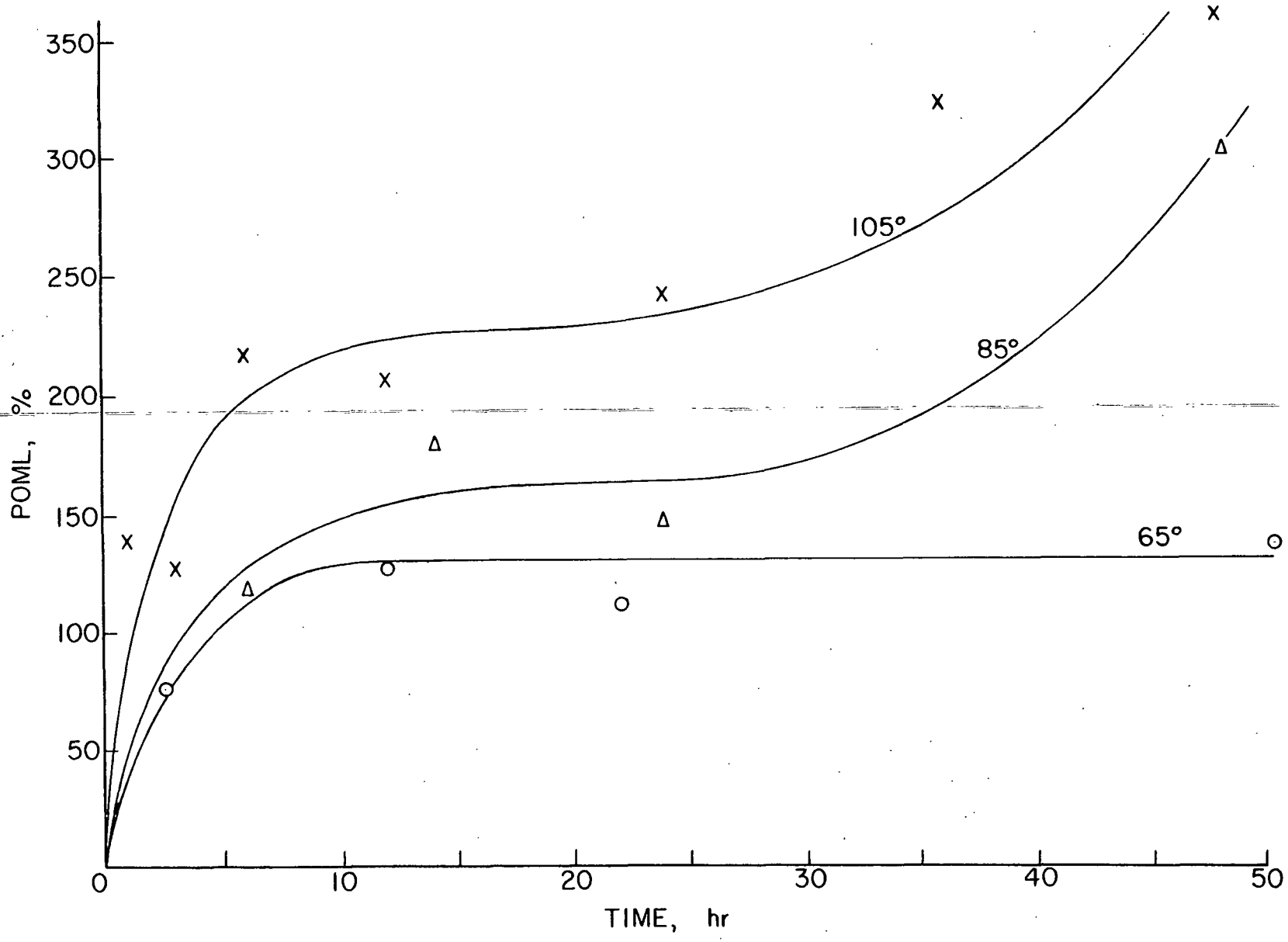

Figure 12. Total Adsorption of Stearic Acid vs. Time

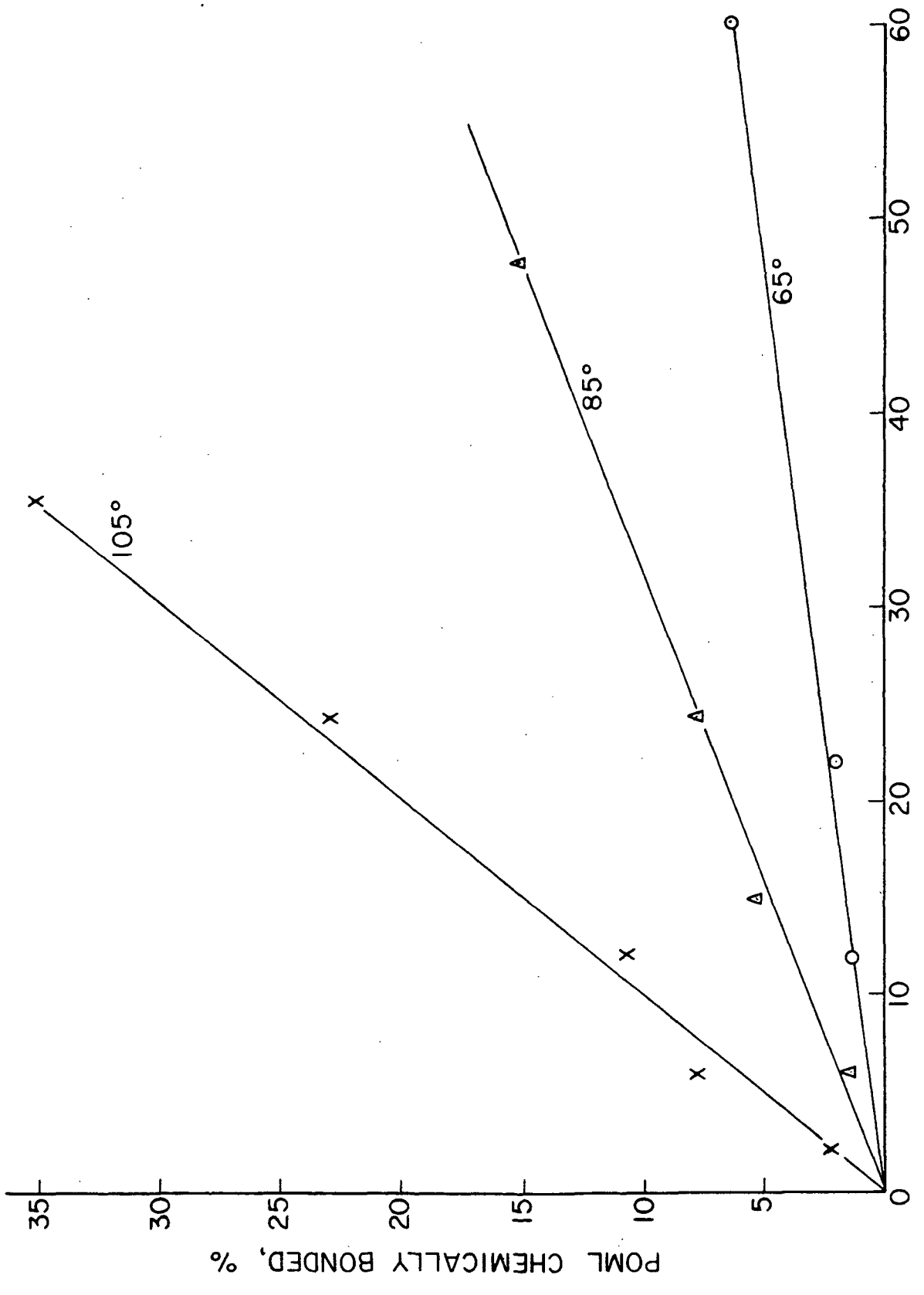

Figure 13. Rate of Chemical Adsorption of Stearic Acid

chemically bonded to the interior surfaces. The result is an eventual departure from linearity once penetration of acid into the film begins.

It is significant that the amount of chemically bonded acid is less than 10% of the total adsorption at 105°C and 24 hours, and is much less than this in all other cases.

DEVELOPMENT OF THE WATER CONTACT ANGLE ON UNEXTRACTED FILMS

The development of the water contact angle on unextracted films appears to occur in stages which may be represented by three linear regions. These three stages are shown in Fig. 14a for adsorption at 105°C. Results for all three temperatures were obtained over the first 60 hours of adsorption and are presented in Fig. 14b. The same mechanism is apparently being followed in each case. An increasing lag time before the water contact angle begins to increase significantly develops at the lower temperature. This is attributable to slower and less adsorption at 65°C. The rate of increase of the water contact angle in the first region is 0.46, 1.37, and 4.5 degrees/hour at 65, 85, and 105°C, respectively.

WATER CONTACT ANGLES ON EXTRACTED FILMS

The water contact angle on extracted film is normally slightly higher than the corresponding unextracted film contact angle. The contact angle *vs.* time curve is therefore very similar and has the same change of rate as does the plot of the unextracted data.

A different viewpoint, available from the extracted film data, is presented in Fig. 15. Here, the increase of the water contact angle is plotted *vs.* the amount of chemically bonded acid on the surface of the film. Data

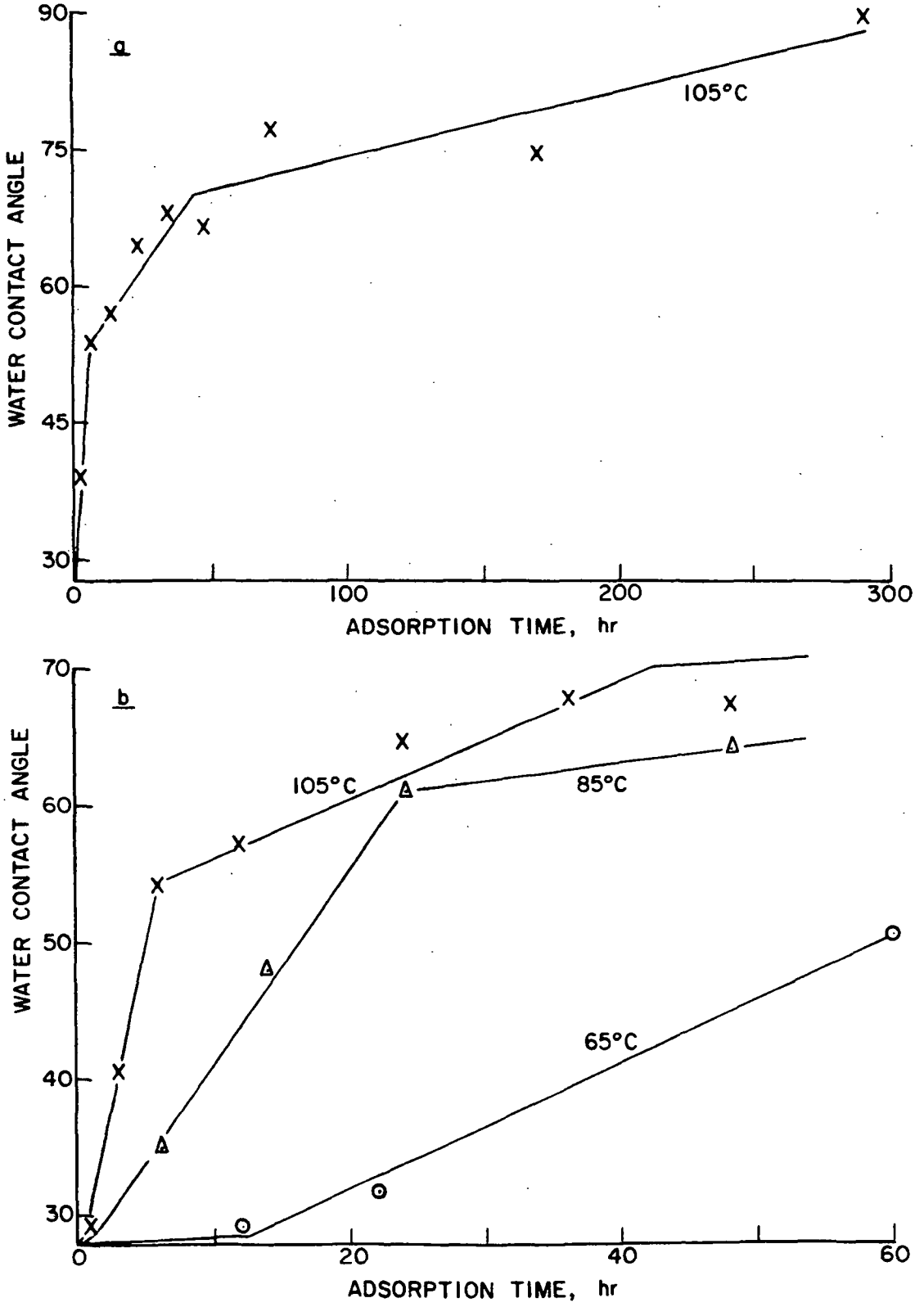

Figure 14. Development of Water Contact Angle on Unextracted Films as a Function of Time. a) Three Regions of 105°C Data. b) Behavior in First 60 Hours

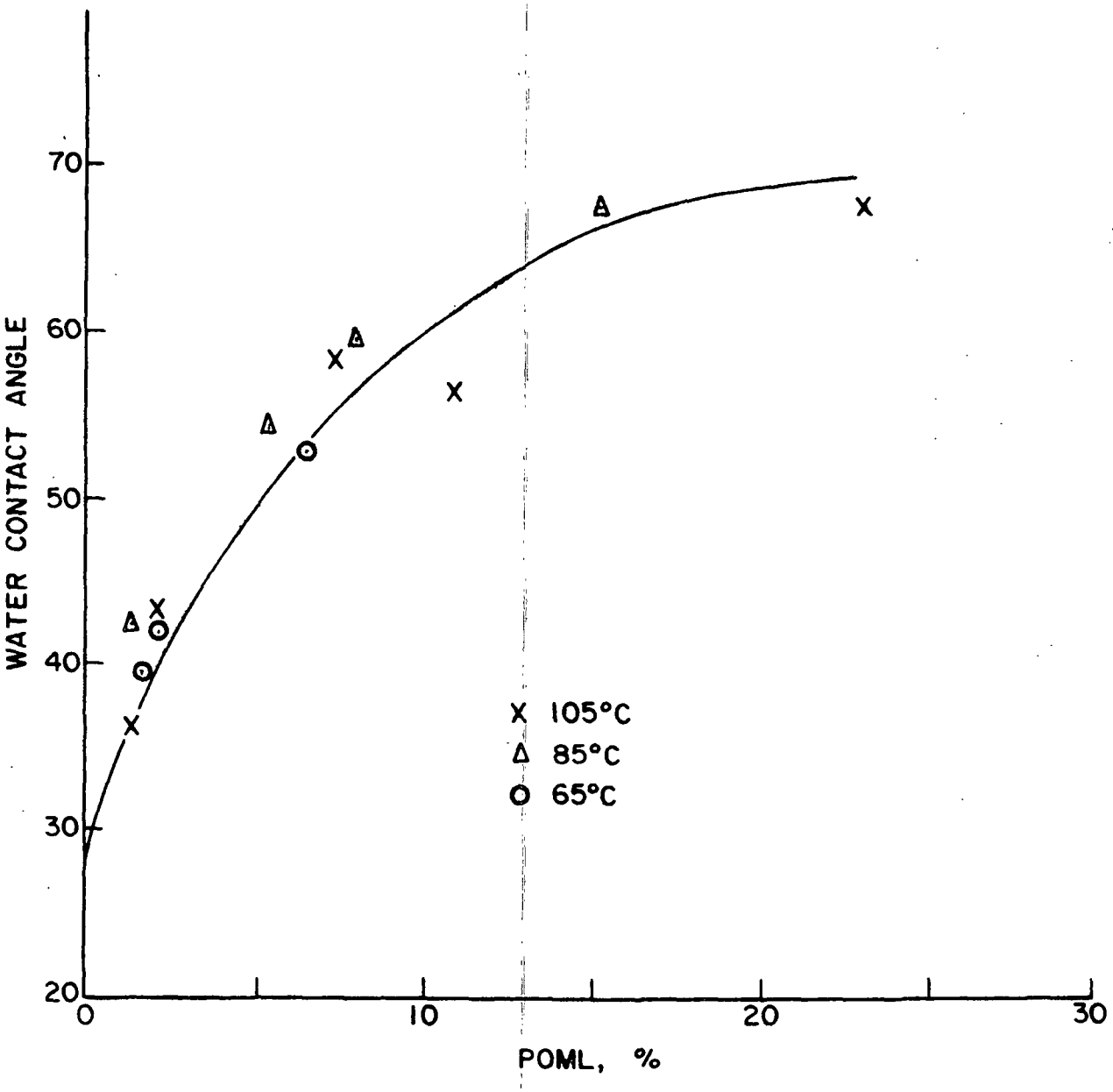

Figure 15. Development of Water Repellency on Extracted Film as Function of Molecular Population on Surface

for adsorption times longer than 24 hours are not included as the amount of chemical bonding can no longer be determined due to the penetration of the acid into the film interior. However, the extracted film contact angle above 24 hours changes only gradually with time as adsorption continues.

The fact that the data for all three temperatures fall resonably well along the same line indicates that there is little difference between the orientation or distribution of the molecules adsorbed at the three temperatures.

METHYLENE IODIDE CONTACT ANGLES

The most consistent methylene iodide contact angle data were obtained for a) saturated methylene iodide on unextracted films and b) pure methylene iodide on extracted films. From previous experiments, it seems likely that the methylene iodide saturated with stearic acid did not disrupt the adsorbed molecules on the unextracted film as much as pure methylene iodide. This would account for the less scattered results with saturated methylene iodide in this case. For extracted films, the stearic acid associated with the saturated methylene iodide could possibly fill in holes in the extracted stearic acid monolayer and give erroneous results. This would account for the better results with pure methylene iodide on extracted films.

The appropriate contact angle is plotted vs. time for unextracted and extracted films in Fig. 16a. The methylene iodide contact angle as a function of surface coverage for extracted film is shown in Fig. 16b.

The methylene iodide contact angles correspond more directly to surface coverage than do the water contact angles reported earlier. For example, the saturated methylene iodide angles on unextracted films increase with time

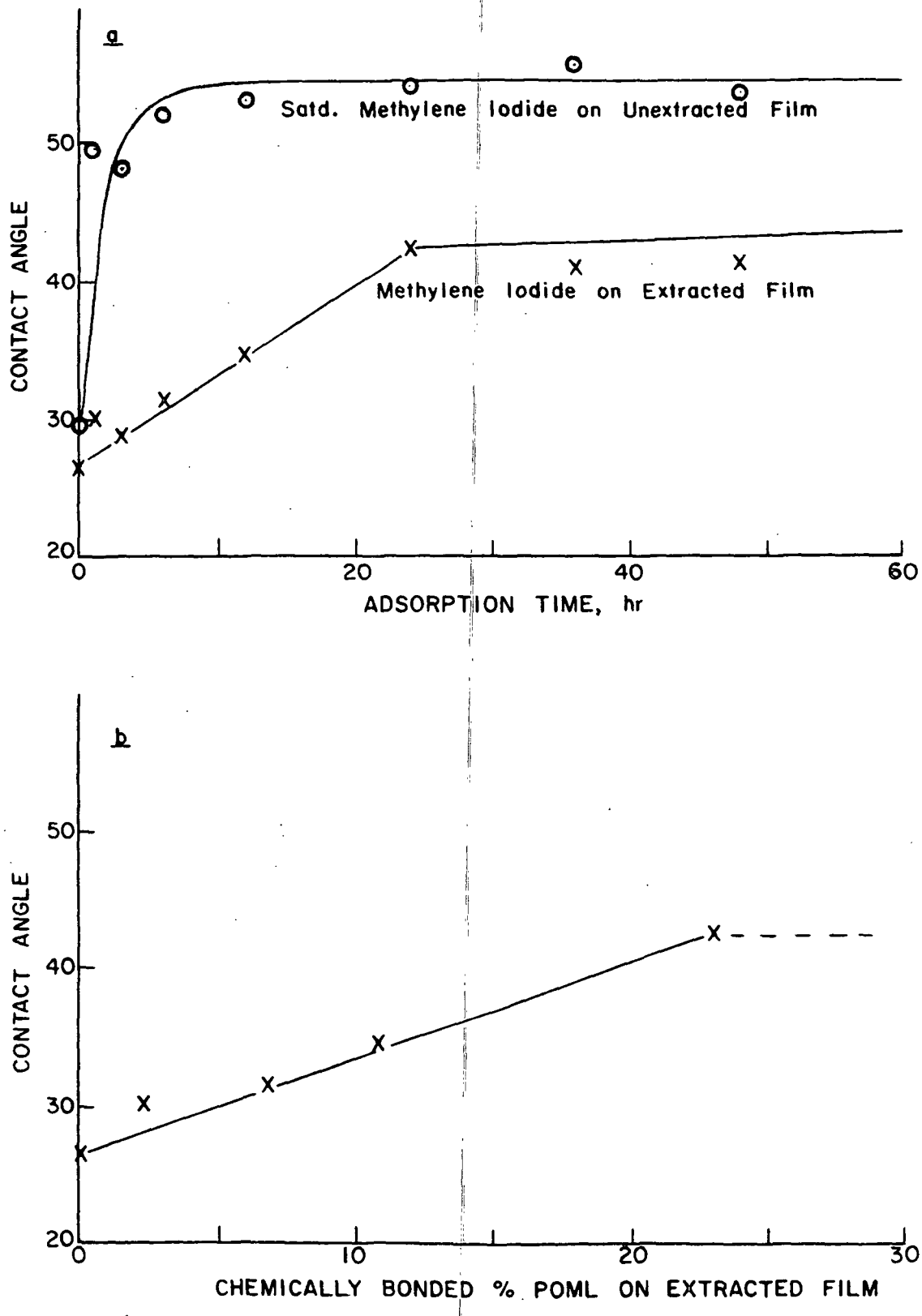

Figure 16. Methylene Iodide Contact Angles. a) As a Function of Time. b) As a Function of Coverage

and level off identically with total adsorption up to 24 hours at 105°C. The pure methylene iodide contact angles increase linearly up to 24 hours after which they increase only very slowly. This suggests that the chemically bonded coverage of the external surfaces increases only gradually after the first 24 hours at 105°C. This suggested linear increase in the amount of chemically bonded coverage for the first 24 hours agrees well with the results found by analytical techniques.

This difference between the development of methylene iodide and water contact angles is an indication of different mechanisms at the interface which may be due to the size differences or chemical differences of the two liquid molecules. A water molecule can penetrate a repellent pseudo-surface more easily than can the larger methylene iodide molecule. This would make it more difficult to increase the water repellency as the packing density increases. Also, the hydrocarbon tails of the acid may tend to dissolve in methylene iodide. This would lead to a methylene iodide contact angle dependent on surface concentration of stearic acid only. In either case, the methylene iodide contact angle would be a better indicator of acid concentration on the film surface.

The dotted line in Fig. 16b indicates that the contact angle for the next adsorption time is essentially unchanged. However, due to penetration of the acid into the cellulose above 24 hours, it is not possible to experimentally determine the corresponding surface coverage for the abscissa.

SURFACE ENERGY PARAMETERS

The Owens-Wendt surface energy parameters from the contact angle data are presented as a function of adsorption time in Fig. 17. The total surface energy parameter and the polar component of the surface energy parameter are

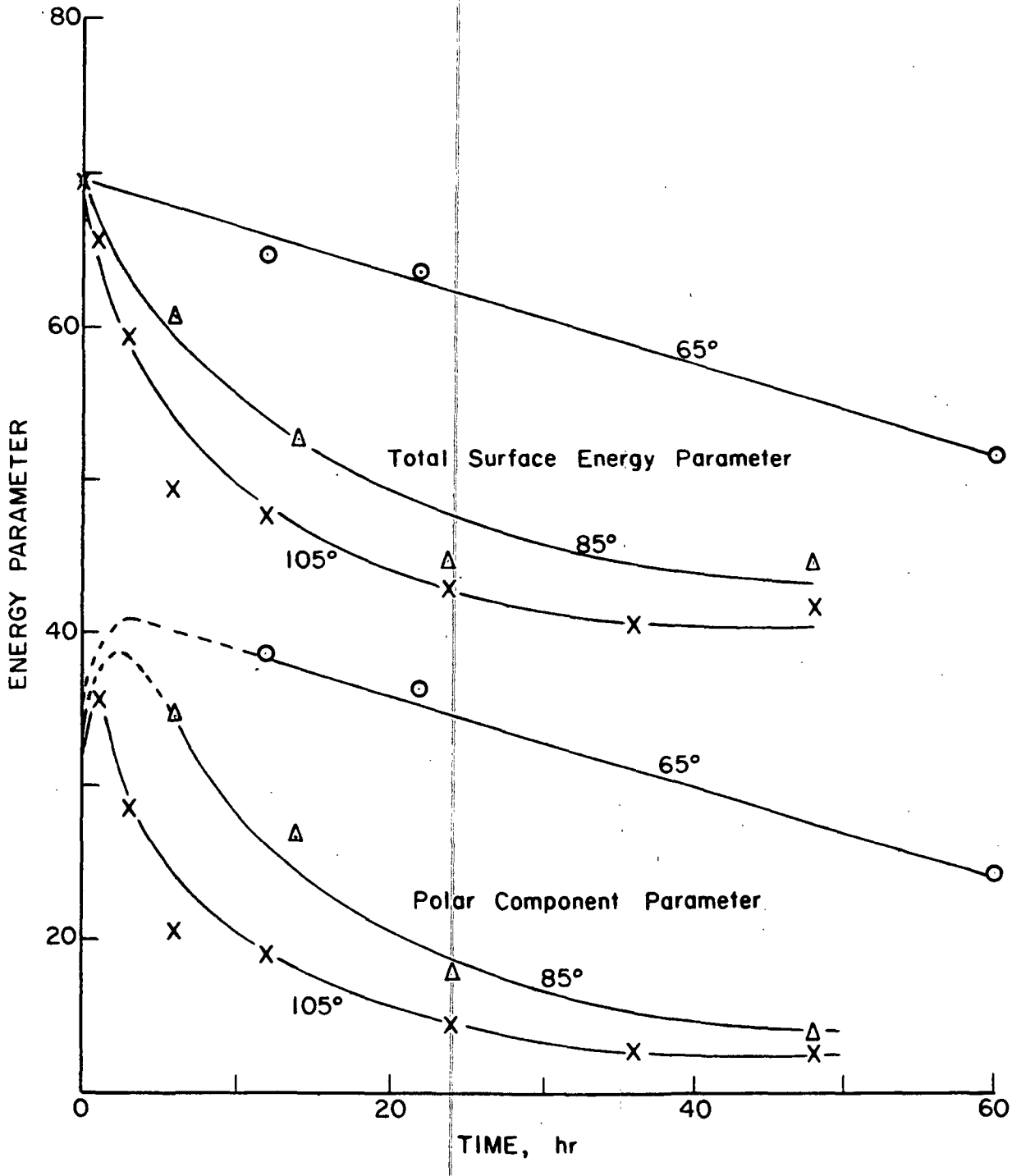

Figure 17. Changes in the Owens-Wendt Surface Energy Parameter with Time (Unextracted Film)

plotted. The dispersion component, the difference between these two values, remains essentially constant. As would be expected, the total surface energy parameter decreases with time, or with continued adsorption, until equilibrium is reached. Of more interest, however, is the behavior of the polar component. The value of the polar component for pure cellulose is 30 parameter units. During initial adsorption, the polar component increases above this value briefly and then decreases rapidly. This phenomenon is indicated for each temperature although the dotted lines for the two lower temperatures are estimated projections.

Figure 18 illustrates the differences between the surface energy parameters of unextracted and extracted films. The primary difference in the dispersion results is the immediate drop in the dispersion component of the unextracted film. This may be due to the smaller polarizability of the stearic acid surface as opposed to the cellulose surface, resulting in a smaller dispersion force contribution to the total energy. The decrease in the extracted film occurs quite gradually as the cellulose is slowly covered up by the aliphatic hydrocarbon tail of the acid.

The initial increase in the polar component found with unextracted film does not occur in the extracted film. The polar and dispersion components of the extracted and unextracted films approach a single polar and single dispersion value at long times of adsorption.

All adsorption, contact angle, and surface energy data are presented in Appendix IX from each major experimental run.

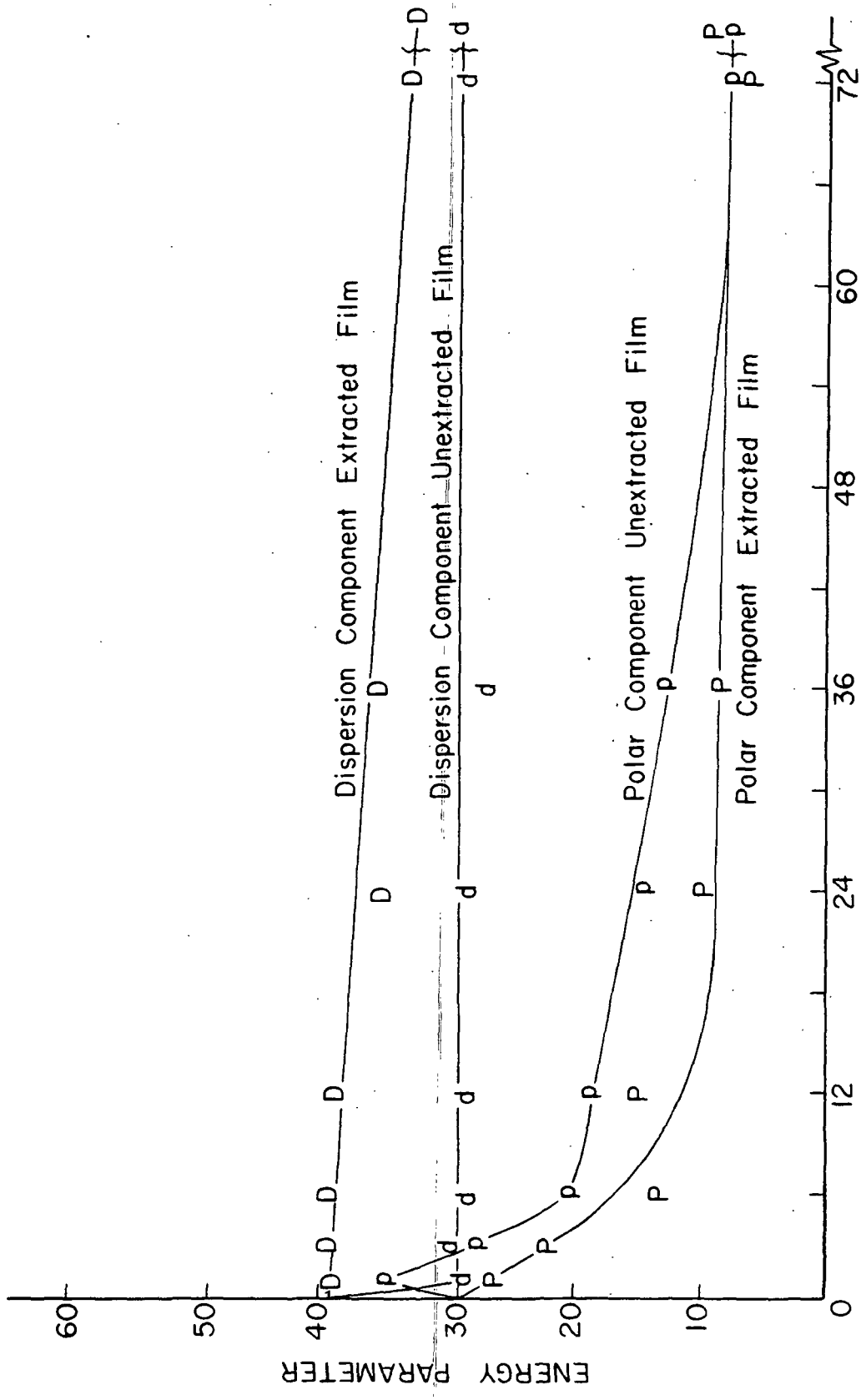

Figure 18. Changes in Polar and Dispersion Components of Unextracted and Extracted Films with Time, 105°C

DISCUSSION OF RESULTS

The experimental results are discussed from two interdependent viewpoints — the adsorption of stearic acid, and the development of water repellency. In addition, the results are specifically interpreted for a number of secondary aspects.

ADSORPTION OF STEARIC ACID

Vapor-phase adsorption results in a complex adsorbed surface layer which is difficult to visualize. However, the data do provide consistent evidence of the adsorption behavior on the surface.

ADSORPTION MODEL

When the adsorption tray is placed in the oven, the stearic acid molecules in the bed gain kinetic energy until thermal equilibrium is reached. A transfer of molecules into the vapor phase occurs, and these molecules diffuse across the intervening space toward the cellulose film. In the gas phase, these molecules exist primarily in the monomer form as indicated in Appendix I.

The first molecules approaching the film collide with the cellulose surface in a random manner where they stick to the surface for a finite time then diffuse back into the vapor to perhaps adsorb elsewhere on the surface. As the molecular population on the surface increases, an equilibrium is eventually reached with the vapor in which an equal amount of molecules are leaving the surface as are adsorbing to it. This corresponds to the equilibrium region of the adsorption isotherms. More importantly, the monomer-dimer equilibrium in the surface adsorbed phase shifts toward dimerization as the molecules become more closely packed.

For a perfectly smooth, energetically homogeneous surface, this equilibrium would imply uniform distribution of the adsorbed species, whether monomer or dimer, on the surface. For cellulose film, however, the surface is neither perfectly smooth nor energetically homogeneous. The film has a definite roughness to it as well as a characteristic system of pores and asperities. As adsorption continues, the higher energy of the surface asperities and lower vapor pressures of the molecules adsorbed in them combine to increase the acid concentration in the pores and crevasses while the equilibrium concentration on the external surface is maintained.

Evidence of this effect is presented in Fig. 19 for the 105°C data. This figure indicates the amount of stearic acid removed by each extraction liquid as the percentage of the initial adsorption on the film at each time. The percentages total 100% since the values are for consecutive benzene-water-caustic extractions on the same piece of film. To interpret the figure properly, the total adsorption isotherm (Fig. 11) must be considered. For example, since the total adsorption increases rapidly after 24 hours, a constant percentage in this figure is an increase in real amount.

The first conclusion drawn from this figure is the striking decrease in percentage of benzene-extractable acid and the corresponding increase in percentage water-extractable acid with time. Since benzene does not swell cellulose while water does, these data suggest that the stearic acid content of the film shifts from primarily benzene accessible sites to primarily benzene inaccessible sites as adsorption continues. This is in agreement with expected adsorption behavior. The rate of increase of the water-extracted value is considered too slow to represent a shift toward a hydrogen bonded species.

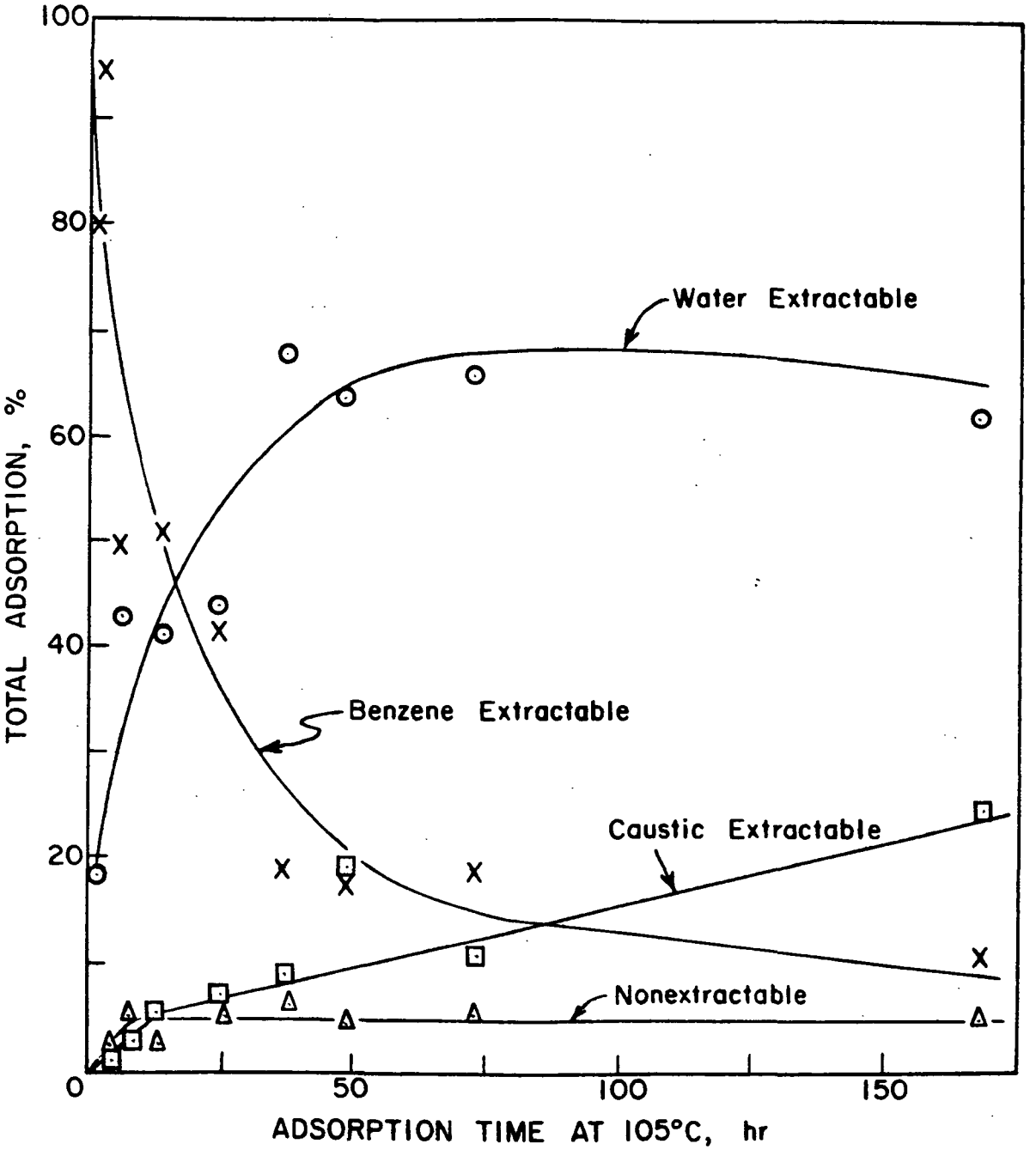

Figure 19. Stearic Acid Extractability in Water, Benzene, and Caustic as Function of Adsorption Time

Further evidence supporting this proposed migration is found in the actual benzene-extractable values as shown in Table V.

TABLE V

BENZENE-EXTRACTABLE ACID PER SQUARE INCH OF FILM

Adsorption Time, 105°C, hr	Total Adsorbed, cpm	Benzene-Extractable, cpm
1	14,030	11,158
3	12,797	12,267
6	21,842	10,846
12	20,644	10,662
24	24,216	10,217
36	32,993	6,157
48	37,911	4,514
72	90,676	15,920
168	279,000	29,000

The relatively constant amount of stearic acid removed by benzene over the first 24 hours strongly suggests that this is the equilibrium concentration on external surfaces at 105°C. This is further strengthened by the temperature dependence of this equilibrium benzene-extractable amount. The acid which is benzene extractable from 65, 85, and 105°C films in the equilibrium region averages 7500, 8570, and 11,030 cpm/sq inch, respectively. These values agree with the concept of higher adsorption at higher temperatures.

Between 6 and 24 hours at 105°C, the total adsorption of stearic acid is relatively constant. The distribution of the acid between external and recessed areas also appears almost constant in this region. (This plateau is not evident in Fig. 19 due to the scale factor.) Only the chemically bonding reaction appears to continue. However, near the end of this equilibrium

period, massive amounts of adsorbed stearic acid begin to penetrate into the film recesses.

EVIDENCE FOR PENETRATION

Above 24 hours at 105°C a very dramatic change occurs in the adsorption isotherm. This phenomenon is observed after longer times at lower temperatures. The films begin to adsorb the equivalent of a planar monolayer every five hours and the shape of the adsorption curve strongly suggests multilayer adsorption as shown previously in Fig. 11. There are two possible explanations for this adsorption behavior: the acid either forms multilayers or penetrates into the film. The conclusion that the penetration interpretation is correct is based on the following three observations.

First, when films from this high adsorption region are boiled in benzene only a very small percentage of the total acid is removed as shown in Fig. 19. Even after lengthy extraction, the radioactivity in the film is unchanged. Since stearic acid is exceedingly soluble in benzene, this suggests the acid is not readily accessible to the solvent. The possibility of the formation of an insoluble polymorph of stearic acid upon cooling from the vapor is not considered likely.

The second observation suggesting penetration is based on experimental data from a film exposed to stearic acid vapor for 290 hours at 105°C. The water contact angle on this unextracted film was 90°, indicating a very slow increase in the water contact angle with time is continuing. If multilayers were forming on the film, each succeeding layer would be identical to the preceding and the water contact angle would not change. That this is not the case must indicate a slow change in a single layer.

The most persuasive indication of penetration is the caustic extraction results in this high adsorption region. Typical data are obtained from the film exposed 168 hours at 105°C. When removed from the oven, this sample contained 2790% POML. After benzene extraction, 2500% POML remained. Brief water extraction at room temperature reduced this value to 800% POML. Alternate benzene and water extractions could not reduce this value further. Also, the water contact angle did not change throughout this procedure. The behavior when the sample was extracted with 3% NaOH at 80°C was revealing and is presented in Fig. 20. After two seconds in the caustic, almost 80% of the radioactivity in the water-extracted film was removed but the water contact angle decreased only 1.5°. As extraction continued, both the water contact angle and the stearic acid content decreased and slowly levelled out.

This behavior is interpreted as further evidence that large amounts of stearic acid had penetrated into the interstices of the molecular structure. Only the greater swelling power of caustic over water could free these penetrated molecules. While stearic acid is relatively insoluble in water, approximately 200 monolayers per square inch can be dissolved in the volume of the water extraction step (100 g). This penetrated liquid has no effect on the contact angle, of course, and its removal does not affect the rate of saponification of the chemically bonded species on the external surface. This figure can be compared to the caustic extraction data of Fig. 10 for films adsorbed below the penetration region. In that figure, the water contact angle decreases proportionately with stearic acid content.

A curious factor illustrated by Fig. 20 can be addressed here. As caustic extraction continues in films adsorbed in the penetration region, the water contact angle drops slowly to approximately 55° and remains there despite

further treatment. Similar extraction in films adsorbed below the penetration region results in a caustic extracted contact angle near that of pure cellulose — 28°. This phenomenon is interpreted by assuming that at the long times and temperatures involved in these cases, a certain amount of the acid molecules

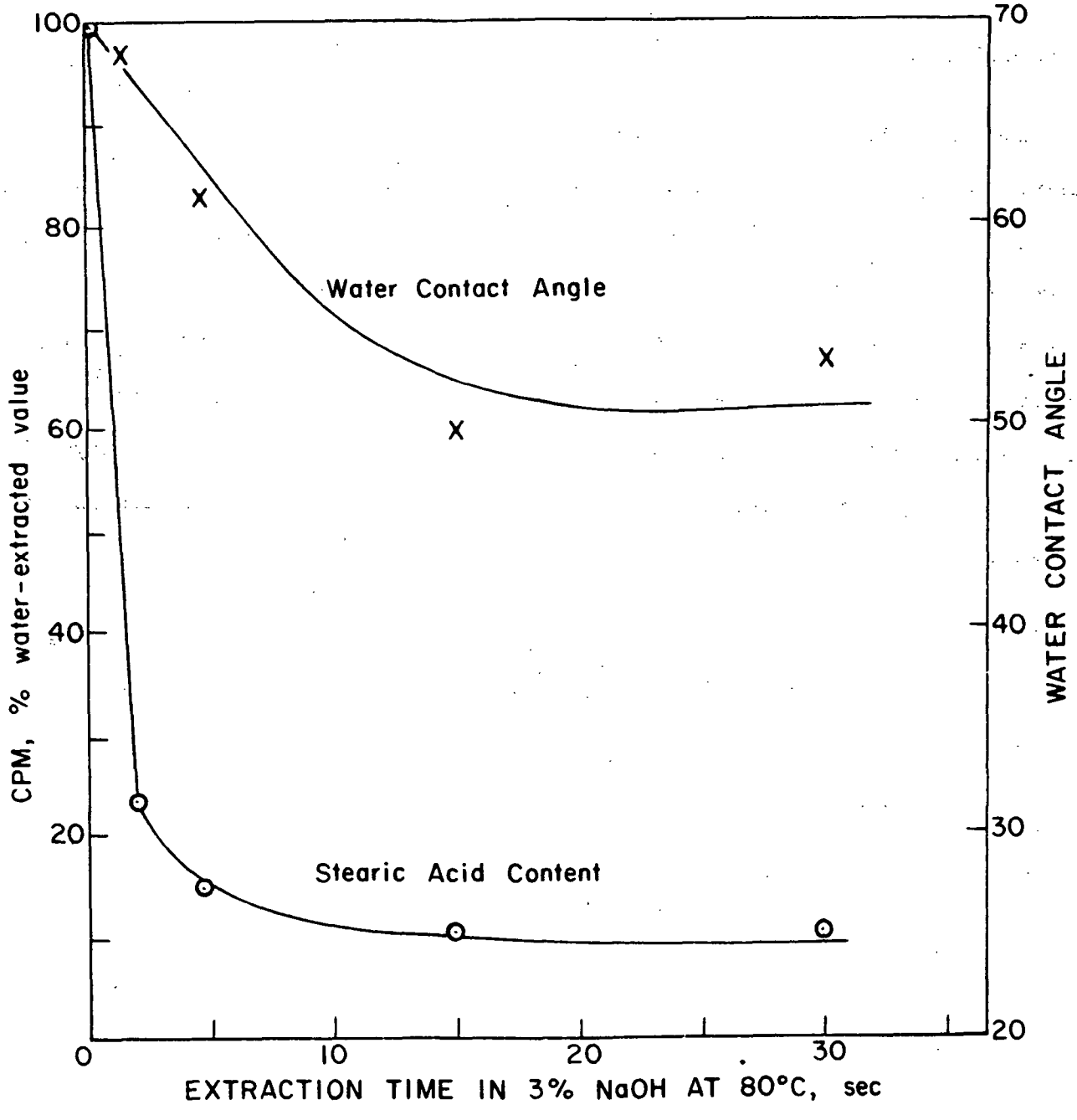

Figure 20. Caustic Extraction Behavior in Penetration Region

actually penetrate between cellulose chains or micelles and become physically held. In this way, tails could extend from the surface while heads are trapped in the surface. Another possible interpretation may be the formation of a very stable bond with time. In either case, the surface coverage of these residual molecules need only be about 1% of a true monolayer.

A PROPOSED MECHANISM OF PENETRATION

The following hypothesis primarily depends on the microporous nature of cellulose film. Jayme and Balser (58) have reviewed the literature on morphology and structure of cellulose films. They cite general agreement that films consist of a very dense but thin external skin which covers an amorphous, spongy center. The skin is reported to be as little as 500-A thick. The center of the film is reported to be physically soft and spongy and filled with vacuoles created during the regeneration from viscose. The entire film consists of both crystalline and amorphous regions. They report the existence of very small cracks and fissures in the surface.

It is proposed that the surface of the cellulose film used in this work, while hand-cast, does contain numerous fissures or asperities which lead to a microporous system of pores in the film interior. Amorphous regions of the skin itself may also present a microporous structure.

As adsorption begins, the walls of these pores begin to adsorb stearic acid. Pores of all sizes become increasingly covered, but the net migration will be to the pores of the smallest effective radius. This is predicted on the basis that the smallest pores exhibit the lowest vapor pressure of adsorbed species. Only when the walls of the smallest accessible pores are covered, will the pore system begin to fill up with acid molecules. This migration

period would correspond to the adsorption curve equilibrium in this model and could easily take several days at lower temperatures. As the pores finally begin to fill up, the penetration region begins. Beginning with the smallest and proceeding through the largest pores, stearic acid deposits into the film interior. At 105 and 85°C an additional aspect of penetration may be a capillary movement of the liquid acid in the pores into even smaller interstices existing in the film.

The net result is that a film in the penetration region contains stearic acid not only on the surface and in cracks and fissures, but also in a microstructure of pores extending even, perhaps, to the molecular interstices of the crystalline region.

When the film is cooled and extracted, benzene would remove the external surface molecules, water would swell the film and dissolve out a portion of the benzene-inaccessible acid, and finally caustic extraction would swell the crystalline regions, perhaps, and remove molecules which had penetrated even into the smallest molecular interstices.

Chemically bonded molecules would be found on internal as well as external surfaces. The penetrated molecules, plus those chemically bonded in the interior would both contribute to the rapid rise of the water-unextractable acid above 24 hours at 105°C. This is the cause of the breakdown in the method to determine the amount of chemically bonded acid on the surface.

DEVELOPMENT OF WATER REPELLENCY

The rate of increase of the water contact angle with time is divided into three stages as shown previously in Fig. 14. In the 105°C adsorption data, the first rate is constant up to approximately 55° after which a second slower

rate predominates. This second rate increases the contact angle to 70° again linearly with time. Above this, the contact angle continues to increase even more slowly but does reach 90° after 290 hours at 105°C.

INITIAL DEVELOPMENT OF REPELLENCY

During the initial period, the water contact angle increases linearly with time until the slope of the line changes suddenly. This linearity is observed at all temperatures. The cause of this linear relationship and the sudden break in the slope are interpreted in the following manner.

As acid monomers first collide with the surface they tend to recline on the cellulose due to the greater interaction and lower free energy. They reside on the surface for an average time, dependent on temperature, then desorb back into the vapor and may readsorb elsewhere. As the surface concentration increases, several things occur. Monomer-dimer equilibrium shifts quickly toward dimerization as the monomers come into close proximity. Also, an increasing amount of acid becomes chemically bonded to the surface. As the experimental evidence indicated, the bonding reaction rate is constant with time over this region, but the total number of molecules chemically bonded is never more than 10% of the total adsorption on the film.

The kinetic energy of these chemically anchored molecules causes the hydrocarbon tail to flail about the surface sweeping out an area far greater than the molecular cross-sectional area. The simplest model to assume is that these long chains sweep out a conical volume by rotating about the bonding site at a constant angle of inclination. A more complex "flip-flop" mode is considered less likely as the flailing hydrocarbon tail in the conical volume model would tend to occupy the more favorable positions of minimum potential

energy, i.e., positions without interaction with the surface. Furthermore, it is considered unlikely that the relatively large hydrocarbon chain could gain kinetic energy fast enough and thereby "flip-flop" fast enough to successfully mask the underlying surface (81).

Along with increasing dimerization and bonding, the polarity of the surface measured by the Owens-Wendt parameters increases briefly as the stearic acid initially adsorbs. This is attributed to the increase in the number of carboxyl groups at the liquid-cellulose interface. The carboxyls of the dimer would affect the polar nature of the surface to a lesser degree than the monomeric carboxyls. This increased polarity is short-lived, however. The polar component begins to decline within one or two hours at all temperatures and decreases at a temperature dependent rate. The most plausible explanation of this effect is that the increasing amount of chemically bonded molecules is masking the underlying polar molecules by sweeping out an increasing volume over the polar surface. This mechanism is supported by a linear decrease in polarity with increased chemical bonding as shown in Fig. 21.

The alternate interpretation of this figure, that the reorientation of the molecules which lowers the polarity is the rate limiting step for the chemical bonding, is rejected since a large number of molecules would initially orient polar end "down" and initial rates would not be so dependent on overturning. Moreover, the three-dimensional structure necessary to support the overturning theory requires close packing of the molecules which would quickly lead to dimerization, rendering overturning functionless.

The masking argument is fully compatible with the observation that the extracted film contact angles are usually 2-4° higher than the water contact angles on the corresponding unextracted films. This increase could be caused

by the removal of a small amount of monomers physically adsorbed to the swinging chains and oriented with polar group outward. Another explanation perhaps is that the underlying monomer-dimer layer hinders the rotation of the chemically bonded molecule. When this underlying layer is removed, the

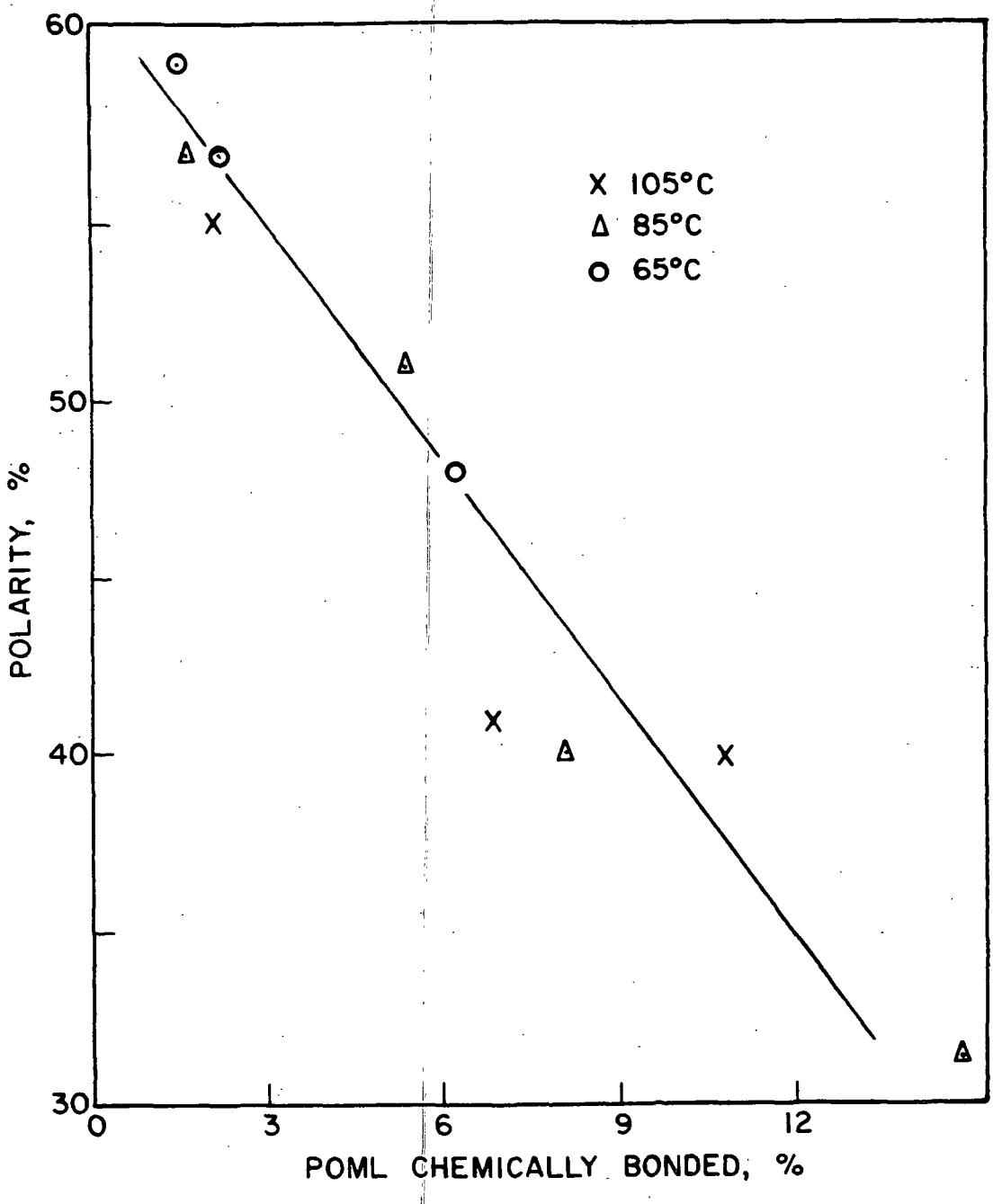

Figure 21. Relationship Between Fractional Polarity and Chemical Bonded Coverage for Unextracted Films

chains can more effectively mask the surface and result in a slightly higher water contact angle.

As chemical bonding progresses, the water contact angle increases linearly as each newly anchored molecule masks another portion of surface. At about 55°, the slope of the contact angle vs. time curve changes abruptly as mentioned above. This break occurs at 6 and 24 hours of adsorption at 105 and 85°C, respectively. From Fig. 13 it is evident that this change occurs in both cases at approximately 8% POML chemically bonded coverage. Since the area per molecule in a tightly packed monolayer is 20.1 A^2 (54), 8% monolayer coverage is equivalent to 250 A^2 per molecule on a planar surface. An estimate of the real area per molecule on these cellulose films is the product of the estimated roughness factor (1.6 to 8.0, see page 31) and this planar area per molecule. Therefore, the real area per molecule is estimated to be 400 to 2000 A^2 at the break in the contact angle curve depending on the roughness factor. Stearic acid molecules would sweep out this range of areas if they inclined between 27 and 90° from the perpendicular and swept out a conical volume. An actual inclination within this range seems reasonable and would allow each portion of the surface to be masked by a chemically bonded molecule at 8% POML coverage.

The break in the water contact angle rate may come at a higher angle (and higher surface coverage) as the adsorption temperature is lowered. This could be a result of a smaller angle of inclination at lower temperatures, due to less kinetic energy of the swinging chain, leading to closer packing before interaction.

This interaction interpretation suggests that up to approximately 8% POML each newly bonded molecule sweeps out and masks new surface but that above this coverage, a significant change in mechanism occurs. The prime difference is considered to be that the anchored molecules are now in close proximity. The molecules added above 8% POML no longer mask new area but increase the packing density above a portion of the surface. Each added molecule, therefore, has less effect on the contact angle.

This concept also introduces the increased possibility of monomers orienting with the polar group outward either by physically adsorbing along an anchored chain or simply by being oriented by the "forest" of chemically bonded molecules. These monomers could then reorient slowly and increase the water contact angle. Another factor which would increase the difficulty of developing repellency above 8% POML is the small size of the water molecule which allows them to penetrate the adsorbed structure even with high packing densities. All these effects would tend to lower the rate at which the water contact angle increases and may explain the decreased rate above 55°.

INTERMEDIATE DEVELOPMENT OF WATER REPELLENCY

From 55 to 70°, the water contact angle increases at a second, slower rate. Continuing chemical bonding contributes to this increase but at a reduced efficiency as suggested above. There is significant evidence that the chemical bonding reaction slows considerably after about 23% chemically bonded POML or about 70° water contact angle. It is at this coverage that methylene iodide contact angles on extracted films stop their linear increase. An approximate linearity between the methylene iodide contact angle and surface concentration of chemically bonded stearic acid on metals has been reported by

Timmons (80). As this is also found (Fig. 16b) for the similar case on cellulose, the almost complete halt of the increasing methylene iodide contact angle on extracted film strongly suggests a significant reduction in the rate of chemical bonding on the surface.

There are two possible causes for the reduction in the reaction rate. Steric hindrance of the reaction is easily visualized as the concentration of chemically bonded molecules increases. Also, as the perpendicularly oriented structure of physically adsorbed molecules grows, more and more molecules become adsorbed in this "forest" and are not available for reaction.

FINAL DEVELOPMENT OF WATER REPELLENCY

In the 105°C adsorption from 72 to 290 hours, experimental data are neither complete nor indisputable. However, contact angles on unextracted film were determined on a 290-hour sample. The saturated methylene iodide contact angle remained unchanged from the 24-hour value but the water contact angle increased to 90°. This is interpreted to be a result of continued physical adsorption of molecules into the "forest" of hydrocarbon tails. The packing density of the methyl surface over the cellulose had increased to the point where the water did not penetrate it significantly. The amount of chemically bonded acid, extracted contact angles, and extractable amounts of acid were not satisfactorily determined on this film.

After only 168 hours of adsorption, however, the amount of stearic acid removable by benzene was up to 29,000 cpm/sq inch or 290% POML as opposed to 100% POML during the equilibrium period. This could be additional evidence that an oriented molecular structure holding more stearic acid/sq inch is present on the surface.

OVERALL CONSIDERATIONS ON WATER REPELLENCY DEVELOPMENT ON CELLULOSE FILM

The development of water repellency by vapor-phase adsorption of stearic acid is very slow and apparently very inefficient where a truly repellent angle of 90° is required. The time required to reach 90° and the penetration which occurs during this time may be unique to high temperature vapor-phase sizing techniques.

The difficulty in attaining a 90° water contact angle may be that an actual contraction of the monolayer coverage occurs when the sample is cooled. At 105°C, for example, the energy of the chemically bonded molecule will cause it to sweep out a larger area than it does at 20°C where the contact angles are measured. At the high temperatures, therefore, the film may be actually water repellent if a contact angle could be measured significantly at that temperature. At room temperature, water would penetrate the layer readily between the smaller volumes swept out at the lower energy level.

A significant increase in repellency is found over the first linear region. This increase is highly temperature dependent and very similar to the rate of chemical bonding as shown in Table VI, where 65°C data are normalized to 1.0.

TABLE VI

COMPARISON OF RATES OF CHEMICAL BONDING AND RATE OF DEVELOPMENT OF REPELLENCY

Temperature, °C	Rate of Chemical Bonding, %POML/hr	Rate of Contact Angle Increase, °/hr
65	1.0	1.0
85	3.3	3.0
105	9.6	8.7

This is further evidence that the chemical bond is the key to increasing the water contact angle. This is a significant departure from expected results, i.e., the physically adsorbed molecules apparently do not contribute to the development of the water contact angle. This is most likely due to the reclining nature of the physically adsorbed species. While the surface of the hydrocarbon tail is indeed water repellent, the water can encompass the chains and contact the cellulose.

The various mechanisms suggested by this work for the development of the water contact angle during 105°C adsorption are summarized in Table VII as a function of the approximate water contact angle range in which they operate.

TABLE VII

SUMMARY OF PROPOSED MECHANISMS OF REPELLENCY DEVELOPMENT DURING 105°C ADSORPTION

Water Contact Angle Range	Mechanisms of Repellency Development on the Surface of Cellulose Film
28-55	Physically adsorbed molecules, primarily dimeric, recline on the surface and do not contribute to repellency. Chemically bonded molecules sweep out conical volumes. Increase in repellency caused by chemical bonding increases. Amount of surface masked by swinging hydrocarbon tails determines the contact angle.
55-70	Additional chemically bonded molecules no longer mask new surface but increase packing density of methyl surface. Chemical bonding continues at a constant rate up to approximately 70° and slows considerably. Reduction in rate may be due to steric hindrance at reaction site or a decline in the amount of physically adsorbed acid at the reaction site. Good possibility that increasing amounts of physically adsorbed molecules are becoming entangled in a three-dimensional adsorbed structure on the surface. This structure is evolving as a result of the close proximity of the chemically bonded molecules and their ability to perpendicularly orient physically adsorbed molecules.
70-90	Chemical bonding very slow, if present. Unextracted water contact angle increases slowly as molecules adsorb into molecular "forest" and slowly increase packing density.

Migration of acid into the porous structure, and the penetration into the film occur concurrently with these surface reactions.

PARTICIPATION OF STEARIC ACID AT THE WATER-CELLULOSE INTERFACE

The exact amount of stearic acid on the film participating in the mechanism for increasing the water contact angle cannot be determined from this work. Since physically adsorbed molecules are most likely unequally distributed over the surface, it is only reasonable to assume that the chemically bonded molecules would be also. Since this would lead to more chemically bonded acid in the asperities, which are precisely the locations that do not contribute to the repellency at the water-cellulose interface, the results only limit the amount of adsorbed molecules required for any degree of repellency.

The determination of the true percentage monolayer coverage from the results of this work is also difficult even if equal distribution of the molecules on the surface is assumed. The %POML must be corrected for the exact roughness factor of the surface and for the actual area effectively masked per molecule, both of which are unknown.

For the above reasons, it is not possible to determine how much coverage is required to develop a set amount of repellency.

THE CHEMICAL BOND

No direct evidence of the formation of a chemical bond between cellulose and stearic acid has been established in this work. However, the evidence is quite strong that 1) the stearic acid molecules do anchor to the cellulose in some manner, 2) this anchoring is both temperature and time dependent, 3) the polar group is the interacting element, and 4) the anchored molecules can be

removed by hot sodium hydroxide treatment. This is considered to be sufficient evidence to demonstrate the existence of a chemical linkage between the stearic acid molecule and cellulose. Furthermore, it is assumed that this linkage is an ester bond formed between the alcoholic cellulose hydroxyls and the acid carboxyl group.

The analysis of the experimental data to determine the rate-controlling step for the bonding process is complex and the results are relatively inconclusive. However, the following possible pathway is consistent with the data and suggests a plausible kinetic order.

Stearic acid in the vapor phase has been shown to be primarily monomeric (Appendix I). The normal pathway from vapor-phase monomer to cellulose stearate must pass through diffusion of the monomer to the surface, dimerization, dissociation, and bonding. This is illustrated in the reaction diagram shown in Fig. 22.

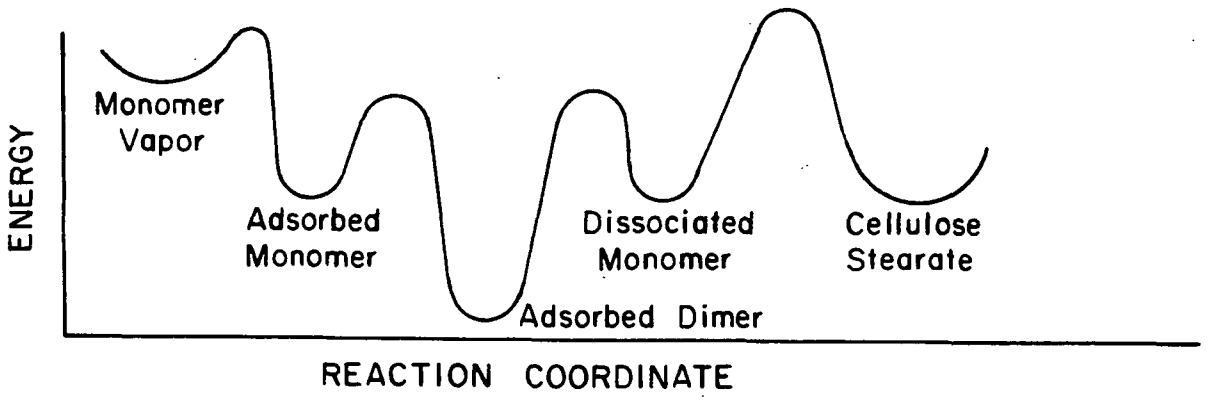

Figure 22. Proposed Reaction Diagram

As monomer units become associated with the surface, they give up sensible heat equal to ΔH_{-ads}, the heat of adsorption. The adsorbed monomers quickly dimerize and release additional energy as the heat of dimerization. The adsorbed dimer is in the lowest energy — and most stable — state. However, the

dimer does dissociate in some equilibrium with the monomer which can then react with cellulose by passing over the energy barrier equal to the energy of activation of the esterification reaction. The heat of reaction passing from the monomer to the stearate is probably near zero since the same type and number of bonds are broken as are formed. It is possible that some monomers may react directly with the surface hydroxyls without intermediate dimerization.

The overall equation for the reaction may be written as shown in Equation (13),

$$MCOOH + HOR \longrightarrow MCOOR + HOH \qquad (13)$$

where MCOOH is the monomer unit and R the cellulose chain. Therefore, the generalized rate equation is $\underline{v} = \underline{k}(MCOOH)^{\underline{p}}(ROH)^{\underline{q}}$ where $\underline{p}$ and $\underline{q}$ are dimensionless constants, $\underline{v}$ is the rate of reaction, and $\underline{k}$ the reaction rate constant. The assumption is made that the concentration of possible hydroxyl bonding sites is much greater than the number consumed in the reaction. The effective concentration of (ROH), therefore, does not change during the time of kinetic measurements. The rate equation is simplified then to $\underline{v} = \underline{k}'(MCOOH)^{\underline{p}}$, where $\underline{k}' = \underline{k}(ROH)^{\underline{q}}$.

In order to determine whether the proposed reaction system provides a reasonable value of $\underline{p}$ for this mechanism, a rough estimate of the monomer concentration in the adsorbed phase can be made. This requires several assumptions.

1. The energy of dissociation of the dimer on the surface lies somewhere between the ΔH_{diss} in the vapor phase (14,000 cal./mole) and the ΔH_{diss} in benzene (8000 cal./mole) (82). This assumes that the heat of interaction of monomer with benzene is greater than the heat of interaction of monomer with dimer (the "solvent" in the stearic acid melt).

2. The ΔS for dissociation is the same for the dimer in benzene as for the dimer in the liquid state of the fatty acid. This is an order of magnitude approximation. This ΔS value is 12 e.u. (82).

3. Monomer-dimer equilibrium in the surface region is described by the function $K_{eq} = X_m^2/X_d$, where X_m and X_d are the mole fraction of monomer and dimer, respectively.

4. The change in k' with temperature is small compared to the change in monomer concentration with temperature.

When the free energy of reaction, $\Delta G^\circ (= \Delta H^\circ - T\Delta S^\circ)$ is calculated and in turn used to determine K_{eq}, ($\text{Log}_{10} K_{eq} = -\Delta G^\circ/2.303RT$), the mole fractions of monomer and dimer can be estimated. These calculations are summarized in Appendix X. The values thus determined substantiate the expectation that the stearic acid in the surface region is overwhelmingly dimeric. When the monomer mole fraction, X_m, is multiplied by the total adsorption in %POML at each temperature, a relative value of the monomer concentration on the surface at each temperature is obtained. When this surface monomer concentration is used in the rate equation and Log v plotted vs. Log (MCOOH), the slope of the line, p, is 1.2 and 1.7 for ΔH_{diss} of 14,000 and 8000 cal./mole, respectively. This suggests 1) the monomer-dimer equilibrium in the adsorbed layer can provide the right order of magnitude of monomer concentration for first-order kinetics in (MCOOH), and 2) the ΔH_{diss} of 14,000 cal./mole is most likely for $p = 1$.

These calculations can be carried one step further to determine the Arrhenius energy of activation, E_a. If this first-order kinetics with respect to monomer is accepted, then the rate constant k' is equal to $v/(\text{MCOOH})$. If ln k' is plotted vs. $1/T$ for each temperature, an E_a of 2450 cal./mole is

obtained. This should represent a very rough approximation of the energy required in the rate-controlling step to form the ester linkage.

The mechanism of formation of the reaction product will determine the $\underline{E}_a$ of the reaction. Ingold (83) describes two acid-catalyzed mechanisms for esterification of carboxylic acids in solution. These reactions are labelled $A_{AC}1$ and $A_{AC}2$ and are analogous to the S_N1 and S_N2 mechanisms.

The applicability of either mechanism to vapor-phase reaction is not certain. The acid catalysis is considered probable in view of dissociation of the monomer acid and the presence of water in the system.

These mechanisms will vary considerably in energy of activation. In the $A_{AC}1$ mechanism complete bonds must be broken to form the carbonium ion, hence $\underline{E}_a$ values of about 20,000 cal./mole would be required by this route. The intermediate transition state of the $A_{AC}2$ mechanism would not require as great an $\underline{E}_a$. Hiller (84) determined an energy of activation of 11,000 cal./mole for the acetylation of cellulose in solution, and felt his data supported the $A_{AC}2$ type mechanism. This type of intermediate is also suggested by Roberts and Urey (85) for the esterification of carboxylic acids.

The low value of the energy of activation from the above speculative calculations may reflect a low $\underline{E}_a$ consistent with the $A_{AC}2$ mechanism. A rate-limiting step of breaking intramolecular hydrogen bonds in the cellulose chain or formation of the $A_{AC}2$ reaction intermediate itself would result in a low activation energy.

This kinetic model readily accounts for the zero-order reaction rate with time since the monomer concentration at the surface would be maintained by the dissociation equilibrium at each temperature. However, the reaction does

$A_{AC}1$

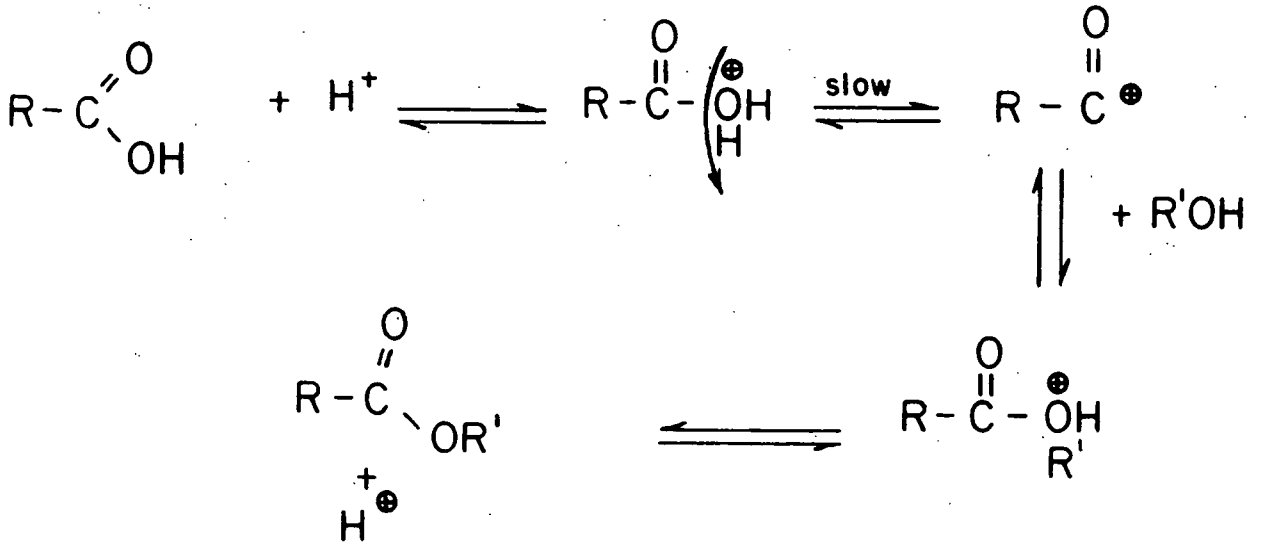
R - C
O
OH
+ H+
R - C
OH
H
slow
R - C
+ R'OH
R - C
OR'
H
R - C
OH
R'

$A_{AC}2$

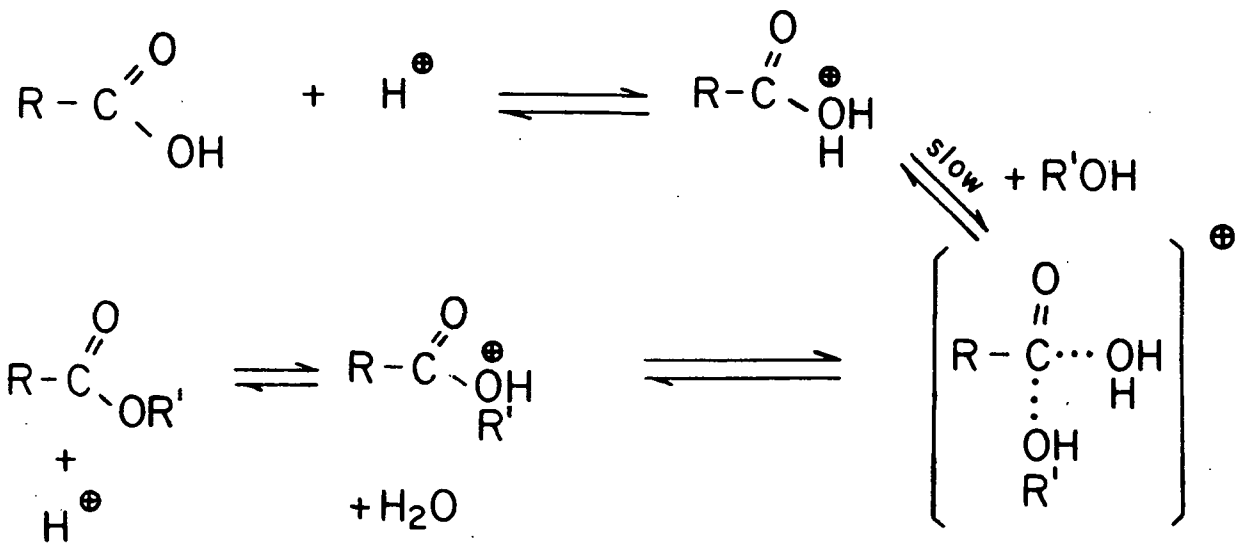
R - C
O
OH
+ H
R - C
OH
H
slow
+ R'OH
R - C
OR'
H
R - C
OH
R'
+ H2O
R - C ··· OH
H
OH
R'

slow markedly after about 23% POML coverage. This is attributed to steric hindrance developing from the concentration of chemically bonded molecules on the surface, and from a tendency of the physically adsorbed molecules to become associated with the tails of the chemically reacted molecules and become unavailable for surface reactions.

Correlations between other variables and the reaction rate have eliminated consideration of some alternate possible schemes: 1) The rate is proportional to surface concentration (primarily dimer) to the 3.2 power. This unusually high order means the dimer is an unlikely participant in the rate-limiting step. 2) The possibility that increased adsorption with temperature is in multilayers and rate increases are due only to increases in $\underline{X}_{\underline{m}}$ at a constant interfacial area is rejected since $\underline{p} = 1.9$ for this relationship. A mechanism involving the second order of the monomer concentration in the rate-controlling step seems improbable. Finally, 3) direct reaction with vapor monomer is rejected since $\underline{p} = 0.45$ for this scheme, which is improbable for a mechanism involving a simple gas species. The plots used for evaluation of $\underline{p}$ are included in Appendix X.

EVALUATION OF THE SURFACE ENERGY PARAMETER

Methylene iodide contact angles were measured in this work to add the dimension of surface energy parameter to the interpretation of results. The parameter values have proved to be quite consistent and useful in visualizing the adsorption process. Other than the first short increase in measured polarity, the results are exactly as predicted for this adsorption system. The water contact angle behavior is totally consistent with the surface energy parameter. This is important to the overall picture and adds confidence to the evaluation of the system.

However, there are some disconcerting results from the methylene iodide data. First, a model-for-wetting approach (see Discussion, p. 102) for methylene iodide on extracted films gives calculated angles far too high. Second, the methylene iodide contact angles show no effect at the 8% POML point where water angles show a sharp break in slope. Finally, methylene iodide contact angles decrease when films are extracted whereas water angles increase.

This behavior is interpreted as evidence that the hydrocarbon tails of the stearic acid dissolve in the methylene iodide. Interaction between water and hydrocarbon tails is very slight since a contact angle of 108° exists between the water and methyl surfaces. A greater attraction exists between methylene iodide and methyl groups as evidence by a 70° contact angle of methylene iodide on pure methyl surfaces (80).

If the stearic acid tails dissolve in methylene idodide, the contact angle would depend on the concentration of the acid at the interface and not on any masking ability of the hydrocarbon chains. Therefore, the wetting model approach would not operate correctly and the contact angles would be expected to decrease when the films are extracted as a result of reduced concentration.

When this solubility is considered, the meaning of the Owens-Wendt parameters becomes questionable since the two liquids are forming angles against different surfaces. As mentioned previously, the Owens-Wendt equations were developed for a two-component system and the presence of the third component at the interface presents fundamental difficulties. However, the agreement of the surface parameter with expected behavior, the consistency of the data, and the linearity of the methylene iodide contact angles with surface coverage all suggest a meaningful empirical interpretation of the parameter value is valid. It is reemphasized that units are purposefully omitted from the

parameter to discourage any interpretation of the value as a surface energy measurement.

It is important to note that the methylene iodide contact angles have become increasingly valuable as a measure of surface concentration of stearic acid.

CONSIDERATIONS ON THE DIMERIZATION AND ORIENTATION OF PHYSICALLY ADSORBED MOLECULES

In the preceding sections, the physically adsorbed molecules have been presented as 1) primarily dimeric, and 2) reclining on the surface. Extensive dimer character is inferred from the thermodynamically preferable association of monomers into a lower energy state and is supported by the speculative calculations presented in the section on the chemical bond.

The orientations of the physically adsorbed molecule which must be considered are complicated by the existence of several possible species on the surface. A true monomer present on the surface could either recline or hydrogen bond to the cellulose and act as a chemically bonded molecule in sweeping out a volume. Likewise, dimers could totally recline or conceivably exhibit the same type of tail swinging mechanism if sufficient attraction existed between the dimer carboxyl center and the cellulose surface. This attraction could be a form of hydrogen bonding between a cellulose hydroxyl and some electronegative element of the carboxyl ring structure, or possibly could be a true hydrogen bond between cellulose and one monomer unit, which in turn is hydrogen bonded to the second monomer unit by a single hydrogen bond. The model evolving in these schemes is one with a much more perpendicular orientation of the physically adsorbed molecules.

This concept is rejected by the following argument. The water contact angle is highly dependent on the molecular packing of oriented molecules as shown in Fig. 15. Here, the water contact angle varies strongly with surface coverage as the chemically reacted population on the extracted film increases. Therefore, if physically adsorbed or hydrogen bonded molecules extend perpendicularly from the surface, the concentration of methyl groups at the water-hydrocarbon interface would be greatly increased and the water contact angle should be much greater on unextracted films. This is not so. Furthermore, if these molecules overturned rapidly, the contact angle should be much smaller on unextracted films than on extracted films due to the polar groups at the interface. This is not found. The obvious conclusion is that the physically adsorbed molecules are not present at the water-hydrocarbon interface in the unextracted film, i.e., they must be reclining on the surface. The possibility that the physically adsorbed molecules reorient immediately upon contact with water to form a relatively stable interface with the water and exhibit the same water contact angle as found on extracted films is improbable. This would require that the attraction of the polar groups toward water be identically offset by the added water repellency of the tails of the nonreoriented molecules — an improbable event.

The existence of significant amounts of hydrogen bonds between stearic acid and cellulose therefore becomes more difficult to accept since the hydrogen bonded molecule should act in the same manner as the chemically anchored monomer, i.e., increase the water contact angle. Only two possibilities exist in view of the fact that extracted and unextracted films exhibit the same contact angle with water. Either, 1) hydrogen bonded molecules are not removed by water and are counted as chemically bonded molecules, or 2) hydrogen bonding of monomer to cellulose does not occur in this system.

The disruption of hydrogen bonds by water seems probable. Moreover, the response of the hypothesized chemical bonds to temperature and caustic suggests a chemical bonding nature to the attraction. However, the energy of activation of 2450 cal./mole calculated for the bonding process could support a hydrogen bonding interpretation.

The overall analysis supports the probability of chemical bonding, and the disruption of any hydrogen bonds during water extraction. This leads to the logical, but difficult, conclusion that monomer-cellulose hydrogen bonds are not a significant phenomenon, and water-extracted acid is removed by swelling of the cellulose structure only.

This possibility is supported by the fact that dimerization is probably an energetically preferable state for a monomer on the surface since dissociation of the dimer may require as much as 14,000 cal./mole, whereas disruption of a single hydrogen bond would probably consume only 3-5000 cal./mole. A wagging of the tails of the dimer is rejected by the same argument used for the monomer.

A MODEL OF WETTING FOR THE EXTRACTED SYSTEM

According to the mechanism of repellency proposed in the previous sections, the chemically bonded molecule is the key to development of repellency. The following argument utilizes this model and makes several assumptions to calculate a water contact angle which is in excellent agreement with the observed water contact angles. This agreement strengthens both the model and the assumptions.

The extracted film is considered to consist of a cellulose surface with chemically bonded molecules adsorbed on it. No unreacted stearic acid is present. The water contact angle on pure cellulose was determined to be 28°,

the water contact angle on pure methyl groups is reported as 108° (31), and the polarity of the pure cellulose surface was found to be 0.44 in this work.

The following assumptions are made:

1. The reduction in polarity of the cellulose surface by adsorption of stearic acid is caused by masking of the polar cellulose surface by the swinging hydrocarbon tail of the acid.
2. The fraction of the surface effectively masked by the hydrocarbon tail is proportional to the reduction in the polarity of the surface as determined by the Owens-Wendt equations.
3. Portions of the surface effectively masked by the acid tails exhibit a 108° water contact angle, and the unmasked cellulose surface will exhibit the normal 28°.
4. The measured contact angle is an arithmetically averaged sum of the two contact angle regions weighted for the proportion of the surface exhibiting each contact angle, i.e.,

$$\frac{\text{calculated water}}{\text{contact angle}} = \left(\frac{\text{polarity}}{0.44}\right) \times 28° + \left(\frac{0.44 - \text{polarity}}{0.44}\right) \times 108°$$

When this model is applied to the 105°C adsorption data, the measured and calculated contact angles compare exceedingly well as shown in Table VIII.

This excellent agreement, especially below 24-hours adsorption time, lends credence to the model, the Owens-Wendt calculations, and the assumptions.

TABLE VIII

COMPARISON OF CALCULATED AND MEASURED WATER CONTACT ANGLES FOR WETTING MODEL

Adsorption Time, hr	Measured Angle	Calculated Angle
1	36.5 ± 1.7	37.1
3	43.4 ± 1.5	42.6
6	55.4 ± 2.2	56.7
12	56.5 ± 3.3	53.6
24	67.7 ± 3.0	68.0
36	70.1 ± 1.4	73.5
48	71.3 ± 1.7	75.0
72	75.1 ± 1.6	77.0

APPLICATIONS TO PAPER SIZING

As mentioned previously, Swanson (70) determined the size times on paper handsheets treated by vapor-phase adsorption of stearic acid at 50, 65, 85, and 105°C. The size time *vs.* adsorption time results for his work are presented in Fig. 23. There are several correlations between sizing development on paper and the rate of contact angle development on cellulose film. In both cases repellency increases to an essentially constant level and remains there. Furthermore, the time required to reach this level is temperature dependent and similar as shown in Table IX.

These results indicate that the two systems respond similarly in the overall view despite major differences between sizing and contact angle mechanisms.

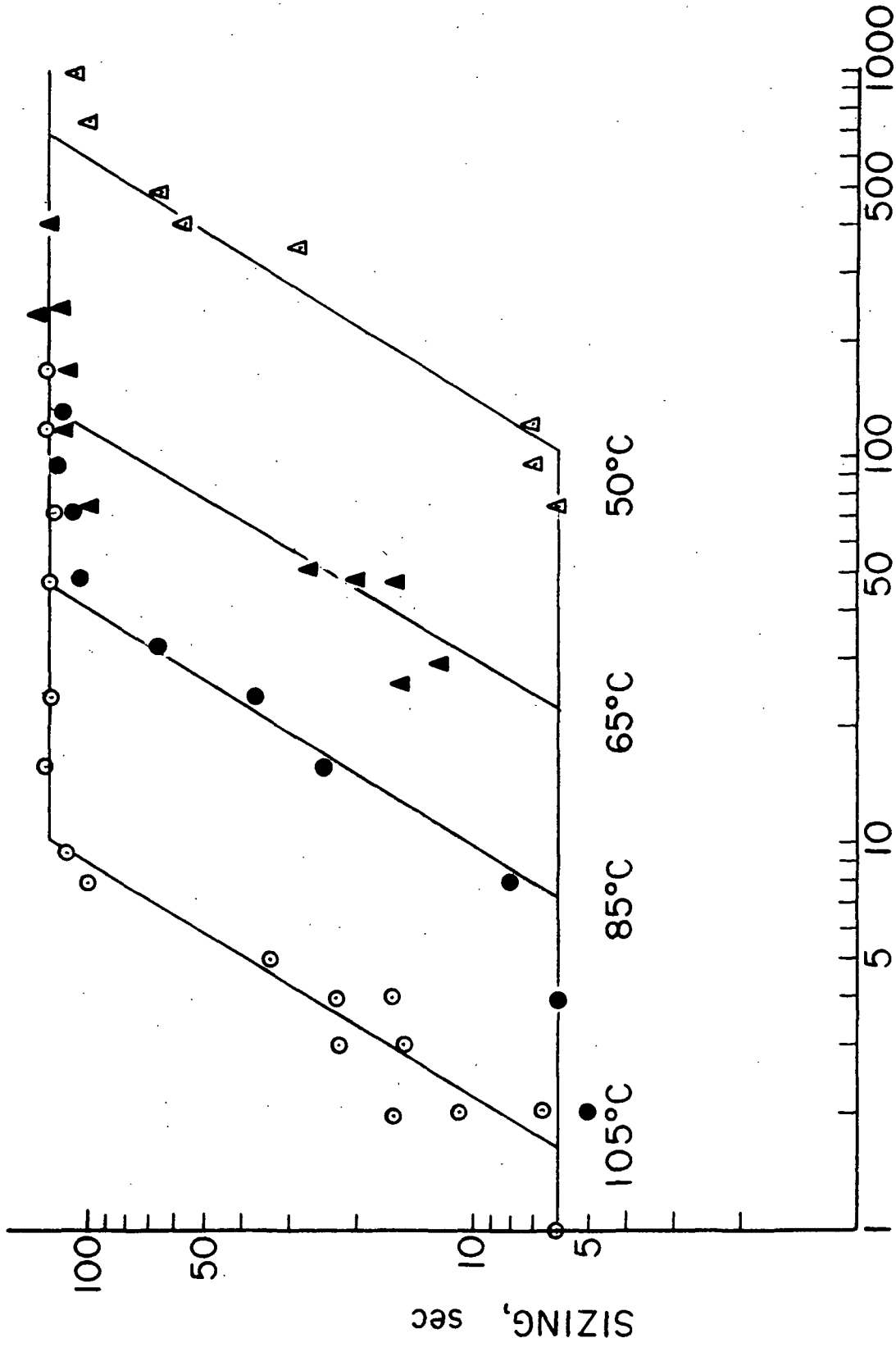

Figure 23. Development of Sizing in Paper Handsheets Exposed to Vapor-Phase Stearic Acid (70)

TABLE IX

CORRELATION BETWEEN SWANSON'S PAPER SIZING DATA AND CELLULOSE FILM CONTACT ANGLE DATA

Temperature, °C	Hours to Reach Plateau	
	Paper	Film
65	130	168
85	48	24
105	10	9

When the paper samples corresponding to the maximum exposure times were extracted in benzene and dried, the paper became totally water repellent. This could possibly occur if the polar groups of the physically adsorbed molecules reoriented toward the water interface during the long periods of the size test. This would cause a lowering of the effective contact angle and a poor size time. However, when the sheet was extracted, the chemically bonded molecules developed and maintained sufficient repellency to provide an essentially infinite size time. A 90° water contact angle would not be required for complete repellency. The Cassie-Baxter equation indicates the apparent contact angle could exceed 90° due to the porosity of the fibrous sheet.

Another aspect of paper sizing which this work may reflect upon is the theory of self-sizing in paper. This term refers to the gradual sizing development in initially unsized paper stored for long periods of time at elevated temperatures. The cause of this increased repellency has been thought to be a vapor-phase transport of fatty acid material from the fines in the sheet to the paper surface. As these materials deposited onto the surface, they were thought to increase repellency and, hence, the size time.

This work suggests that this may not be the entire story. Both the vapor-phase diffusion of fatty materials to the fiber surface and the chemical bonding reaction are temperature dependent and may play a part in the self-sizing process. Separate experiments would be required to distinguish between the two mechanisms to determine which is limiting the development of water repellency.

SUMMARY OF CONCLUSIONS

The adsorption of stearic acid from the vapor phase onto cellulose film does increase the water repellency of that film in a predictable manner. The amount of acid picked up by the film increases with temperature in a system where concentration of acid in the vapor is directly dependent on temperature. The cellulose film adsorbs stearic acid in three distinct adsorption regions: an initial drive toward equilibrium with the vapor, an equilibrium region which may extend over days at lower temperatures, and finally a period during which penetration of stearic acid into the film occurs. Equilibrium acid concentrations are established quickly on the film surface and maintained into the penetration region. The migration of physically adsorbed acid into surface pores and asperities is quite marked, while the equilibrium surface coverage on the external surfaces is maintained.

A chemical bond is formed between the stearic acid molecule and the cellulose surface. The rate of this esterification reaction is zero order with time and depends strongly on temperature. The reaction may be first order with monomer stearic acid concentration on the surface. The reaction rate at 105°C has been found to be constant up to 24 hours of adsorption or 23% POML. Above this level, the reaction is very slow and cannot be analytically followed due to the complexities caused by the penetration phenomenon.

The water contact angle on pure cellulose film is 28°. The water contact angle on treated films increases in three stages, each a function of the rate and extent of chemical bonding and approaches 90° only after 290 hours at 105°C. There is evidence that the physically adsorbed molecules do not increase the water contact angle to any significant degree.

The development of water repellency by extremely small numbers of chemically bonded molecules is explained by assuming the swinging hydrocarbon tails of the bonded molecules sweep out a conical volume about the bonding site. A reasonable angle of inclination of the swinging molecular chains from the perpendicular adequately explains the water contact angle data.

The Owens-Wendt equations for surface energy adapted well to an estimation of a surface energy parameter and confirmed expected results. However, fundamental difficulties in the treatment of the third component at the interface make its usefulness highly questionable.

SUGGESTIONS FOR FURTHER RESEARCH

The possibilities for further work in this area are numerous and only a few are suggested below.

Directly related to this work is the search for direct proof of a chemical bond between stearic acid and cellulose. ATR techniques on the infrared spectrophotometer have been tried in this work. The results were not straightforward and additional effort would be required to determine if this technique is useful.

A very valuable contribution could be made by determining exact stearic acid vapor pressures at the operating temperatures. This could lead to adsorption isotherms over a range of partial pressures. This information is extremely vital to the interpretation of the adsorption mechanism.

An extremely challenging problem is a determination of the monomer-dimer equilibrium on the surface — especially at low coverages. The monomer concentration appears very important in the reaction mechanism. Along with this, a study of chemical reactions at the vapor-solid interface would be interesting in terms of energy of activation and molecular orientation.

Methods to increase the rate of reaction should be studied if any useful technique is to come from this concept. Pretreatment of the films with alum is an enticing experiment to consider.

The change in the water contact angle with drop-aging time at different surface coverages would make a real contribution to this area. The water contact angles in this work are only initial values. The ability of a specified surface coverage of bonded molecules to maintain water repellency with time is certainly of profound importance.

The role of porosity in promoting repellency must be determined. Does a more porous surface become nonwettable faster than a nonporous surface? How much planar repellency is required to provide total repellency to paper?

This system also provides a basis to compare the efficiency of different sizing molecules on the grounds of reactivity and geometry.

The paths are numerous and challenging and all contribute directly to an important aspect of papermaking.

NOMENCLATURE

cpm	counts per minute
f_1	Cassie-Baxter roughness factor, dimensionless
f_2	Cassie-Baxter porosity factor, dimensionless
MI	methylene iodide
POML	Planar Oriented MonoLayer
r	Wenzel's roughness factor, dimensionless
RH	relative humidity
SMI	saturated methylene iodide
W_A	work of adhesion, ergs/cm^2
W_C	work of cohesion, ergs/cm^2
γ	surface free energy, ergs/cm^2
γ_{12}	interfacial free energy between Phases 1 and 2, ergs/cm^2
γ_c	Zisman's critical surface tension, dynes/cm
γ_i^d	dispersion force component to the surface free energy of substance i, ergs/cm^2
γ_i^p	polar component to the surface free energy of substance i, ergs/cm^2
γ_l	liquid surface free energy, ergs/cm^2
γ_s	solid surface free energy, ergs/cm^2
γ_{sl}	solid-liquid interfacial free energy, ergs/cm^2
γ_{sv}	solid-vapor interfacial free energy, ergs/cm^2
π_e	equilibrium film pressure of adsorbed vapor, ergs/cm^2
θ	contact angle, degrees
θ_A	apparent contact angle, degrees
θ_o	true contact angle, degrees

ACKNOWLEDGMENTS

The author is deeply indebted to a great many persons for their aid and advice during the period of this work. First and foremost, thanks are due to Dr. J. W. Swanson, under whose challenging guidance this work was performed. Dr. D. G. Williams and Dr. D. B. Easty also contributed significantly as members of the Thesis Advisory Committee. Counsel of Dr. R. H. Atalla is also acknowledged. Members of the Institute staff who gave unselfishly of their time and effort include Don Beyer, John Church, Marvin Filz, Hillka Kaustinen, Fred Sweeney, and Paul Van Rossum. To these persons I am tremendously indebted. However, it is no overstatement that every member of the Institute faculty and staff with whom I have worked has helped generously and without reservation.

The financial support of the Institute and its member companies is gratefully acknowledged.

Finally, my wife, Virginia, must be thanked for her unswerving support and patience as well as for her professional help in preparing the final manuscript.

LITERATURE CITED

1. Johnson, R. E., J. Phys. Chem. 63(10):1655-8(Oct., 1959).
2. Dupre, A. Theorie mechanique de la chaleur. p. 368-9. Paris, 1869.
3. Young, T., Phil. Trans. Royal. Soc. (London) 16:65(1805); Ref. (86), p. 2.
4. Adamson, A. W., and Ling, I. Ref. (86), p. 57.
5. Lester, G. R., J. Colloid Sci. 16(4):315-26(Aug., 1961).
6. Michaels, A. S., and Dean, S. W., J. Phys. Chem. 66(10):1790-7(Oct., 1962).
7. Bangham, D. H., and Razouk, R. I., Trans. Faraday Soc. 33:1459-63(1937).
8. Wenzel, R. N., Ind. Eng. Chem. 28(8):988-94(Aug., 1936).
9. Bartell, F. E., and Shepard, J. W., J. Phys. Chem. 57(2):211-15(Feb., 1953).
10. Bartell, F. E., and Shepard, J. W., J. Phys. Chem. 57(4):455-63(April, 1953).
11. Bikerman, J. J., J. Phys. Colloid Chem. 54(5):653-8(May, 1960).
12. Tamai, Y., and Aratani, K., J. Phys. Chem. 76(22):3267-71(Oct., 1972).
13. Cassie, A. B. D., and Baxter, S., Trans. Faraday Soc. 40(12):546-51(1944).
14. Herzberg, W. J., Marian, J. E., and Vermeulen, T., J. Colloid Sci. 33(1): 164-71(May, 1970).
15. Dettre, R. H., and Johnson, R. E., Jr., J. Phys. Chem. 68(7):1744-50(July, 1964).
16. Dettre, R. H., and Johnson, R. E., Jr., J. Phys. Chem. 69(5):1507-15(May, 1965).
17. Ruch, R. J., and Bartell, L. S., J. Phys. Chem. 64(5):513-19(May, 1960).
18. Timmons, C. O., and Zisman, W. A., J. Colloid Interface Sci. 22(2):165-71 (Aug., 1966).
19. Neumann, A. W., Haage, G., and Renzow, D., J. Colloid Interface Sci. 35(3): 379-85(March, 1971).
20. Petke, F. D., and Ray, B. R., J. Colloid Interface Sci. 31(2):216-27(Oct., 1969).
21. Herzberg, W. H., and Marian, J. E., J. Colloid Interface Sci. 33(1):161-3 (May, 1970).
22. Ellison, A. H., and Zisman, W. A., J. Phys. Chem. 58(3):260-5(March, 1954).
23. Fox, H. W., and Zisman, W. A., J. Colloid Sci. 7(2):109-21(April, 1952).

24. Fox, H. W., and Zisman, W. A., J. Colloid Sci. 7(4):428-42(Aug., 1952).

25. Ray, B. R., Anderson, J. R., and Scholz, J. J., J. Phys. Chem. 62(10): 1220-7(Oct., 1958).

26. Bernett, M. K., and Zisman, W. A., J. Phys. Chem. 63(8):1241-6(Aug., 1959).

27. Hoernschemeyer, D., J. Phys. Chem. 70(8):2628-33(Aug., 1966).

28. Shafrin, E., and Zisman, W. A., J. Phys. Chem. 76(22):3259-66(Oct., 1972).

29. Fowkes, F. M., Ind. Eng. Chem. 56(12):40-52(Dec., 1964).

30. Girifalco, L. A., and Good, R. J., J. Phys. Chem. 61(7):904-9(July, 1957).

31. Owens, D. K., and Wendt, R. C., J. Appl. Polymer Sci. 13(8):1741-7(Aug., 1969).

32. Wu, S., J. Polymer Sci., Part C(34):19-30(1971).

33. Langmuir, I., Trans. Faraday Soc. (15):62-74(1920).

34. Bernett, M. K., and Zisman, W. A., J. Colloid Interface Sci. 28(2):243-9 (Oct., 1968).

35. Bartell, F. E., and Bristol, K. E., J. Phys. Chem. 44(1):86-101(Jan., 1940).

36. Shafrin, E. G., and Zisman, W. A., J. Colloid Sci. 7(2):166-72(Feb., 1952).

37. Langmuir, I., Science 87:493(1938).

38. Rideal, E., and Tadayon, J., Proc. Royal Soc. (London) A225:346-56(1954).

39. Yiannos, P. N. Molecular reorientation of some fatty acids when in contact with water. Doctor's Dissertation. Appleton, Wis., The Institute of Paper Chemistry, 1960. 115 p.; J. Colloid Sci. 17(4):334-47(April, 1962).

40. Rideal, E., and Tadayon, J., Proc. Royal Soc. (London) A225:357-62(1954).

41. Young, J. E., Austral. J. Chem. 8(2):173-93(May, 1955).

42. Beischer, D. E., J. Phys. Chem. 57(1):135-8(Feb., 1953).

43. Cook, H. D., and Ries, H. E., J. Phys. Chem. 63(2):226-33(Feb., 1959).

44. Bartell, L. S., and Ruch, R. J., J. Phys. Chem. 60(8):1231-4(Sept., 1956).

45. Sharpe, L. H., Proc. Chem. Soc. (London) 1961:461-3.

46. Adamson, A. Physical chemistry of surfaces. New York, Interscience, 1960. 629 p.

47. Gregg, S. J. The surface chemistry of solids. 2nd ed. New York, Reinhold, 1961. 393 p.

48. Zettlemoyer, A. C., J. Colloid Interface Sci. 28(3/4):343-69(Nov.-Dec., 1968).

49. Bigelow, W. C., Pickett, D. L., and Zisman, W. A. J. Colloid Sci. 1(6): 513-38(Dec., 1946).

50. Bigelow, W. C., and Brockway, L. O., J. Colloid Sci. 11(1):60-8(Feb., 1956).

51. Langmuir, I., J. Chem. Phys. 1(11):756-76(Nov., 1933).

52. Epstein, H. T., J. Phys. Coll. Chem. 54(7):1053-69(Oct., 1950).

53. Brockway, L. O., and Jones, R. L. Ref. (86), p. 275.

54. Gaines, G. L., J. Colloid Sci. 15(4):321-39(Aug., 1960).

55. Bartell, L. S., and Ruch, R. J., J. Phys. Chem. 63(7):1045-9(July, 1959).

56. Clint, J. H., J. Chem. Soc., Faraday Trans. I. 68(12):2239-46(Dec., 1972).

57. Back, E., and Lundin, B., Svensk Papperstid. 58(20):758-63(Oct. 31, 1955).

58. Jayme, G., and Balser, K., Papier 18(12):746-58(Dec., 1964).

59. Stone, J. E., Treiber, E., and Abrahamson, B., Tappi 52(1):107-10(Jan., 1969).

60. Borgin, K., Norsk Skogind. 13(3):81-92(March, 1959).

61. Borgin, K., Norsk Skogind. 13(11):429-42(Nov., 1959).

62. Borgin, K., Norsk Skogind. 14(11):485-95(Nov., 1960).

63. Borgin, K., Norsk Skogind. 15(9):384-91(Sept., 1961).

64. Hermans, H. P. Physics and chemistry of cellulose fibers. New York, Elsevier, 1949.

65. Bartell, F. E., and Ray, B. R., J. Am. Chem. Soc. 74(3):778-83(Feb. 5, 1952).

66. Ray, B. R., and Bartell, F. E., J. Phys. Chem. 57(1):49-56(Jan., 1953).

67. Luner, P., and Sandell, M., J. Polymer Sci., Part C(28):115-42(1969).

68. Dann, J. R., J. Colloid Interface Sci. 32(2):302-20(Feb., 1970).

69. Dann, J. R., J. Colloid Interface Sci. 32(2):321-31(Feb., 1970).

70. Swanson, J. W. Unpublished work, 1965.

71. Swanson, J. W., and Cordingly, S., Tappi 42(10):812-18(Oct., 1959).

72. Lee, S. J., and Luner, P., Tappi 55(1):116-21(Jan., 1972).

73. Panzer, J., J. Colloid Interface Sci. 44(1):142-61(July, 1973).

74. Bikerman, J. J. Surface chemistry. 2nd ed. New York, Academic Press, 1958. 501 p.

75. Neuman, R. D. The properties, structure, and multilayer deposition of stearic acid-calcium stearate monolayers. Doctor's Dissertation. Appleton, Wis., The Institute of Paper Chemistry, 1973. 206 p.

76. Brown, P. F. The role of surface chemistry in the bonding of a cellulose substrate treated in a corona discharge. Doctor's Dissertation. Appleton, Wis., The Institute of Paper Chemistry, 1971. 120 p.

77. Browning, B. L. Methods in wood chemistry. Vol. II. New York, Interscience, 1967. 436 p.

78. White, M. L. The detection and control of organic contaminants. In Goldfinger's Clean surfaces. p. 361. New York, Marcel Dekker, 1970.

79. Guide, R. G. A study of the sodium aluminate-abietate size precipitates. Doctor's Dissertation. Appleton, Wis., The Institute of Paper Chemistry, 1959. 102 p.

80. Timmons, C. O., J. Colloid Interface Sci. 43(1):1-9(April, 1973).

81. Atalla, R. H. Personal communication, 1974.

82. Allen, G., and Caldin, E. F., Quart. Rev. 7:255-78(1953).

83. Ingold, C. K. Structure and mechanisms in organic chemistry. 2nd ed. Ithaca, N. Y., Cornell University, 1969. 1266 p.

84. Hiller, L. A., Jr., J. Polymer Sci. 10(4):385-421(April, 1953).

85. Roberts, I., and Urey, H. C., J. Am. Chem. Soc. 61(10):2584-7(Oct., 1939).

86. Fowkes, F. M., Symposium Chairman. Advances in Chemistry Series No. 43. Contact angle, wettability and adhesion. Washington, D.C., American Chemical Soc., 1964. 389 p.

87. Hodgman, C. D., Chief Ed. Handbook of chemistry and physics. 42nd ed. Cleveland, The Chemical Rubber Co., 1960.

88. Pool, W. O., and Ralston, A. W., Ind. Eng. Chem. 34(9):1104-5(Sept., 1942).

89. Littlewood, R., J. Chem. Soc. 1957:2419-20.

APPENDIX I

STEARIC ACID VAPOR PRESSURE AND VAPOR-PHASE MONOMER-DIMER EQUILIBRIUM AT 65, 85, 105°C

A. LITERATURE VALUES FOR VAPOR PRESSURE

Temperature, °C	Vapor Pressure, mm Hg	Reference
225	10.0	(87)
173	1.0	(87)
158	0.25	(88)
91	0.02	(41)
60	1.42×10^{-6}	(89)

B. DATA CONVERSION

Temp., °C	Temp., °K	Vapor Pressure, mm Hg	Log_{10} V.P.	1/T
225	498	10.0	1.000	0.00201
173	456	1.0	0.000	0.00220
158	431	0.25	-0.603	0.00232
91	364	0.02	-1.700	0.00275
60	333	1.42×10^{-6}	-5.850	0.00300

C. DATA PLOT

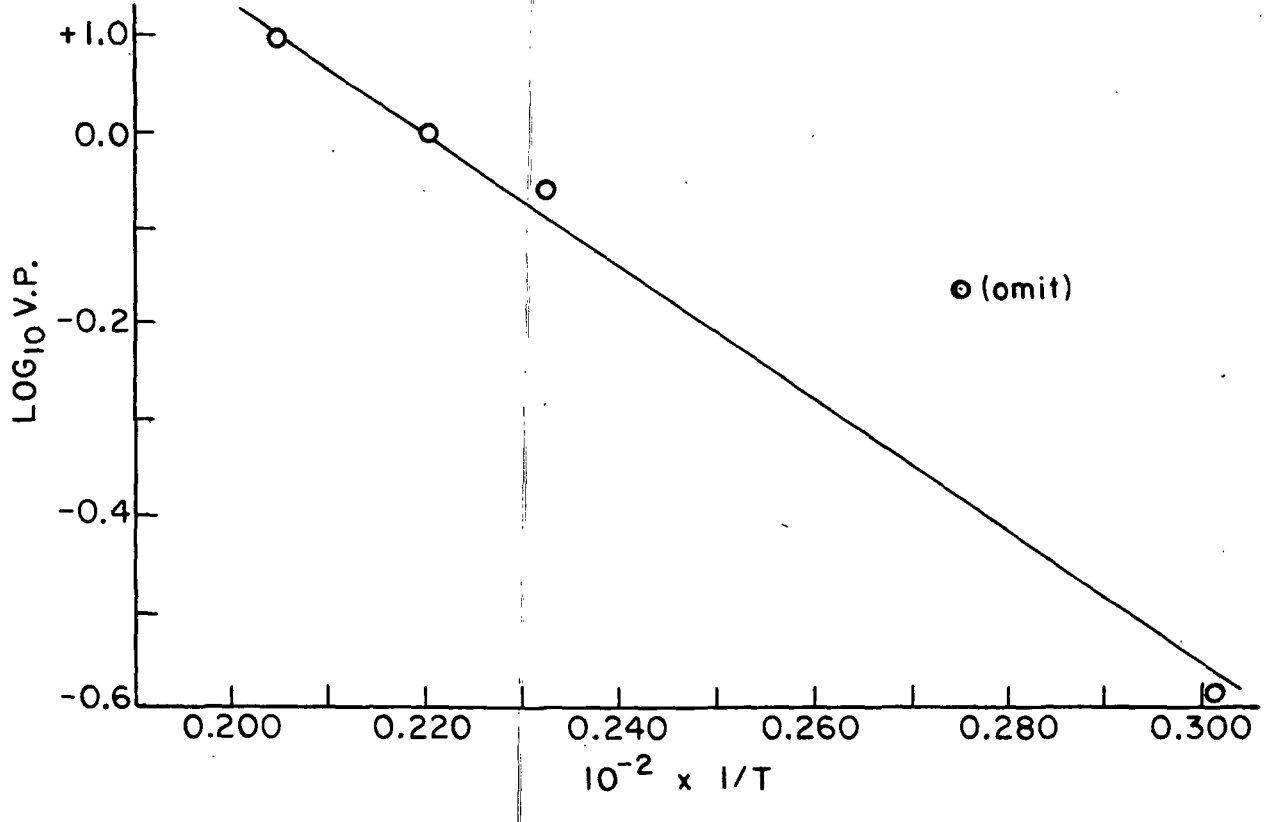

Figure 24. Data Plot for Vapor Pressure Interpolation

D. VAPOR PRESSURE ESTIMATES

Temp., °C	Temp., °K	$1/\underline{T} \times 10^{-2}$	Log_{10} V.P.	Vapor Pressure, mm Hg
65	338	0.296	-5.508	3.11×10^{-6}
85	358	0.279	-4.343	45.4×10^{-6}
105	378	0.265	-3.384	413.0×10^{-6}

E. RATIO OF VAPOR PRESSURES RELATIVE TO 65°C

Temperature, °C	Relative Vapor Pressure
65	1.0
85	14.5
105	134.0

F. VAPOR-PHASE MONOMER-DIMER EQUILIBRIUM

$\text{Log}_{10} \underline{K}_{eq} = 10.13 - 3075/\underline{T}$ for lower fatty acids. $\Delta\underline{H}_{diss}$ changes little with R in RCOOH (82). Assume valid for stearic acid.

$\underline{K}_{eq} = \underline{P}_{m}^{2}/\underline{P}_{d}$, where $\underline{P}_{m}$ = partial pressure of monomer,

$\underline{P}_{d}$ = partial pressure of dimer,

$\underline{P}_{m} + \underline{P}_{d}$ = vapor pressure at each temperature,

so, $\underline{P}_{m} + (\underline{P}_{m}^{2}/\underline{K}_{eq}) - \text{V.P.} = 0$ ($\underline{K}_{eq}$ and V.P. must be in same units).

Temp., °C	$\underline{K}_{eq}$, atm	V.P., mm Hg	$\underline{P}_{m}$	$\underline{P}_{d}$	$\underline{X}_{m}$
65	0.0197	3.11×10^{-6}	3.11×10^{-6}	6.4×10^{-13}	1.0
85	0.0632	4.54×10^{-5}	4.54×10^{-5}	4.3×10^{-11}	1.0
105	0.1783	4.13×10^{-4}	4.13×10^{-4}	1.3×10^{-9}	1.0

Stearic acid is completely monomeric at these temperatures.

APPENDIX II

ANALYSIS OF STEARIC ACID

A. SAMPLES

1. Radioactive stearic — [1-^{14}C] — acid. Lot number C17622 Dhom Products, Ltd.
2. Nonradioactive stearic acid, Fluka.

B. TESTING METHOD

Gas liquid chromatography.

C. TESTING CONDITIONS

Column: 8% EGSS-X on Gas Chrom Q.

Temperatures: Column - 170°C
Injector - 200°C
Detector - 235°C

Carrier gas: Helium at 30 cc/min.

Sample was 1% solution in cyclohexane, 2 µl injected.

D. ANALYSIS

Sample	C-16 Palmitic, %	C-17 Margaric, %	C-18 Stearic, %
Radioactive IPC File No. 72-74524	0.1	0.0	99.9
Nonradioactive IPC File No. 72-74526	0.28	0.08	99.64

APPENDIX III

DETERMINATION OF OPERATING VOLTAGE OF NUCLEAR CHICAGO COUNTING EQUIPMENT

A. CONDITIONS

Model D-47 gas flow detector
Micromil window in place
β-Proportional operation
Gas flow: 50 cc/min at 10 psig

B. RESULTS

Voltage	CPM	Voltage	CPM
1800	210	2050	638
1900	438	2100	682
1950	570	2150	1380
2000	625	2200	8000

C. PLATEAU CURVE

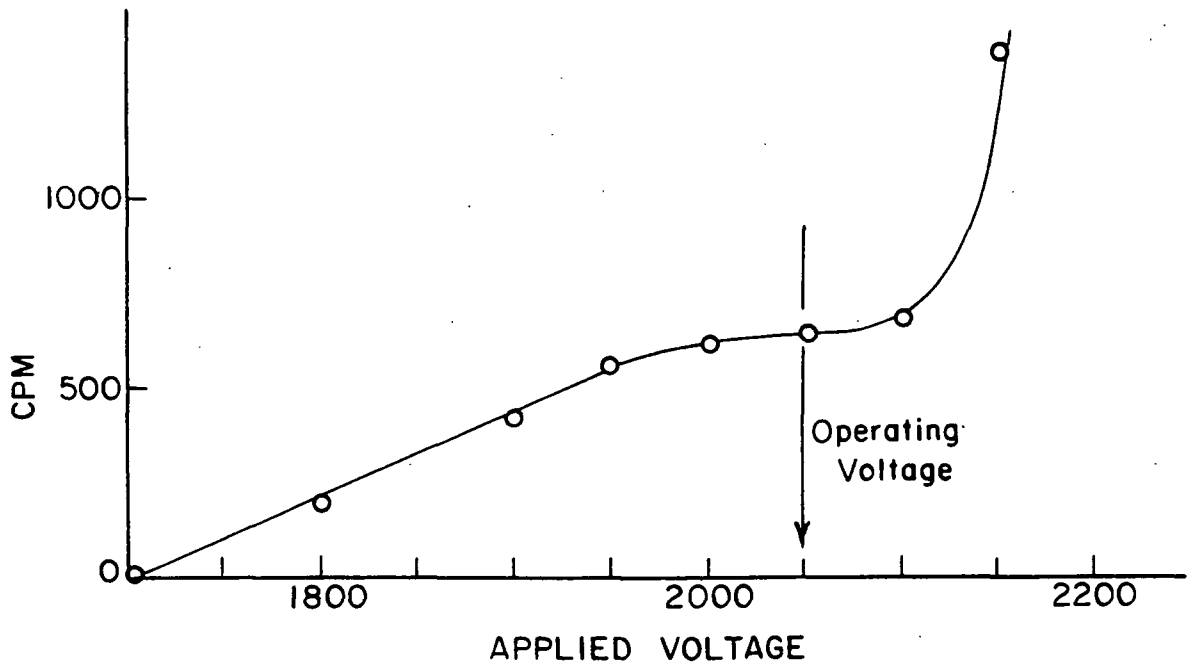

Figure 25. Cpm-Applied Voltage Curve

APPENDIX IV

ELEMENTAL ANALYSIS OF CELLULOSE FILMS

ASH, 550°C, %: 0.091

EMISSION SPECTROGRAPHIC ANALYSIS FOR CONCENTRATION OF ELEMENTS, PPM IN ASH

Element	Ash, ppm
Aluminum	2.9
Barium	0.18
Boron	5.1
Calcium	223.0
Copper	12.0
Iron	9.7
Lead	1.4
Magnesium	59.0
Manganese	0.39
Silicon	12.0
Sodium	73.0
Zinc	11.0

Total sulfur, %: 0.02 (Total film basis)

APPENDIX V

CALCULATION OF LIQUID SURFACE TENSION PARAMETERS FOR SATURATED METHYLENE IODIDE

A. γ_L MEASUREMENT

Cenco-DuNuoy Interfacial Tensiometer used to determine γ_L. Using correction factor of 0.838 (76), γ_L = 47.6.

B. γ_L^p, AND γ_L^d ESTIMATION

Contact angles of pure methylene iodide (MI) and saturated methylene iodide (SMI) were measured on clean Lucite (polymethylmethacrylate) and polyethylene surfaces.

Cos θ_{MI} vs. $\sqrt{\gamma_L^d}/\gamma_L$ is plotted to establish the Fowkes plot for each surface. (The slope is $2\sqrt{\gamma_s^d}$.)

Cos θ_{SMI} values were used to read off $\sqrt{\gamma_L^d}/\gamma_L$ for saturated methylene iodide.

C. DATA PLOT

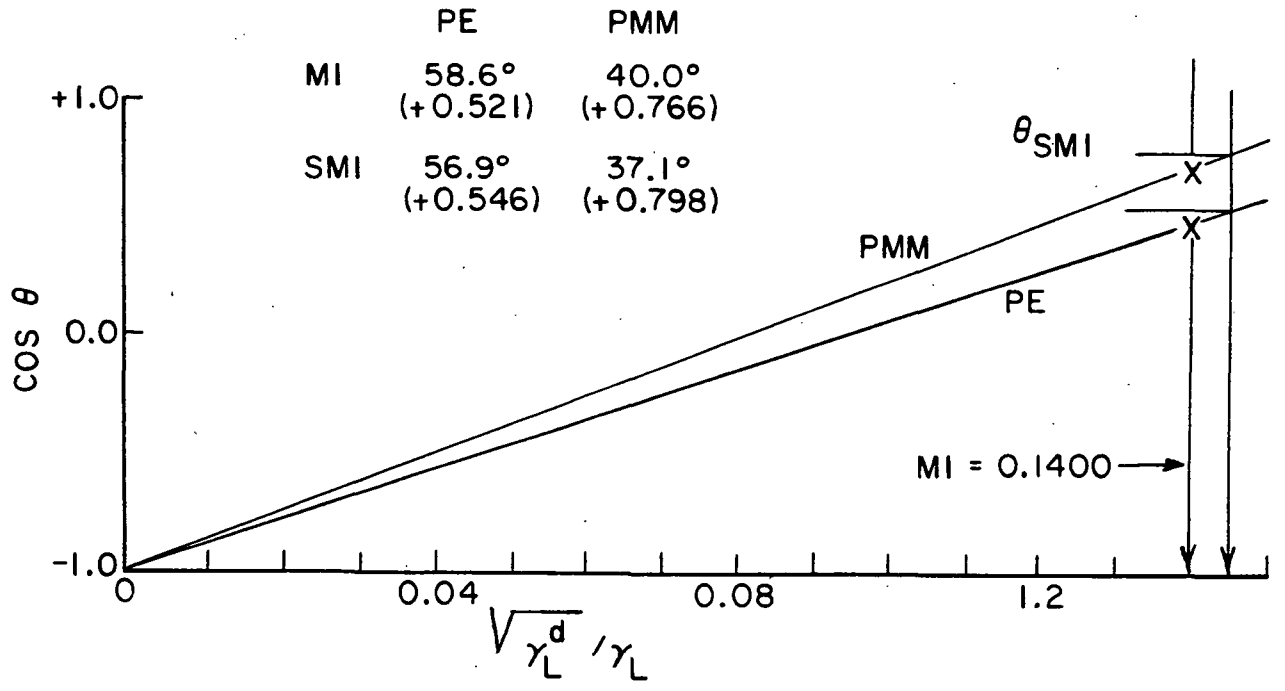

Figure 26. Fowkes' Plot for SMI Properties

D. INITIAL (UNREFINED) VALUES FOR $\gamma_{\underline{L}}^{p}$, AND $\gamma_{\underline{L}}^{d}$

From Fig. 26, $\sqrt{\gamma_{\underline{L}}^{d}/\gamma_{\underline{L}}}$ for saturated methylene iodide is 0.1435.

This calculates into $\gamma_{\underline{L}}^{d} = 46.5$, and $\gamma_{\underline{L}}^{p} = 1.1$.

E. REFINEMENT OF DETERMINED VALUES

The estimates were refined by computer simulation to give exact agreement of surface energy parameters calculated from water-MI and water-SMI pairs on pure cellulose. The final results:

$$\gamma_{\underline{L}}^{d} = 48.0 \qquad \gamma_{\underline{L}}^{p} = 0.1 \qquad \gamma_{\underline{L}} = 48.1.$$

APPENDIX VI

DARKROOM PROCEDURES

A. AUTORADIOGRAMS

Film: Kodak No-Screen X-ray Film

Developer: Kodak Liquid X-ray Developer

1 minute with continuous agitation
4 minutes with agitation, 15 seconds per minute
5 minutes total

Stop Bath: Kodak X-ray Indicator and Stop Bath

1 minute with continuous agitation
1 minute with agitation, last 15 seconds
2 minutes total

Fixer: Kodak Liquid X-ray Fixer

2 minutes continuous agitation
8 minutes with agitation, 15 seconds every minute
10 minutes total

Wash: Running Tap Water, 68°F, 20 minutes
Kodak Photo-Flo 200, 30 seconds

Dry: 30 Minutes in Drying Cabinet

B. PHOTOGRAPHIC FILM

Film: Kodak High Contrast (HC 135-36)

Developer: Kodak D-19 Liquid Developer, room temperature

1 minute continuous agitation
3.5 minutes agitation, once every 30 seconds
4.5 minutes total

Fixer: Kodak Rapid Photographic Fixer

5-Minute total, no agitation

Wash: Running Tap Water, 10 minutes
Kodak Photo-Flo 200, 30 seconds

Dry: 10 Minutes in Drying Cabinet

APPENDIX VII

COMPUTER PROGRAMS

```
C     THIS PROGRAM IS USED TO CALCULATE THE FOWKES, OWENS-WENDT,
C     AND WU SOLUTIONS FOR SURFACE ENERGY CONTRIBUTIONS FROM
C     CONTACT ANGLE DATA FROM TWO OR THREE LIQUIDS.
C     DATA INPUT IS ONE DESCRIPTION CARD(10A4), FOLLOWED BY ONE CARD
C     CONTAINING WATER, SAT.M.I., AND M.I. CONTACT ANGLES IN THREE F15
C     FIELDS. NO SPACING CARD IS REQUIRED BETWEEN DATA SETS.
        DIMENSION CODE(10),GLT(5),GLD(5),GLP(5),THETA(5),GSDF(5),BETA(6),
      1 ALFA(6),DENOM(10,10),GSDO(10,10),GSPO(10,10),GSTO(10,10),Q(6),
      2 R(6),S(6),T(6),GSDW(5,5),GSPW(5,5),GSTW(5,5), FACT(5),PLRTY(5,5)
      3 ,PLRTW(5,5)
C
C     THE FOLLOWING INPUTS ARE (1) = WATER (2) = SAT M.I.  (3) = METHYLENE I
C     IODIDE
        GLD(1) = 21.8
        GLP(1) = 51.0
        GLD(2) = 48.00
        GLP(2) = 0.10
        GLD(3) = 50.38
        GLP(3) = 0.38
        DO 79 I = 1,3
   79   GLT(I) = GLP(I) + GLD(I)
        WRITE(6,75)
   75   FORMAT('J. L. FERRIS-PROGRAM CALC')
   50   IDEX = 0
       KDEX = 0
       NDEX = 0
        READ(5,52) CODE
   51   READ(5,1) THETA(1),THETA(2), THETA(3)
        WRITE(6,76) CODE, THETA(1),THETA(2),THETA(3)
   76   FORMAT(////,' SURFACE ENERGY CALCULATIONS FOR ',10A4,//,
      1 5X,' WATER = ',F4.1,' SAT M.I. =',F6.1,' METH.IODIDE =',F6.1)
        DO 145 I = 1,3
  145   THETA(I) = THETA(I)/57.29
   52   FORMAT(10A4)
    1   FORMAT( 3F10.2)
        IF(THETA(1))2,2,3
    3   IF(THETA(2))4,4,5
    5   IF(THETA(3))6,6,7
    2   NGONE = 1
        GO TO 8
    4   NGONE = 2
        GO TO 8
    6   NGONE = 3
        GO TO 8
    7   NGONE = 0
    8   DO 9  I = 1,3
        IF(I - NGONE)11,9,11
   11   GSDF(I) =(((COS(THETA(I))+ 1.)*GLT(I))/(2.*SQRT(GLD(I))))**2.
    9   CONTINUE
C       OWENS-WENDT SOLUTION
   12   DO 14 I = 1,3
        BETA(I) =(2.*SQRT(GLP(I)))/GLT(I)
   14   ALFA(I) = (2.* SQRT(GLD(I)))/GLT(I)
        DO 15  I = 1,2
        IF(I - NGONE)17,15,17
   17   DO 15 J = 2,3
        IF(J - NGONE)18,15,18
```

```
 18     IF(I -J)16,15,16
 16     DENOM(I,J) = (ALFA(J) * BETA(I) -ALFA(I) *BETA(J))
        GSDO(I,J) = ((BETA(I)*(1.+COS(THETA(J)))-BETA(J)*(1.+COS(THETA
     1(I))))/DENOM(I,J))**2
        GSPO(I,J) =((ALFA(J)*(1.+COS(THETA(I))) - ALFA(I)*(1.+COS
     2(THETA(J))))/DENOM(I,J))**2
        GSTO(I,J) = GSDO(I,J) + GSPO(I,J)
        PLRTY(I,J) = GSPO(I,J)/GSTO(I,J)
 15     CONTINUE
C      WU SOLUTION
        DO 19  I = 1,3
        IF(I-NGONE)20,19,20
  20    FACT(I) = GLT(I) * (1. + COS(THETA(I)))/4.
        Q(I) = GLD(I) +GLP(I) - FACT(I)
        R(I) = GLP(I) *(GLD(I) -FACT (I) )
        S(I) = GLD(I)*(GLP(I) -  FACT(I))
        T(I) = FACT(I) * GLD(I) * GLP(I)
  19    CONTINUE
        DO 21 I = 1,1
        IF(I-NGONE)22,21,22
   22   DO 21 J = 2,3
        IF(J-NGONE)23,21,23
  23    IF(I-J)24,21,24
  24   KDEX = 0
       NDEX = 0
       IDEX = 0
        GSP = 100.
  67    GSD =((Q(J)*T(I) - Q(I)*T(J))/(Q(J)*R(I)-Q(I)*R(J)) )
     1 - ((Q(J)*S(I) - Q(I)*S(J))/(Q(J)*R(I)- Q(I)*R(J)))*GSP
        SUM     = Q(I)*GSP*GSD +R(I)*GSD + S(I)*GSP - T(I)
        ABSUM =  ABS(SUM)
        IF(KDEX-1)44,41,44
   44   IF(NDEX-1) 43,42,43
 43     IF(ABSUM - SUM) 42,41,42
 41     KDEX = 1
        IF(ABSUM - SUM) 27,27,29
  42    NDEX = 1
        IF(ABSUM - SUM) 29,29,27
   29   IDEX = 1
        GO TO 28
  27    IF(IDEX-1)25,26,25
 25     GSP = GSP - 1.0
        GO TO 67
 28     GSP = GSP +0.001
        GO TO 67
 26     GSDW(I,J) = GSD
        GSPW(I,J) = GSP
        GSTW(I,J) = GSP + GSD
        PLRTW(I,J) = GSPW(I,J)/GSTW(I,J)
 21     CONTINUE
C       OUT PUT OF ALL DATA
        WRITE(6,30)       (GSDF(I), I =1,3  )
  30    FORMAT(//,'FOWKES SOLUTION ',20X,'WATER',12X,'SAT M.I.',8X,
     1 'METH-IODIDE',/,5X,'DISPERSION',5X,3F20.1,/)
 32     WRITE(6,33)GSDO(1,2),GSDO(1,3),GSDO(2,3),GSPO(1,2),GSPO(1,3),
     1  GSPO(2,3),GSTO(1,2),GSTO(1,3),GSTO(2,3),PLRTY(1,2),PLRTY(1,3),
     2 PLRTY(2,3)
       WRITE(6,38) GSDW(1,2),GSDW(1,3),GSDW(2,3),GSPW(1,2),GSPW(1,3),
     1 GSPW(2,3),GSTW(1,2),GSTW(1,3),GSTW(2,3),PLRTW(1,2),PLRTW(1,3)
     2 , PLRTW(2,3)
```

```
 33   FORMAT(' OWENS-WENDT SOLUTION      WATER-SAT M.I.   WATER-METH.'
     1 ,'IODIDE        1122 TBE-M.I',/,5X,'DISPERSION',5X,3F20.1,/,
     2 5X,'POLAR',10X,3F20.1,/,5X,'TOTAL',10X,3F20.1,/,5X,'POLARITY',
     37X,3F20.2,/)
 38   FORMAT(' WU SOLUTION',14X,'WATER-SAT M.I.',10X,'WATER-M.I.',
     1 7X,'1122 TBE-M.I.',/,5X,'DISPERSION',5X,   3F20.1,/,5X,'POLAR',
     2 10X,3F20.1,/,5X,'TOTAL',10X,3F20.1,/,5X,'POLARITY',7X,3F20.2)
      GO TO 50
      END
```

```
      SUBROUTINE TFIT(TIME,ANG,  THETA, IK)
C     FOR USE WITH MAINLINE PROGRAM ANG
      DIMENSION ANG(99), TM(99),Z(99),ANGC(99),TIME(99)
      IO = 5
      JO = 6
 101  NDEX = 1
      QDEX = 1
      PD = 1000.
      DELT = 0.1
      TDELT = DELT/10.
  6   N = IK-1
      TN = N
      IDEX = 1
      ALF = 0.01
 12   RFAC = 0.
      ZFAC = 0.
      QFAC = 0.
      PFAC = 0.
      SFAC = 0.
  77  DO 7 I =1,N
      IF(QDEX)78,79,78
 78   Z(I) = TIME(I)
      GO TO 81
  79  Z(I) = EXP(-ALF*TIME(I))
 81   RFAC = RFAC + ANG(I)
      ZFAC = ZFAC + Z(I)
      QFAC = QFAC + ANG(I)*Z(I)
      PFAC = PFAC + Z(I)**2
 7    SFAC = SFAC + Z(I)
      REM = TN*PFAC - SFAC*ZFAC
      IF(REM - .0001)223,500,500
 500  ALPHA = (TN*QFAC - SFAC*RFAC)/(TN*PFAC-SFAC*ZFAC)
      BETA = (RFAC-(ZFAC*ALPHA))/TN
      DIFF = 0.
      DO 8 I = 1,N
      ANGC(I) = ALPHA * Z(I) + BETA
 8    DIFF = (ANGC(I) - ANG(I))**2  + DIFF
      IF(QDEX) 95,96,95
  95  THETA = BETA
      WRITE (6,199)THETA,DIFF
 199  FORMAT(5X, 'LINEAR EXTRAPOLATION          ANGLE =' F8.2,4X,
     1' LEAST SQUARES =',F8.2)
 208  QDEX = 0.
 96   IF(IDEX)15,46,15
 15   IF(NDEX) 17,18,17
 17   IF(PD -DIFF)18,16,20
 20   ALF = ALF + DELT
      PD = DIFF
      GO TO 12
 18   IF(NDEX)25,27,25
 25   NDEX = 0
      GO TO 28
 27   IF(PD-DIFF) 16,16,28
 28   ALF = ALF - TDELT
       PD = DIFF
      GO TO 12
  16    ALF = ALF + TDELT
       IDEX = 0
```

```
       GO TO 12
46     THETA = ALPHA + BETA
      WRITE(JO,19) THETA,DIFF, ALF,BETA
 19   FORMAT(5X, 'EXPONENTIAL EXTRAPOLATION    ANGLE = ',F8.2,
     2'    LEAST SQUARES =',F8.2,/,
     1                      35X,'EXPNT = ',F8.2,  '    BETA =',F8.2)
      GO TO 534
 223  WRITE (6,225)
 225   FORMAT(5X,'EXPONENTIAL SOLUTION APPROACHES LINEAR')
534   CONTINUE
     RETURN
     END
```

```
C       PROGRAM ANG  .  TO CALCULATE  CONTACT ANGLES FROM DROP PROFILE
C       INPUT WITH ONE  DATA    CARD CARRYING  THREE  F5.0 FIELDS
C       FOLLOWED BY AN A4 FIELD WITH DROP ID, AND AN F5.2 WITH TIME.
C       STOPS ARE (0,0) FOR CONTINUE,(0,1) FOR NEW ROLL,(1,0) FOR ANGLE
C       ONLY. A 1 IN COLUMN 61 OF FIRST CARD WILL GIVE ANGLES PLUS
C       STANDARD DEVIATION OF THE SET. ONE DEFN  CARD BEFORE EACH
C       SET OF DATA   REQUIRED. SUBROUTINE TFIT IS CALLED IF BACK
C       EXTRAPOLATION DESIRED.
      DIMENSION X(10), Y(10),       CVOL(50),KIQ(50),CMA(90),CMAS(90)
      DIMENSION TIME(90), ANG(90),CODE(15),RATE(90),VOL(90)
       IGIT = 0
      Y(1) = 1.
  2   IF(Y(1) - 1.0)20,21,21
 21   READ(5,23) CODE, IGIT
      WRITE(6,25) CODE
      WRITE(6,500)
 500  FORMAT(1HO,'J. L. FERRIS--PROGRAM ANG')
 23   FORMAT(15A4,I1)
  25  FORMAT(1H1,'CONTACT ANGLE CALCULATIONS FOR ',15A4  )
  20  WRITE(6,49)
  49  FORMAT(1HO,//,'DROP'
     1          '    DROP COORDINATES X(I)/Y(I) BASE  HEIGHT  VOLUME  '
     1,'         TIME     ANGLE    PCVOL ')
      TM = 0.
      SQM = 0.
      IC = 0
      IO = 5
      JO = 6
      DO 5 IK= 1,200
  3   READ (IO,10)      (X(I),Y(I), I = 1,3),ID,TIME(IK)
  10  FORMAT(       3(F5.0,F5.0), A4,F5.2)
      IF(X(1))1,8,1
  1   IF(X(1)-1.)2,2,11
 11   YZ = (Y(1) + Y(3))/2.
      AMS = (X(3) - X(1))/2.
      HM = Y(2) - YZ
      VOL(IK)= 3.14156*HM*(3.*AMS**2 + HM**2)/6000000000.
      PVOL = VOL(IK)/VOL(1) *100.
      CONAM = (ATAN (HM/AMS))*2.*57.29577
      ANG(IK) = CONAM
      IC = IC+1
      CMA(IC)=CONAM
      WRITE(JO,48)ID,X(1),X(2),X(3),Y(1),Y(2),Y(3),AMS,HM,VOL(IK),
     1TIME(IK),CONAM,PVOL
  5   CONTINUE
   8   ND = IC
      PND = ND - 1
      XND = ND
      DO 120 I = 1,ND
 120  TM = TM + CMA(I)
      AVM =  TM/XND
      DO 83 I = 1,ND
      CMAS(I) = (CMA(I) - AVM)**2
  83  SQM = SQM + CMAS(I)
      SDEVM = SQRT(SQM/PND)
      ERR = SDEVM/SQRT(XND)
      T = (.856278 +XND * (.0703808 + 1.96 *XND))/
```

```
     1 (.40068466 -XND * (1.1734961 -XND))
      CL = T * ERR
      WRITE(JO,102) AVM,SDEVM , ND, CL
      IF(IGIT  - 1 )156,2,2
156   CALL TFIT(TIME,ANG,THETA,IK)
102   FORMAT(1HO,5X,'AVERAGE OF THE ABOVE SET = 'F7.2,'  STANDARD DEV
     1 OF THE ABOVE SET = ' F7.2,/,6X,'NUMBER OF POINTS = ',I2,15X,
     1 '95 PC CL ARE +/- ',F5.2)
      DO 70  IS =1,IC
 70   RATE(IS) = ANG(IS)/THETA * 100.
      WRITE(6,71)(TIME(I),RATE(I),I = 1,IC)
71    FORMAT('0    RATE DATA',/,(F15.2,F8.2,F15.2,F8.2,F15.2,F8.2,F15.2
     1,F8.2,/))
      GO TO  2
 48   FORMAT(1HO,A4,3F10.0,/,5X,3F10.0,1F6.0,2F8.2,9X, F5.2,2F10.2)
      CALL EXIT
      END
```

APPENDIX VIII

CALIBRATION OF RADIOACTIVE COUNTS PER MINUTE TO PERCENT PLANAR ORIENTED MONOLAYER

A. SOLUTIONS

Solution I. 1 Ampule [1.0 millicurie (mC_i) of 58 mC_i/mM in 1 ml of benzene] + 99 ml benzene.

Solution II. 1 ml Solution I + 99 ml benzene = 0.001724 µm/1 ml II.

B. CPM/MILLILITER I

10 λ II on cellulose film = 388 cpm, so

1 λ I = 3880 cpm, or

1 ml I = 3,880,000 cpm.

C. MICROMOLES (µM) PER SQUARE INCH OF PACKED MONOLAYER

1 $Inch^2$ = 6.45 cm^2

Packed monolayer = 4.94×10^{14} molecules/cm^2 (54)

$\mu M/inch^2 = 6.45 \times 4.94 \times 10^{14}$ moles/$cm^2 \times 1\ \mu M/6.02 \times 10^{17}$ molecules

$= 5.3 \times 10^{-3}\ \mu M/inch^2$

D. CPM PER SQUARE INCH PACKED MONOLAYER

$$\frac{0.1724\ \mu M}{3{,}880{,}000\ cpm} = \frac{0.0053\ \mu M}{X\ cpm}$$

X, cpm/$inch^2$ packed monolayer = 119,000

E. DILUTION FACTOR FOR 100% POML = 10,000 CPM

Desire 10/119 of total stearic acid in monolayer to be radioactive, or 8.4% of stearic acid in bed is labelled.

F. PREPARED SOLUTION

Mixed 11.3 nonradioactive with 1.0 radioactive or 8.1% labelled.

This is equivalent to 9600 cpm/100% POML.

This difference is within experimental error expected in measurement of cpm/ml I.

G. EFFICIENCY OF COUNTING ON CELLULOSE FILM

1.0 mC_i diluted in benzene to 100 ml (Solution I)

1 λ Solution I = 1.0 $mC_i \times 10^{-5}$

1.0 mC_i = 3.7×10^7 disintegrations per second

1 λ Solution I = 3.7×10^2 dps

= 22,200 disintegrations per minute

Efficiency = 3880/22,200 = 17.4%

APPENDIX IX

EXPERIMENTAL DATA FOR FILM NAA - TEMP 65 - TIME 12 HR

ADSORPTION DATA COUNTING STANDARD = 683.

TOTAL ADSORPTION

13800. 11400. 11100. 11000. 12600. 11200. 12800. 11600. 12600. 16400.

MEAN IS 12759.86 +/- 1201.3

CPM AFTER BENZENE EXTRACTION

5180. 4580. 3950. 4620. 5400. 6900.

MEAN IS 5232.06 +/- 1040.0

CPM AFTER WATER EXTRACTION

350. 650. 250. 336. 640. 505.

MEAN IS 466.50 +/- 172.5

CPM AFTER CAUSTIC EXTRACTION

270. 344.

MEAN IS 314.64 +/- 163.2

AMOUNT BENZENE EXTRACTED 7527.00+/- 1663.4

AMOUNT WATER EXTRACTED 4766.00+/- 960.0

AMOUNT CAUSTIC EXTRACTED 152.00+/- 318.0

CALCULATED PER CENT POML BONDED 1.5

UNEXTRACTED FILM CONTACT ANGLES

WATER

27.50 27.60 27.71 28.50 28.63 28.98 29.62 29.66 29.75 29.79 30.76 32.33

MEAN = 29.24 +/- 0.89

SAT.M.I.

55.78 55.96 56.16 56.70 56.87 57.02

MEAN = 56.41 +/- 0.52

METH.IOD.

47.24 48.99 50.42 50.91 53.13 53.21

MEAN = 50.65 +/- 2.33

SURFACE ENERGY PARAMETER	WATER-SAT.M.I.	WATER-METH.IOD.
TOTAL ENERGY	64.59	65.09
POLARITY	0.60	0.57

EXTRACTED FILM CONTACT ANGLES

WATER

29.95 36.32 37.51 37.53 38.29 39.25 39.52 39.58 40.14 41.34 44.22 51.28

MEAN = 39.58 +/- 3.15

SAT.M.I.

19.06 19.78 23.34 25.56 27.42

MEAN = 23.03 +/- 4.15

METH.IOD.

15.80 23.57 26.70 28.01 28.21 31.14 39.59

MEAN = 27.57 +/- 6.46

SURFACE ENERGY PARAMETER	WATER-SAT.M.I.	WATER-METH.IOD.
TOTAL ENERGY	64.70	63.89
POLARITY	0.36	0.37

RESIDUAL WATER CONTACT ANGLE 27.5

APPENDIX IX(CONTD.)

EXPERIMENTAL DATA FOR FILM NAP - TEMP 65 - TIME 168 HR

ADSORPTION DATA COUNTING STANDARD = 645.

TOTAL ADSORPTION

71000. 67000. 55700. 59000. 65000. 65000. 55800. 55000. 58600.

MEAN IS 66575.31 +/- 4735.0

CPM AFTER BENZENE EXTRACTION

62500. 50800. 60000. 59700. 53000.

MEAN IS 62077.50 +/- 6262.0

CPM AFTER WATER EXTRACTION

4340. 4800. 4450. 4440. 4120.

MEAN IS 4807.75 +/- 306.6

CPM AFTER CAUSTIC EXTRACTION

1750. 1150.

MEAN IS 1573.64 +/- 1401.0

AMOUNT BENZENE EXTRACTED 4498.00+/- 7309.8

AMOUNT WATER EXTRACTED 57270.00+/- 5624.6

AMOUNT CAUSTIC EXTRACTED 3234.00+/- 677.7

CALCULATED PER CENT POML BONDED 52.0

UNEXTRACTED FILM CONTACT ANGLES

WATER

66.22 76.19 78.49 79.42 79.64 80.45 80.48 81.94 83.62 84.21 84.40 84.57

MEAN = 79.97 +/- 3.19

SAT.M.I.

53.62 55.46 56.16 56.33 57.00 57.43

MEAN = 56.00 +/- 1.35

METH.IOD.

49.50 50.99 51.62 51.84 52.12 52.14

MEAN = 51.37 +/- 1.01

SURFACE ENERGY PARAMETER	WATER-SAT.M.I.	WATER-METH.IOD.
TOTAL ENERGY	34.41	36.81
POLARITY	0.18	0.15

EXTRACTED FILM CONTACT ANGLES

WATER

66.86 68.19 69.90 70.14 70.53 70.56 71.48 71.56 72.03

MEAN = 70.14 +/- 1.26

SAT.M.I.

33.38 33.83 34.44

MEAN = 33.89 +/- 0.97

METH.IOD.

31.51 32.22 32.35 33.41 34.04 35.17

MEAN = 33.12 +/- 1.35

SURFACE ENERGY PARAMETER	WATER-SAT.M.I.	WATER-METH.IOD.
TOTAL ENERGY	46.38	47.37
POLARITY	0.16	0.15

RESIDUAL WATER CONTACT ANGLE 54.0

APPENDIX IX(CONTD.)

EXPERIMENTAL DATA FOR FILM NAM - TEMP 85 - TIME 48 HR

ADSORPTION DATA COUNTING STANDARD = 663.

TOTAL ADSORPTION

29400. 28100. 28600. 27800. 26300. 28900. 25800. 29400.
31600. 31400.

MEAN IS 30333.30 +/- 1404.1

CPM AFTER BENZENE EXTRACTION

19800. 15600. 18800. 17700. 17300. 18100.

MEAN IS 18881.33 +/- 1502.5

CPM AFTER WATER EXTRACTION

2700. 1960. 2160. 1920. 1940. 2100.

MEAN IS 2248.87 +/- 311.4

CPM AFTER CAUSTIC EXTRACTION

600. 770.

MEAN IS 723.23 +/- 386.2

AMOUNT BENZENE EXTRACTED 11452.00+/- 2030.5

AMOUNT WATER EXTRACTED 16633.00+/- 1397.3

AMOUNT CAUSTIC EXTRACTED 1525.00+/- 577.8

CALCULATED PER CENT POML BONDED 15.2

UNEXTRACTED CONTACT ANGLES

WATER

58.11 59.32 62.07 62.10 62.58 62.72 64.15 64.47
65.10 66.05 68.31 69.35

MEAN = 63.69 +/- 2.07

SAT.M.I.

47.40 47.44 48.17 49.96 49.99 51.74

MEAN = 49.12 +/- 1.73

METH.IOD.

44.24 45.29 45.51 45.88 46.72 47.06

MEAN = 45.78 +/- 1.02

SURFACE ENERGY PARAMETER	WATER-SAT.M.I.	WATER-METH.IOD.
TOTAL ENERGY	44.84	46.04
POLARITY	0.31	0.28

EXTRACTED CONTACT ANGLES

WATER

63.99 66.81 66.82 67.14 67.63 67.68 67.70 67.74
68.27 69.06 69.13 69.25

MEAN = 67.60 +/- 0.89

SAT.M.I.

30.96 33.47 33.70 34.05 34.48 37.76

MEAN = 34.07 +/- 2.19

METH.IOD.

27.53 30.68 31.64 31.77 33.54 33.94

MEAN = 31.52 +/- 2.31

SURFACE ENERGY PARAMETER	WATER-SAT.M.I.	WATER-METH.IOD.
TOTAL ENERGY	47.44	48.88
POLARITY	0.19	0.17

RESIDUAL WATER CONTACT ANGLE 30.1

APPENDIX IX(CONTD.)

EXPERIMENTAL DATA FOR FILM NX - TEMP 105 - TIME 48 HOUR

ADSORPTION DATA COUNTING STANDARD = 666.

TOTAL ADSORPTION
34000. 34000. 35880. 33200. 37600. 36000. 37100. 36200.
37000. 39800.
MEAN IS 37919.79 +/- 1461.3

CPM AFTER BENZENE EXTRACTION
32300. 30400. 32500. 31900. 31700. 31900.
MEAN IS 33405.88 +/- 775.6

CPM AFTER WATER EXTRACTION
7310. 7400. 8320.
MEAN IS 8068.57 +/- 1079.1

CPM AFTER CAUSTIC EXTRACTION
1270. 1310.
MEAN IS 1355.86 +/- 90.5

AMOUNT BENZENE EXTRACTED 4514.00+/- 1912.1
AMOUNT WATER EXTRACTED 25337.00+/- 1216.3
AMOUNT CAUSTIC EXTRACTED 6713.00+/- 1394.0
CALCULATED PER CENT POML BONDED 71.0

UNEXTRACTED FILM CONTACT ANGLES

WATER
59.25 62.10 63.61 66.51 67.38 67.80 68.01 68.54
68.57 68.61 71.41 72.73
MEAN = 67.04 +/- 2.38

METH.IOD.
48.47 49.61 51.59 51.86 52.21 53.39 53.96 54.68
55.94 56.09 56.63
MEAN = 53.13 +/- 1.77

SURFACE ENERGY PARAMETER	WATER-SAT.M.I.	WATER-METH.IOD.
TOTAL ENERGY		41.87
POLARITY		0.30

EXTRACTED FILM CONTACT ANGLES

WATER
68.90 71.03 71.74 71.74 72.93
MEAN = 71.27 +/- 1.71

METH.IOD.
41.53 41.55 41.67
MEAN = 41.58 +/- 0.14

SURFACE ENERGY PARAMETER	WATER-SAT.M.I.	WATER-METH.IOD.
TOTAL ENERGY		43.95
POLARITY		0.18

RESIDUAL WATER CONTACT ANGLE 45.3

APPENDIX IX(CONTD.)

EXPERIMENTAL DATA FOR FILM NAK - TEMP 105 - TIME 72

ADSORPTION DATA COUNTING STANDARD = 650.

TOTAL ADSORPTION

71000. 72500. 88500. 89000. 92000. 102000. 98000. 76000.
78000. 75000.

MEAN IS 90676.88 +/- 8431.1

CPM AFTER BENZENE EXTRACTION

60500. 67500. 76500. 69000. 78000. 65000.

MEAN IS 74756.38 +/- 7243.7

CPM AFTER WATER EXTRACTION

10700. 12600. 14500. 16100. 14000. 13500.

MEAN IS 14610.25 +/- 1962.1

CPM AFTER CAUSTIC EXTRACTION

3680. 3750.

MEAN IS 4000.77 +/- 162.2

AMOUNT BENZENE EXTRACTED 15920.00+/-11659.6

AMOUNT WATER EXTRACTED 60146.00+/- 6834.0

AMOUNT CAUSTIC EXTRACTED 10610.00+/- 3582.5

CALCULATED PER CENT POML BONDED 126.0

UNEXTRACTED FILM CONTACT ANGLES

WATER

71.96 72.56 72.95 75.43 76.32 76.54 76.89 77.49
78.57 79.29 80.32 81.01

MEAN = 76.61 +/- 1.88

SAT.M.I.

50.25 52.38 53.07 53.83 54.80

MEAN = 52.87 +/- 1.97

METH.IOD.

51.42 52.07 53.43 53.51 56.87

MEAN = 53.46 +/- 2.42

SURFACE ENERGY PARAMETER	WATER-SAT.M.I.	WATER-METH.IOD.
TOTAL ENERGY	37.01	37.21
POLARITY	0.20	0.20

EXTRACTED FILM CONTACT ANGLES

WATER

70.61 70.74 73.18 73.99 74.13 75.61 75.94 76.35
77.34 77.59 77.69 78.14

MEAN = 75.11 +/- 1.64

SAT.M.I.

42.60 43.75 44.46 44.80 45.83

MEAN = 44.29 +/- 1.38

METH.IOD.

44.68 45.38 46.44 46.95 47.28

MEAN = 46.15 +/- 1.25

SURFACE ENERGY PARAMETER	WATER-SAT.M.I.	WATER-METH.IOD.
TOTAL ENERGY	40.79	40.70
POLARITY	0.16	0.17

RESIDUAL WATER CONTACT ANGLE 70.4

APPENDIX IX(CONTD.)

EXPERIMENTAL DATA FOR FILM NAJ - TEMP 105 - TIME 36 HR

ADSORPTION DATA COUNTING STANDARD = 656.

TOTAL ADSORPTION

27200. 30000. 32000. 29400. 33000. 32500. 31600. 29700.
32300. 31500.

MEAN IS 32993.88 +/- 1353.7

CPM AFTER BENZENE EXTRACTION

24400. 25200. 29200. 23200. 25700. 23200.

MEAN IS 26836.86 +/- 2377.5

CPM AFTER WATER EXTRACTION

4560. 4580. 4480. 4430. 4580.

MEAN IS 4829.57 +/- 83.0

CPM AFTER CAUSTIC EXTRACTION

1910. 1920.

MEAN IS 2043.44 +/- 23.0

AMOUNT BENZENE EXTRACTED 6157.00+/- 2322.2

AMOUNT WATER EXTRACTED 22007.00+/- 2430.9

AMOUNT CAUSTIC EXTRACTED 2786.00+/- 139.1

CALCULATED PER CENT POML BONDED 35.7

UNEXTRACTED FILM CONTACT ANGLES

WATER

57.20 61.46 64.22 64.58 64.99 67.82 69.59 70.32
70.84 72.62 74.07 75.72

MEAN = 67.79 +/- 3.43

SAT.M.I.

50.25 53.13 54.10 57.27 60.15 60.88

MEAN = 55.96 +/- 4.18

METH.IOD.

47.83 51.15 53.00 53.01 54.13 54.87

MEAN = 52.33 +/- 2.53

SURFACE ENERGY PARAMETER	WATER-SAT.M.I.	WATER-METH.IOD.
TOTAL ENERGY	40.46	41.74
POLARITY	0.32	0.29

EXTRACTED FILM CONTACT ANGLES

WATER

65.45 67.39 68.88 69.28 69.31 70.15 70.26 70.95
71.42 71.82 72.42 73.38

MEAN = 70.06 +/- 1.38

SAT.M.I.

39.31 40.38 42.79 43.89 44.73

MEAN = 42.22 +/- 2.65

METH.IOD.

38.32 41.04 41.85 41.90 41.93

MEAN = 41.01 +/- 1.78

SURFACE ENERGY PARAMETER	WATER-SAT.M.I.	WATER-METH.IOD.
TOTAL ENERGY	43.72	44.66
POLARITY	0.20	0.19

RESIDUAL WATER CONTACT ANGLE 57.7

APPENDIX IX(CONTD.)

EXPERIMENTAL DATA FOR FILM NAH - TEMP 85 - TIME 14 HR

ADSORPTION DATA COUNTING STANDARD = 669.

TOTAL ADSORPTION

18700. 18400. 17000. 16200. 16400. 16400. 15200. 15800.
17500. 19400.

MEAN IS 17892.36 +/- 1007.3

CPM AFTER BENZENE EXTRACTION

11000. 10000. 7100. 7500. 7150. 8040.

MEAN IS 8857.25 +/- 1716.6

CPM AFTER WATER EXTRACTION

1210. 1400. 1380. 1410. 1220. 1040.

MEAN IS 1335.82 +/- 153.1

CPM AFTER CAUSTIC EXTRACTION

735. 790.

MEAN IS 797.83 +/- 123.8

AMOUNT BENZENE EXTRACTED 9035.00+/- 1704.5

AMOUNT WATER EXTRACTED 7522.00+/- 1569.4

AMOUNT CAUSTIC EXTRACTED 538.00+/- 281.6

CALCULATED PER CENT POML BONDED 5.4

UNEXTRACTED FILM CONTACT ANGLES

WATER

45.65 46.76 47.55 47.64 48.16 48.16 48.63 48.67
48.97 49.09 49.78 50.04

MEAN = 48.26 +/- 0.78

SAT.M.I.

53.67 56.62 59.01 59.79 59.94 61.19

MEAN = 58.37 +/- 2.75

METH.IOD.

49.81 52.47 53.04 53.06 53.22 58.72

MEAN = 53.39 +/- 2.91

SURFACE ENERGY PARAMETER	WATER-SAT.M.I.	WATER-METH.IOD.
TOTAL ENERGY	52.44	53.22
POLARITY	0.51	0.48

EXTRACTED FILM CONTACT ANGLES

WATER

51.54 52.79 53.06 53.40 53.40 53.61 54.10 54.56
55.24 56.56 57.80 58.17

MEAN = 54.52 +/- 1.29

SAT.M.I.

25.85 26.76 27.83 29.50 29.55 31.11

MEAN = 28.43 +/- 1.97

METH.IOD.

25.94 26.86 27.37 28.60 29.03 29.18

MEAN = 27.83 +/- 1.31

SURFACE ENERGY PARAMETER	WATER-SAT.M.I.	WATER-METH.IOD.
TOTAL ENERGY	55.53	55.96
POLARITY	0.27	0.27

RESIDUAL WATER CONTACT ANGLE 31.7

APPENDIX IX(CONTD.)

EXPERIMENTAL DATA FOR FILM NAF - TEMP 85 - TIME 6 HR

ADSORPTION DATA COUNTING STANDARD = 625.

TOTAL ADSORPTION

9850. 10300. 11500. 10700. 9900. 10000. 10100. 9800.
10500. 12800.

MEAN IS 11810.40 +/- 745.5

CPM AFTER BENZENE EXTRACTION

3500. 2320. 2380. 2460. 2950. 4000.

MEAN IS 3287.20 +/- 769.5

CPM AFTER WATER EXTRACTION

340. 332. 282. 283. 395. 390.

MEAN IS 377.44 +/- 55.1

CPM AFTER CAUSTIC EXTRACTION

318. 290.

MEAN IS 340.48 +/- 67.5

AMOUNT BENZENE EXTRACTED 8523.00+/- 1069.0

AMOUNT WATER EXTRACTED 2910.00+/- 702.6

AMOUNT CAUSTIC EXTRACTED 37.00+/- 102.3

CALCULATED PER CENT POML BONDED 1.4

UNEXTRACTED FILM CONTACT ANGLES

WATER

33.41 34.75 34.91 35.11 35.21 35.22 35.30 35.37
35.89 36.97 37.29 42.16

MEAN = 35.97 +/- 1.38

SAT.M.I.

50.99 55.81 56.10 57.43 58.51 58.84

MEAN = 56.28 +/- 2.86

METH.IOD.

46.34 49.15 49.22 51.01 51.53 51.97

MEAN = 49.87 +/- 2.09

SURFACE ENERGY PARAMETER	WATER-SAT.M.I.	WATER-METH.IOD.
TOTAL ENERGY	60.75	61.51
POLARITY	0.57	0.53

EXTRACTED FILM CONTACT ANGLES

WATER

35.40 41.52 42.61 42.78 42.80 43.05 43.28 43.52
43.68 43.92 44.74 45.12

MEAN = 42.70 +/- 1.57

SAT.M.I.

21.46 23.99 24.24 25.41 28.26 28.30

MEAN = 25.28 +/- 2.66

METH.IOD.

23.33 24.08 26.90 28.21 28.75 31.13

MEAN = 27.07 +/- 2.95

SURFACE ENERGY PARAMETER	WATER-SAT.M.I.	WATER-METH.IOD.
TOTAL ENERGY	62.64	62.34
POLARITY	0.35	0.35

RESIDUAL WATER CONTACT ANGLE 32.2

APPENDIX IX(CONTD.)

EXPERIMENTAL DATA FOR FILM NAE - TEMP 85 - TIME 24 HR

ADSORPTION DATA COUNTING STANDARD = 663.

TOTAL ADSORPTION

13800. 14400. 13700. 12300. 13500. 13800. 13300. 13700. 14200. 16200.

MEAN IS 14665.14 +/- 736.0

CPM AFTER BENZENE EXTRACTION

6390. 6430. 5600. 6000. 6250. 6300.

MEAN IS 6505.53 +/- 331.1

CPM AFTER WATER EXTRACTION

1180. 1110. 1070. 980. 1000. 1040.

MEAN IS 1122.67 +/- 78.0

CPM AFTER CAUSTIC EXTRACTION

280. 560.

MEAN IS 443.44 +/- 636.0

AMOUNT BENZENE EXTRACTED 8160.00+/- 953.2

AMOUNT WATER EXTRACTED 5383.00+/- 309.7

AMOUNT CAUSTIC EXTRACTED 679.00+/- 222.1

CALCULATED PER CENT POML BONDED 8.0

UNEXTRACTED FILM CONTACT ANGLES

WATER

56.36 57.85 58.30 59.91 60.61 60.74 60.74 61.13 62.76 62.88 63.05 64.81

MEAN = 60.76 +/- 1.53

SAT.M.I.

53.23 55.43 56.80 57.58 59.85 60.19

MEAN = 57.18 +/- 2.65

METH.IOD.

44.56 44.76 47.97 51.26 53.86 54.93

MEAN = 49.56 +/- 4.48

SURFACE ENERGY PARAMETER	WATER-SAT.M.I.	WATER-METH.IOD.
TOTAL ENERGY	44.37	46.47
POLARITY	0.40	0.34

EXTRACTED FILM CONTACT ANGLES

WATER

52.73 56.48 58.92 58.93 59.05 59.30 59.47 59.89 59.96 63.56 63.86 64.74

MEAN = 59.74 +/- 2.06

SAT.M.I.

26.74 26.96 28.64 29.90 30.37 37.48

MEAN = 30.01 +/- 3.94

METH.IOD.

27.38 28.20 29.97 30.33 30.90 31.65

MEAN = 29.74 +/- 1.63

SURFACE ENERGY PARAMETER	WATER-SAT.M.I.	WATER-METH.IOD.
TOTAL ENERGY	52.39	52.88
POLARITY	0.24	0.23

RESIDUAL WATER CONTACT ANGLE 33.2

APPENDIX IX(CONTD.)

EXPERIMENTAL DATA FOR FILM NAC - TEMP 65 - TIME 60 HR

ADSORPTION DATA COUNTING STANDARD = 666.

TOTAL ADSORPTION

18100. 20100. 12400. 13200. 12800. 14500. 14000. 13900. 14600.

MEAN IS 15602.24 +/- 2037.3

CPM AFTER BENZENE EXTRACTION

6500. 6420. 6420. 6130. 5950. 6900.

MEAN IS 6712.71 +/- 343.5

CPM AFTER WATER EXTRACTION

800. 715. 690. 725. 805. 720.

MEAN IS 780.40 +/- 50.4

CPM AFTER CAUSTIC EXTRACTION

120. 158.

MEAN IS 146.10 +/- 85.9

AMOUNT BENZENE EXTRACTED 8890.00+/- 2425.4

AMOUNT WATER EXTRACTED 5932.00+/- 316.1

AMOUNT CAUSTIC EXTRACTED 634.00+/- 94.9

CALCULATED PER CENT POML BONDED 6.4

UNEXTRACTED FILM CONTACT ANGLES

WATER

48.23 48.34 48.98 49.10 49.87 50.68 51.46 51.93 52.13 55.74

MEAN = 50.65 +/- 1.62

SAT.M.I.

49.85 53.81 57.69 58.16 58.80 59.04

MEAN = 56.23 +/- 3.65

METH.IOD.

51.13 52.80 54.47

MEAN = 52.80 +/- 3.07

SURFACE ENERGY PARAMETER	WATER-SAT.M.I.	WATER-METH.IOD.
TOTAL ENERGY	51.24	51.81
POLARITY	0.48	0.45

EXTRACTED FILM CONTACT ANGLES

WATER

45.84 47.47 48.17 50.06 51.64 53.42 54.66 54.87 55.70 55.97 56.72 60.27

MEAN = 52.90 +/- 2.71

SAT.M.I.

21.16 21.83 22.22 23.14 24.12 35.68

MEAN = 24.69 +/- 5.47

METH.IOD.

19.49 21.24 22.60 23.59 25.11 32.30

MEAN = 24.05 +/- 4.47

SURFACE ENERGY PARAMETER	WATER-SAT.M.I.	WATER-METH.IOD.
TOTAL ENERGY	57.20	57.63
POLARITY	0.27	0.27

RESIDUAL WATER CONTACT ANGLE 32.1

APPENDIX IX(CONTD.)

EXPERIMENTAL DATA FOR FILM NAB - TEMP 65 - TIME 22 HR

ADSORPTION DATA COUNTING STANDARD = 687.

TOTAL ADSORPTION

12600. 9700. 9000. 10400. 10300. 10000. 10500. 10800.
11300. 14700.

MEAN IS 11136.81 +/- 1175.3

CPM AFTER BENZENE EXTRACTION

3640. 3550. 3020. 4040. 4100. 7450.

MEAN IS 4381.36 +/- 1620.0

CPM AFTER WATER EXTRACTION

445. 440. 440. 320. 480. 620.

MEAN IS 466.16 +/- 98.2

CPM AFTER CAUSTIC EXTRACTION

248. 435.

MEAN IS 347.96 +/- 409.9

AMOUNT BENZENE EXTRACTED 6755.00+/- 1829.3

AMOUNT WATER EXTRACTED 3915.00+/- 1477.9

AMOUNT CAUSTIC EXTRACTED 119.00+/- 210.4

CALCULATED PER CENT POML BONDED 2.1

UNEXTRACTED FILM CONTACT ANGLES

WATER

31.04 31.16 31.26 31.45 31.62 31.67 31.70 32.25
32.29 32.48 32.58 32.69

MEAN = 31.85 +/- 0.37

SAT.M.I.

50.12 52.28 53.78 54.00 56.49 57.48

MEAN = 54.03 +/- 2.69

METH.IOD.

43.39 45.07 45.92 46.41 48.47 48.97

MEAN = 46.37 +/- 2.09

SURFACE ENERGY PARAMETER	WATER-SAT.M.I.	WATER-METH.IOD.
TOTAL ENERGY	63.45	64.38
POLARITY	0.57	0.52

EXTRACTED FILM CONTACT ANGLES

WATER

30.88 39.39 41.07 41.08 41.81 42.90 42.94 43.12
43.70 45.21 45.48 46.84

MEAN = 42.04 +/- 2.57

SAT.M.I.

15.55 22.42 22.98 25.34 25.89 27.00

MEAN = 23.20 +/- 4.13

METH.IOD.

22.12 22.55 23.38 23.67 24.18 24.62

MEAN = 23.42 +/- 0.95

SURFACE ENERGY PARAMETER	WATER-SAT.M.I.	WATER-METH.IOD.
TOTAL ENERGY	63.36	63.38
POLARITY	0.34	0.34

RESIDUAL WATER CONTACT ANGLE 28.4

APPENDIX IX(CONTD.)

EXPERIMENTAL DATA FOR FILM NV - TEMP 105 - TIME 24 HR

ADSORPTION DATA COUNTING STANDARD = 703.

TOTAL ADSORPTION

22100. 23400. 30200. 23000. 24100. 24800. 21000. 24800.
24200. 25600.

MEAN IS 24216.19 +/- 1738.7

CPM AFTER BENZENE EXTRACTION

13200. 12700. 14200. 14200. 16000.

MEAN IS 13999.98 +/- 1446.9

CPM AFTER WATER EXTRACTION

3150. 3230. 3060. 2900. 3100.

MEAN IS 3074.82 +/- 140.5

CPM AFTER CAUSTIC EXTRACTION

1150. 1040.

MEAN IS 1090.33 +/- 235.7

AMOUNT BENZENE EXTRACTED 10217.00+/- 2566.2

AMOUNT WATER EXTRACTED 10925.00+/- 1304.2

AMOUNT CAUSTIC EXTRACTED 1984.00+/- 246.6

CALCULATED PER CENT POML BONDED 23.0

UNEXTRACTED FILM CONTACT ANGLES

WATER

53.32 58.62 58.82 60.72 64.09 64.42 65.09 65.95
67.15 69.49 74.02 74.83

MEAN = 64.71 +/- 3.97

SAT.M.I.

52.71 53.41 53.93 54.14 55.22 55.99

MEAN = 54.23 +/- 1.20

METH.IOD.

42.28 46.36 47.34 47.64 50.20 50.36

MEAN = 47.36 +/- 2.96

SURFACE ENERGY PARAMETER	WATER-SAT.M.I.	WATER-METH.IOD.
TOTAL ENERGY	42.75	45.00
POLARITY	0.34	0.28

EXTRACTED FILM CONTACT ANGLES

WATER

58.67 62.58 62.82 65.38 67.71 67.97 67.97 68.97
70.94 71.36 71.83 75.69

MEAN = 67.66 +/- 2.96

SAT.M.I.

37.73 37.87 38.19 39.10 42.11

MEAN = 39.00 +/- 2.09

METH.IOD.

38.67 40.39 42.94 44.57 44.70

MEAN = 42.25 +/- 3.05

SURFACE ENERGY PARAMETER	WATER-SAT.M.I.	WATER-METH.IOD.
TOTAL ENERGY	45.90	45.28
POLARITY	0.21	0.22

RESIDUAL WATER CONTACT ANGLE 45.1

APPENDIX IX(CONTD.)

EXPERIMENTAL DATA FOR FILM NU - TEMP 105 - TIME 1 HR

ADSORPTION DATA COUNTING STANDARD = 692.

TOTAL ADSORPTION

11700. 15300. 13900. 14600. 13100. 14000. 13800. 14800.
13900. 13600.

MEAN IS 14030.32 +/- 706.4

CPM AFTER BENZENE EXTRACTION

2780. 2610. 2740. 2580. 3180. 3150.

MEAN IS 2872.83 +/- 265.7

CPM AFTER WATER EXTRACTION

410. 360. 386. 690. 295. 340.

MEAN IS 418.28 +/- 142.6

CPM AFTER CAUSTIC EXTRACTION

130. 236.

MEAN IS 185.12 +/- 230.7

AMOUNT BENZENE EXTRACTED 11158.00+/- 907.6

AMOUNT WATER EXTRACTED 2454.00+/- 274.6

AMOUNT CAUSTIC EXTRACTED 233.00+/- 267.5

CALCULATED PER CENT POML BONDED 2.1

UNEXTRACTED FILM CONTACT ANGLES

WATER

24.72 25.75 27.24 28.10 28.83 29.31 29.57 30.57
30.76 31.52 32.71 33.16

MEAN = 29.35 +/- 1.64

SAT.M.I.

43.53 45.19 48.01 48.56 55.87 58.19

MEAN = 49.89 +/- 5.87

METH.IOD.

39.46 41.53 42.30 42.76 42.90 43.53 45.80

MEAN = 42.61 +/- 1.72

SURFACE ENERGY PARAMETER	WATER-SAT.M.I.	WATER-METH.IOD.
TOTAL ENERGY	65.37	66.29
POLARITY	0.55	0.51

EXTRACTED FILM CONTACT ANGLES

WATER

32.23 33.17 34.71 35.59 35.69 36.96 37.39 37.51
38.50 38.64 40.82

MEAN = 36.47 +/- 1.67

SAT.M.I.

21.80 21.81 22.61 23.72

MEAN = 22.49 +/- 1.26

METH.IOD.

27.61 29.40 30.57 31.40 31.64

MEAN = 30.12 +/- 1.90

SURFACE ENERGY PARAMETER	WATER-SAT.M.I.	WATER-METH.IOD.
TOTAL ENERGY	66.40	65.01
POLARITY	0.37	0.40

RESIDUAL WATER CONTACT ANGLE 29.7

APPENDIX IX(CONTD.)

EXPERIMENTAL DATA FOR FILM NT - TEMP 105 - TIME 6 HR

ADSORPTION DATA COUNTING STANDARD = 731.

TOTAL ADSORPTION

22800. 23700. 25100. 24700. 24200. 22100. 20200. 22200.
21000. 22100.

MEAN IS 21842.65 +/- 1078.8

CPM AFTER BENZENE EXTRACTION

13000. 12000. 10100. 10600. 10800. 12400.

MEAN IS 10996.34 +/- 1096.4

CPM AFTER WATER EXTRACTION

1880. 1620. 1690. 1800. 1620. 1630.

MEAN IS 1634.29 +/- 104.7

CPM AFTER CAUSTIC EXTRACTION

870. 1100.

MEAN IS 943.23 +/- 473.9

AMOUNT BENZENE EXTRACTED 10846.00+/- 1541.6

AMOUNT WATER EXTRACTED 9362.00+/- 1002.9

AMOUNT CAUSTIC EXTRACTED 691.00+/- 229.6

CALCULATED PER CENT POML BONDED 7.6

UNEXTRACTED FILM CONTACT ANGLES

WATER

46.47 52.98 53.87 54.30 54.92 55.29 55.79 55.79
55.84 55.94 56.01 56.09

MEAN = 54.44 +/- 1.70

SAT.M.I.

50.27 51.96 52.02 52.04 54.00

MEAN = 52.06 +/- 1.52

METH.IOD.

46.14 47.51 47.66 48.06 48.20

MEAN = 47.51 +/- 0.94

SURFACE ENERGY PARAMETER	WATER-SAT.M.I.	WATER-METH.IOD.
TOTAL ENERGY	49.68	50.77
POLARITY	0.41	0.38

EXTRACTED FILM CONTACT ANGLES

WATER

51.14 51.47 55.40 56.49 58.07 58.54 59.51 60.30
60.31 64.76 65.49

MEAN = 58.32 +/- 3.06

SAT.M.I.

30.99 31.77 37.31 39.65 40.03

MEAN = 35.95 +/- 4.95

METH.IOD.

29.86 30.24 30.83 31.50 32.70 33.51

MEAN = 31.44 +/- 1.43

SURFACE ENERGY PARAMETER	WATER-SAT.M.I.	WATER-METH.IOD.
TOTAL ENERGY	51.60	53.12
POLARITY	0.28	0.25

RESIDUAL WATER CONTACT ANGLE 31.6

APPENDIX IX(CONTD.)

EXPERIMENTAL DATA FOR FILM NR/NZ - TEMP 105 - TIME 12 HR

ADSORPTION DATA COUNTING STANDARD = 690.

TOTAL ADSORPTION(NZ)

20800. 19700. 18400. 19800. 24500. 21000. 20100. 18500.

MEAN IS 20644.91 +/- 1589.7

CPM AFTER BENZENE EXTRACTION

9910. 10900. 11100. 7450.

MEAN IS 9982.61 +/- 2360.2

CPM AFTER WATER EXTRACTION

1460. 1620. 1660. 1470. 1790. 1320.

MEAN IS 1575.84 +/- 170.7

CPM AFTER CAUSTIC EXTRACTION

452. 515.

MEAN IS 490.51 +/- 137.5

AMOUNT BENZENE EXTRACTED 10662.00+/- 2563.2

AMOUNT WATER EXTRACTED 8407.00+/- 1563.0

AMOUNT CAUSTIC EXTRACTED 1085.00+/- 313.9

CALCULATED PER CENT POML BONDED 10.7

UNEXTRACTED FILM CONTACT ANGLES

WATER

51.14 51.98 52.94 53.95 56.26 56.50 57.33 58.11

59.86 60.57 63.25 63.50

MEAN = 57.12 +/- 2.61

SAT.M.I.

48.71 52.14 52.86 53.11 55.22 57.00

MEAN = 53.17 +/- 2.82

METH.IOD.

45.28 46.42 49.10 49.60 52.16 52.52

MEAN = 49.18 +/- 2.93

SURFACE ENERGY PARAMETER	WATER-SAT.M.I.	WATER-METH.IOD.
TOTAL ENERGY	47.70	48.71
POLARITY	0.40	0.37

EXTRACTED FILM CONTACT ANGLES

WATER

48.40 50.35 50.84 53.93 55.21 55.67 57.16 57.99

60.18 60.19 61.99 66.59

MEAN = 56.54 +/- 3.32

SAT.M.I.

36.61 38.00 38.29 38.86 40.11 50.92

MEAN = 40.46 +/- 5.24

METH.IOD.

33.04 33.28 33.32 33.50 36.68 38.71

MEAN = 34.76 +/- 2.37

SURFACE ENERGY PARAMETER	WATER-SAT.M.I.	WATER-METH.IOD.
TOTAL ENERGY	51.39	53.12
POLARITY	0.32	0.28

RESIDUAL WATER CONTACT ANGLE 30.7

APPENDIX IX(CONTD.)

EXPERIMENTAL DATA FOR FILM NQ/NY - TEMP 105 - TIME 3 HR

ADSORPTION DATA COUNTING STANDARD = 675.

TOTAL ADSORPTION(NY)

13100. 12400. 11900. 11700. 12500. 10700. 11200. 13300.
12900. 13700.

MEAN IS 12797.02 +/- 701.0

CPM AFTER BENZENE EXTRACTION

460. 420. 535. 630.

MEAN IS 530.19 +/- 133.0

CPM AFTER WATER EXTRACTION

248. 210. 240. 270.

MEAN IS 250.96 +/- 35.7

CPM AFTER CAUSTIC EXTRACTION

335. 405.

MEAN IS 383.70 +/- 156.2

AMOUNT BENZENE EXTRACTED 12267.00+/- 1112.4

AMOUNT WATER EXTRACTED 280.00+/- 121.4

AMOUNT CAUSTIC EXTRACTED -133.00+/- 81.7

CALCULATED PER CENT POML BONDED -1.3

UNEXTRACTED FILM CONTACT ANGLES

WATER

36.22 38.93 39.04 39.23 40.43 40.50 40.74 41.27
41.95 42.61 43.10 44.45

MEAN = 40.71 +/- 1.39

SAT.M.I.

44.80 45.98 46.16 46.30 50.99 55.23

MEAN = 48.24 +/- 4.03

METH.IOD.

47.61 50.01 51.71 52.43 53.34 53.58

MEAN = 51.45 +/- 2.28

SURFACE ENERGY PARAMETER	WATER-SAT.M.I.	WATER-METH.IOD.
TOTAL ENERGY	59.19	58.39
POLARITY	0.48	0.51

EXTRACTED FILM CONTACT ANGLES

WATER

39.17 39.79 41.20 42.60 42.80 43.23 44.08 44.75
45.10 45.37 45.98 46.20

MEAN = 43.36 +/- 1.47

SAT.M.I.

25.68 26.00 30.13 30.33 31.09

MEAN = 28.65 +/- 2.98

METH.IOD.

23.52 25.46 28.61 30.36 30.94 35.05

MEAN = 28.99 +/- 4.12

SURFACE ENERGY PARAMETER	WATER-SAT.M.I.	WATER-METH.IOD.
TOTAL ENERGY	61.65	61.61
POLARITY	0.36	0.36

RESIDUAL WATER CONTACT ANGLE 27.9

APPENDIX X

CALCULATIONS FOR REACTION RATE ANALYSIS

A. REACTION ORDER IN MONOMER CONCENTRATION

	Case I			Case II		
Temp., °C	65	85	105	65	85	105
Temp., °K	338	358	378	338	358	378
$T\Delta S$[a]	4050	4296	4536	4050	4296	4536
$\Delta H°$	———	14,000	———	———	8000	———
ΔG	9950	9704	9464	3950	3704	3464
$\text{Log}_{10} K_{eq}$	-6.4	-5.9	-5.5	-2.6	-2.3	-2.0
K_{eq}	3.71×10^{-7}	1.20×10^{-6}	3.38×10^{-6}	2.85×10^{-3}	5.49×10^{-3}	1.00×10^{-2}
X_m	0.61×10^{-3}	1.09×10^{-3}	1.85×10^{-3}	0.053	0.071	0.095
%POML	120	160	240	120	160	240
M	7.32	17.44	44.4	6.36	11.42	22.8
$\text{Log}_{10} M$	0.865	1.24	1.65	0.803	1.06	1.36
v	0.11	0.33	0.96	0.11	0.33	0.96
$\text{Log}_{10} v$	-0.959	-0.482	-0.018	-0.959	-0.482	-0.018
p (from Fig. 27)	———	1.2	———	———	1.7	———

[a] ΔS = 12.0 e.u.

B. ARRHENIUS ENERGY OF ACTIVATION CALCULATIONS

	Case I (ΔH = 14,000 cal./mole)			Case II (ΔH = 8000 cal./mole)		
Temp., °C	65	85	105	65	85	105
Temp., °K	338	358	378	338	358	378
$1/T$, °K	0.00296	0.00279	0.00265	0.00296	0.00279	0.00265
v/M (=k)	0.0150	0.0189	0.0216	0.0173	0.0289	0.0421
$\text{Log}_{10}\ k$	-1.82	-1.72	-1.66	-1.76	-1.54	-1.38
Slope of plot (Fig. 28)	534			1265		
E_a	2450			5780		

C. PLOTS OF DATA

Plot A, Fig. 27, $\text{Log}_{10}\ v$ vs. $\text{Log}_{10}\ M$, Case I

Plot B, Fig. 27, $\text{Log}_{10}\ v$ vs. $\text{Log}_{10}\ M$, Case II

Plot C, Fig. 28, $\text{Log}_{10}\ k$ vs. $1/T$, Case I

Plot D, Fig. 28, $\text{Log}_{10}\ k$ vs. $1/T$, Case II

Plot E, Fig. 29, $\text{Log}_{10}\ v$ vs. Log_{10} (total adsorption)

Plot F, Fig. 29, $\text{Log}_{10}\ v$ vs. $\text{Log}_{10}\ X_m$, Case I

Plot G, Fig. 29, $\text{Log}_{10}\ v$ vs. Log_{10} (vapor pressure)

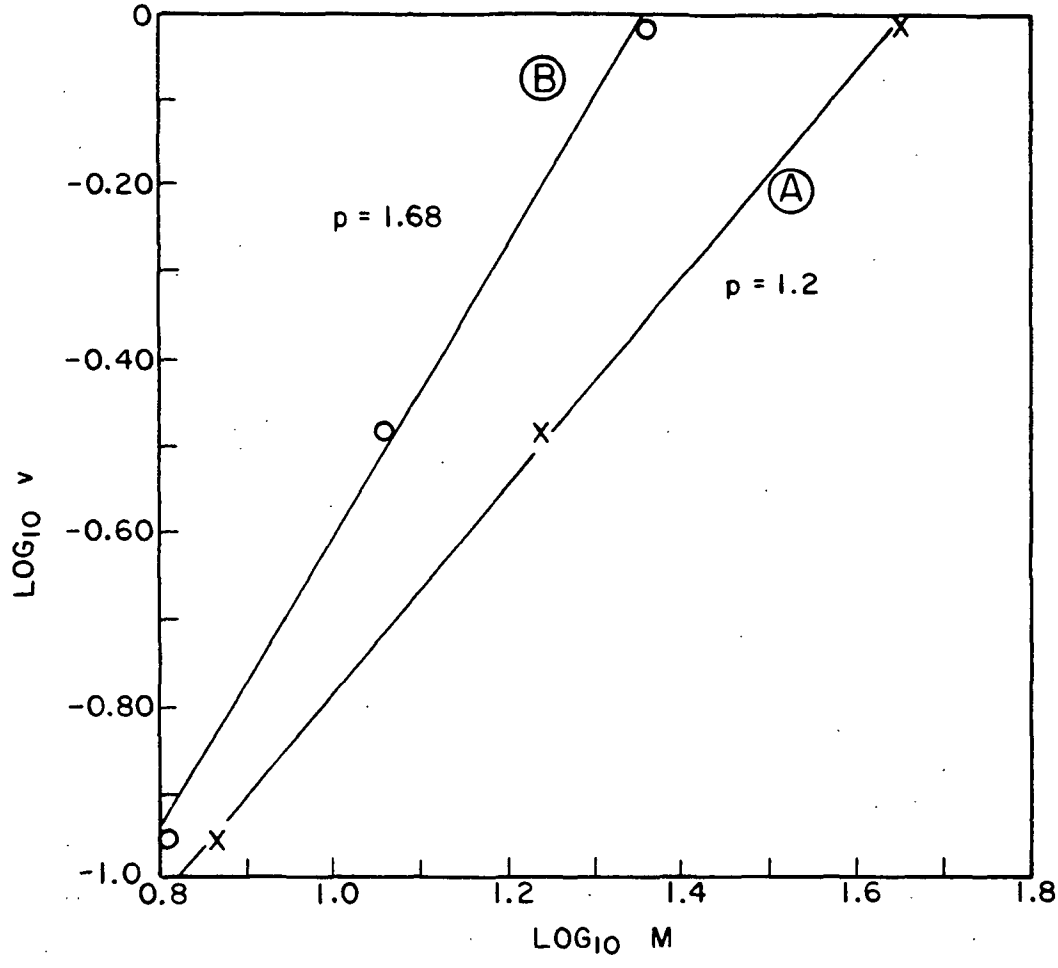

Figure 27. Log-Log Plots, A,B

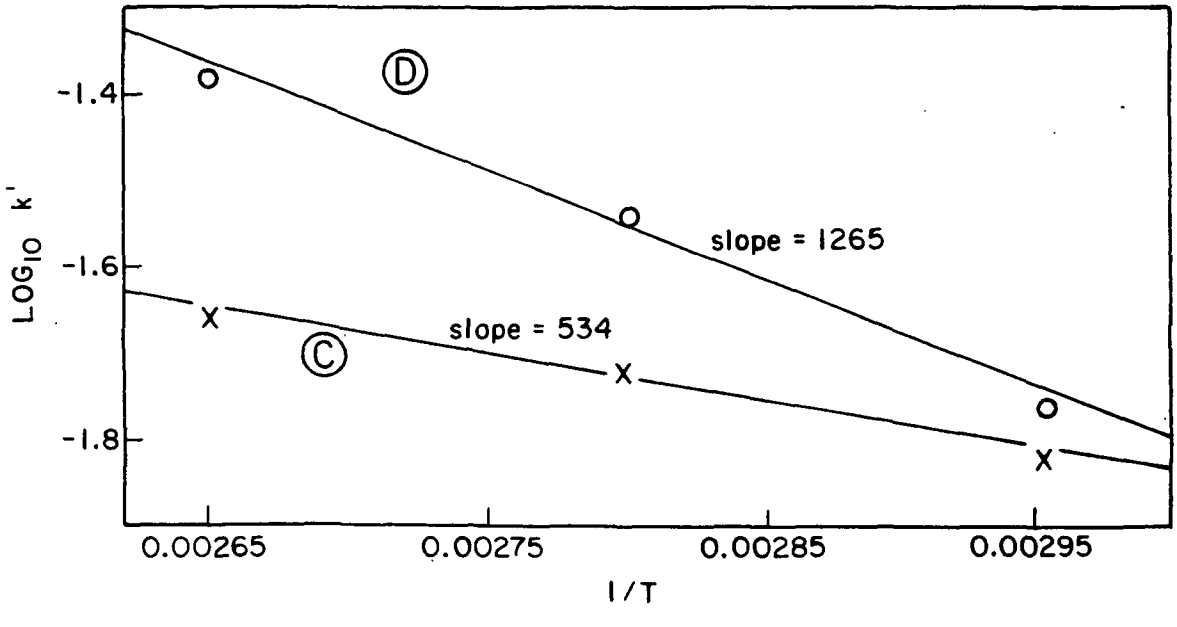

Figure 28. Arrhenius Plots, C,D

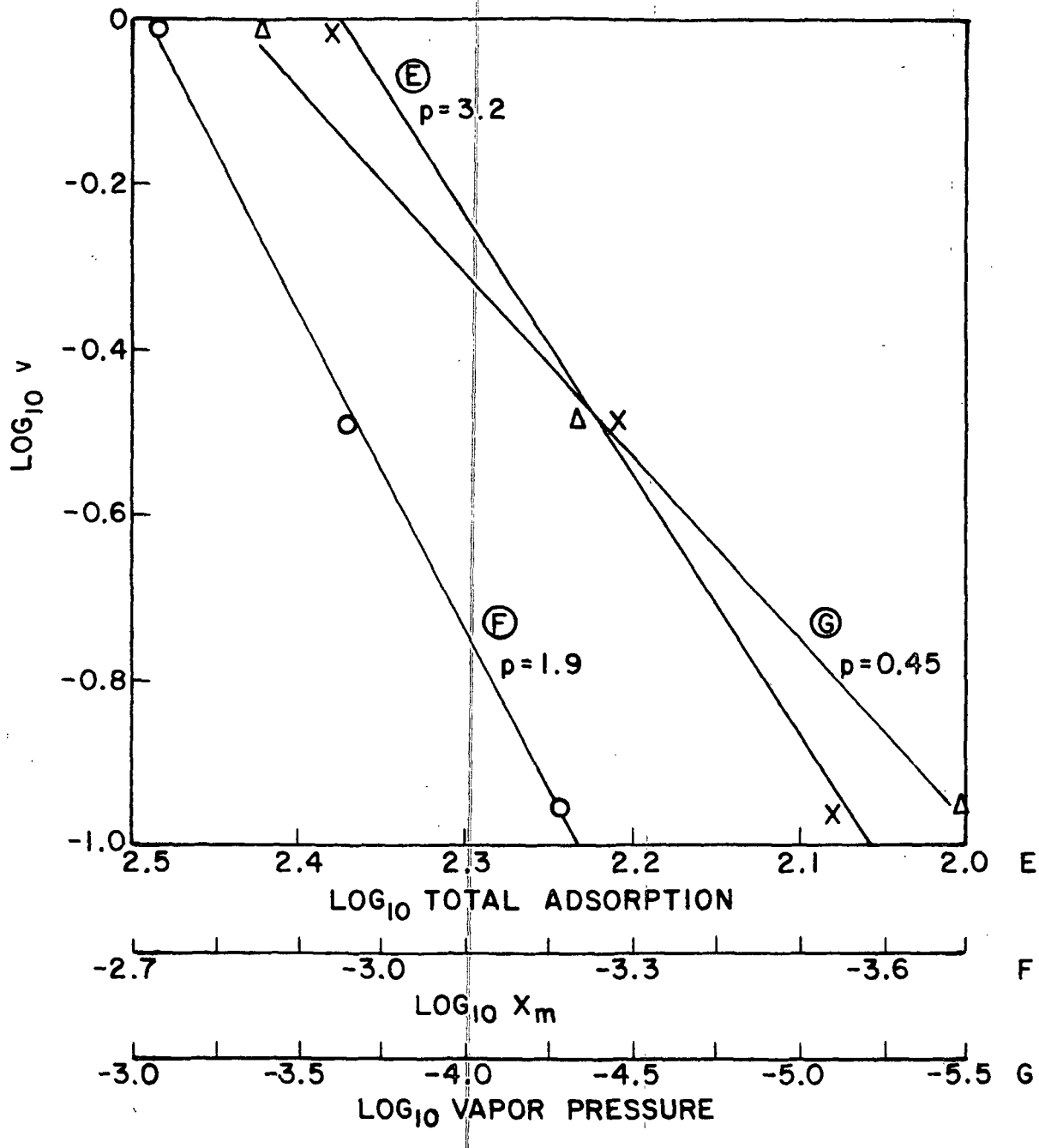

Figure 29. Data Plots for E, F, G